



universität
wien

DIPLOMARBEIT

Titel der Diplomarbeit

Identification of Regulatory Phosphorylation Sites
on the Human Kinetochore

angestrebter akademischer Grad

Magister der Naturwissenschaften (Mag. rer. nat.)

Verfasser:	Stephan Zettl
Matrikel-Nummer:	0247642
Studienrichtung (lt. Studienblatt):	Molekulare Biologie (A490)
Betreuer:	Dr. Jan-Michael Peters

Wien, im September 2009

Table of Contents

Table of Contents	1
Abstract.....	4
Zusammenfassung.....	5
1. INTRODUCTION	6
1.1. The cell cycle	6
1.1.1. The phases of the cell cycle	6
1.1.2. The stages of mitosis	7
1.1.3. Chromosome segregation, instability and cancer	9
1.1.4. Molecular mechanisms controlling cell cycle progression.....	9
1.1.5. Mitotic kinases	10
1.2. The Kinetochore	10
1.2.1. Organisational model of the human kinetochores.....	11
1.3. Specific kinetochore complexes	14
1.3.1. Features of the Hec1 complex	14
1.3.2. Features of the Mis12 complex	15
1.3.3. Features of the RZZ complex.....	16
1.4. Aims of the study	18
1.5. Experimental approach	19
2. RESULTS	20
2.1. Generation of cell lines stably expressing 9myc-tagged human kinetochore proteins	20
2.1.1. Generation of expression constructs	20
2.1.2. Test expression of myc-tagged proteins by IVT.....	21
2.1.3. Creating and testing stably expressing HeLa cells	22
2.1.5. Result summary of the first strategy	26
2.2. Generation and characterisation of kinetochore antibodies	28
2.2.1 Preparation of peptides and proteins for immunisation.....	28

2.2.2. Characterisation of kinetochore anti-sera by western blot	29
2.2.3. Testing the specificity of the kinetochore antibodies by western blot	32
2.2.4. Testing the kinetochore antibodies for immunoprecipitation	34
2.2.5. Optimising IP conditions (IP-WB, IP-silver, IP-MS)	40
2.3. Identification of interaction partners and phospho-sites by liquid chromatography-tandem mass-spectrometry (LC-MS/MS)	44
2.3.1. Identification of interaction partners from DC8-IP	45
2.3.2. Phosphorylation-site mapping of interaction partners from DC8-IP	49
3. DISCUSSION	54
3.1. Expressing tagged kinetochore proteins	54
3.2. Interpretation of interaction results	54
3.2.1. Categorisation of protein hits	55
3.2.2. Ranking and confidence of MS protein hits	57
3.2.3. Possible improvement of IP-MS quality	57
3.2.3. Follow-up experiments for interaction analysis	58
3.3. Interpretation of phospho-site mapping results	60
3.3.1. Kinase consensus sequences	62
3.3.2. Conservation of phospho-sites across species	62
3.3.3. Follow-up experiments for phospho-site analysis	64
3.4. Outlook: Kinetochore regulation by phosphorylation	65
4. MATERIALS AND METHODS	66
4.1. DNA and Cloning	66
4.1.1. Agarose gel electrophoresis	66
4.1.2. Polymerase chain reaction (PCR)	66
4.1.3. Primer design for cloning	66
4.1.4. Restriction enzyme digest	68
4.1.5. Ligation of PCR fragments into a vector	68
4.1.6. Transformation	68
4.1.7. Preparation of DNA	68
4.1.8. cDNA	69

4.2. Expression and purification of recombinant protein	70
4.2.1. Expression in E.coli BL21 (DE3)	70
4.2.2. In vitro translation / transcription (IVT) and phosphoimaging	70
4.3. Antibodies and peptides	71
4.3.1. Antibodies for western blotting	71
4.3.2. Antibody generation	71
4.4. Protein purification and analysis.....	74
4.4.1. Preparation of cell extract.....	74
4.4.2. SDS-polyacrylamide gel electrophoresis (SDS-PAGE)	75
4.4.3. Coomassie staining.....	75
4.4.4. Silver staining.....	76
4.4.5. Western blotting	76
4.4.6. Stripping of PVDF membrane for reprobing.....	77
4.5. Immunoprecipitation and Mass Spectrometry	77
4.5.1. Antibody coupling and cross-linking	77
4.5.2. Immunoprecipitation (IP)	78
4.5.3. In-solution digest.....	78
4.5.4. Mass spectrometry.....	79
4.6. Cell culture and immunofluorescence microscopy	80
4.6.1. Growth and harvesting of HeLa cells.....	80
4.6.2. siRNA transfection	81
4.6.3. Establishment of stable cell pools	82
4.6.4. Immunofluorescence microscopy.....	82
5. APPENDIX.....	84
6. REFERENCES.....	88
7. ABBREVIATIONS.....	97
Acknowledgements.....	99
Curriculum Vitae.....	100

Abstract

A vital feature of mitosis is the accurate segregation of genetic material to the daughter cells. This process crucially depends on biorientation of the sister chromatids on the mitotic spindle. The attachment of spindle microtubules to the mitotic chromosomes occurs via kinetochores, proteinaceous structures which form on the centromeres. Kinetochores are dynamic structures capable of sensing microtubule attachment and tension as well as signaling to the spindle assembly checkpoint (SAC) and therefore are critically involved in formation of the metaphase spindle and the segregation of sister chromatids in anaphase. Kinetochores are known to be made of many protein complexes which are still being characterised. Among those characterised so far, are the Mis12, Hec1 and RZZ complexes, which are thought to regulate the assembly and the maintenance of tension and recruitment of spindle checkpoint components to the kinetochore. The kinetochore is the location for several mitotic kinases, including Cdk1, Aurora B, Plk1, Mps1 and BubR1, and therefore kinetochore proteins would be prime candidates as substrates for these kinases. With the aim of investigating the components and phosphorylation of these complexes in mitotic human cells, I raised antibodies against kinetochore proteins and generated HeLa cells expressing affinity tagged kinetochore components to perform affinity purification and mass spectrometry experiments. Of the five antibodies, one of them (against the Mis12 component DC8) was found to be highly specific and effective for immuno-precipitation. By contrast, the expression of tagged kinetochore components was not sufficient for affinity purification purposes.

The total set of proteins immuno-purified from HeLa extracts using the anti-DC8 antibody was found to contain many known Mis12 components plus the complete Hec1 tetrameric complex, additional mitotic spindle proteins (including HP1-gamma, SPAG5 and dynein light chain) and several novel interactors (including C15orf23, RABGAP1 and claspin). Phosphorylation site analysis identified 44 sites in six of these proteins, DC8, Q9H410, C15orf23, PFKFB2, RABGAP1 and SPAG5, purified from extracts of HeLa in interphase and mitosis. By comparing the phosphorylation states of these proteins under those conditions 18 sites were found to be mitosis specific. Identification of these phospho-sites could help in understanding the dynamic regulation of kinetochores in mitosis.

Zusammenfassung

Ein grundlegendes Merkmal der Mitose ist die exakte Aufteilung des genetischen Materials auf die Tochterzellen. Ausschlaggebend für diesen Prozess ist die Aufteilung der Schwesterchromatiden zu jeweils entgegengesetzten Zellpolen durch die Mitotische Spindel. Die Anheftung der Spindel-Mikrotubuli erfolgt über Kinetochore, proteinöse Strukturen die sich an den Zentromeren der Chromosomen befinden. Kinetochore sind dynamische Strukturen, die sensibel auf Mikrotubuli-Anheftung, Zugspannung sowie auf die Signalübertragung des „Spindle Assembly Checkpoint“ (SAC) reagieren, sie spielen daher eine außerordentlich wichtige Rolle bei der Ausbildung der Metaphase Spindeln sowie der Teilung der Schwester-Chromatiden in der Anaphase. Kinetochore bestehen aus vielen Proteinkomplexen, deren molekulare Charakterisierung gerade andauert. Zu den bereits näher charakterisierten Kinetochor-Proteinkomplexen gehören unter anderem die Komplexe Mis12, Hec1 und RZZ, von denen man annimmt, dass sie die Generierung und Aufrechterhaltung der Zugspannung sowie die Rekrutierung von Spindel Checkpoint Komponenten an die Kinetochore regulieren. Weiterhin ist bekannt, dass sich viele Kinasen, wie Cdk1, Aurora B, Plk1, Mps1 und BubR1 an den Kinetochoren befinden, was darauf hinweist, dass Kinetochor-Proteine potentiell wichtige Substrate für diese Kinasen darstellen. Mit dem Ziel, Komponenten und Phosphorylierungen dieser Proteinkomplexe in mitotischen humanen Zellen zu untersuchen, habe ich Antikörper gegen Kinetochor-Proteine hergestellt sowie HeLa Zellen generiert, die Kinetochor-Proteine mit Affinitäts-tags exprimieren. Ein Affinitäts-tag erleichtert die Aufreinigung der Proteine und ermöglicht Massenspektrometrie Experimente durchzuführen. Von fünf generierten Antikörpern, zeigte sich einer (gegen die Mis12 Komponente DC8) als hoch spezifisch und effektiv für die Immunpräzipitation. Die Expression der getaggten Kinetochor-Komponenten war hingegen nicht ausreichend für die angedachten Affinitäts-Aufreinigungen. Mittels des generierten anti-DC8 Antikörpers, reinigte ich viele der bekannte Mis12 Komponenten, den kompletten Hec1 Komplex, weitere mitotische Spindel-Proteine (wie HP1-gamma, SPAG5 und dynein light chain) sowie einige neue Interaktionspartner (wie C15orf23, RABGAP1 und claspin) aus mitotischen sowie Interphase HeLa Zellextrakten auf. Durch weitere Analyse dieser aufgereinigten Proteinkomplexe identifizierte ich insgesamt 44 Phosphorylierungsstellen in sechs der Proteine, DC8, Q9H410, C15orf23, PFKFB2, RABGAP1 and SPAG5. Beim Vergleich der Phosphorylierungs-Muster dieser Proteine aus Interphase und Mitose, wurden 18 Mitose-spezifische Stellen gefunden. Die Identifizierung von Phosphorylierungsstellen leistet einen wichtigen Beitrag zum Verständnis der dynamischen Steuerung der Kinetochore in der Mitose.

1. Introduction

All living organisms are made up from fundamental building block known as cells. One of the main defining characteristics of life is the ability to replicate genetic material and to reproduce. For eukaryotic cells, the process of duplicating the billions of base-pairs of DNA within the chromosomes, separating the chromosomes and the subcellular organelles, followed by splitting the cell into two daughter cells is an enormous logistic task. Maintaining the integrity of the genome throughout this process is of paramount importance. Thus, the cell invest much of its resources to the faithful replication of the genomic material and accurate separation of the chromosomes (Elledge, 1996).

Passage through the cycle of cell division is regulated by hundreds of gene products, whose role is to co-ordinate the initiation of various events of the cell cycle, and to ensure that these occur in a precise and ordered manner. Throughout the cell cycle it is important that the completion of one event occurs before a later one can be initiated, e.g. the DNA replication has been completed before separation of the chromosomes and cell division can take place. It is also essential that cells can respond to damage to its chromosomes, so that the progression of the cell cycle can be halted until the damage is repaired. Failure to do so would lead to a loss of genomic integrity, possibly leading to permanent mutation and either loss of viability of the progeny cells, or in case of multicellular organisms, transformation of the cell to a tumorigenic phenotype.

Experiments using diverse range of organisms and types of cells have demonstrated that despite enormous variations of cell types, all eukaryotic cells share common mechanisms for timing and regulation of growth and cell division. In this study, I was interested in the identification of regulatory phosphorylation sites on human kinetochore.

1.1. The cell cycle

1.1.1. The phases of the cell cycle

Before a cell is able to successfully divide, two key events must occur: the duplication and the segregation of the chromosomes. When eukaryotic cells are observed during consecutive divisions, each division cycle can be seen to consist of two temporally separated stages, known as interphase and mitosis. Interphase is a morphologically relatively inactive period between two successive mitoses, it can be divided into four phases: 'G1', 'S', 'G2' and 'M' phase (Figure 1.1). At first, cells are in an apparently quiet state, a 'gap phase' (G1) to accumulate the resources needed for the most significant event during interphase, the faithful duplication of the genomic information stored on chromosomes. The period of time

when duplication occurs, is known as 'S-phase' (S for synthesis). This is then followed by a second 'gap phase' (G₂) in which the cell grows, produces proteins, prepares enzymes and machinery required for the subsequent division. The division of the genome takes place during mitosis (or 'M-phase'), which is a phase of dramatic morphological changes, where the nuclear envelope breaks down, the chromosomes become visible and separate, the mitotic spindle forms, chromosomes segregate to opposite poles of the cell and finally the whole cell divides in two (cytokinesis). The cell then either enters a new G₁-phase, ready for a new round of division or ceases to divide and enters a reversibly quiescent state (G₀), whereas some cells (e.g. neurons) exit permanently from the cell cycle and stay in an 'post-mitotic' state.

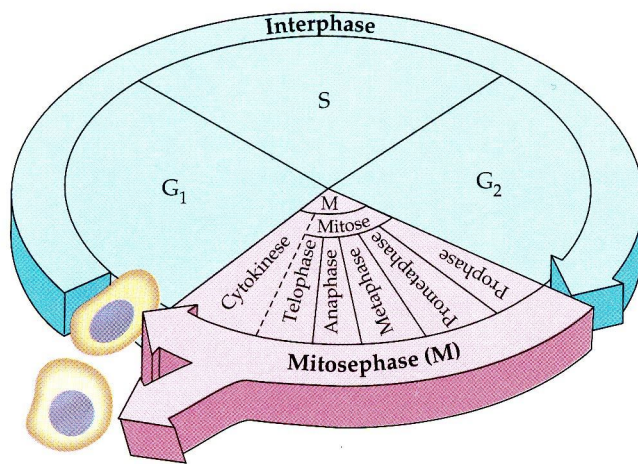


Figure 1.1. Scheme of the cell cycle phases. The cell cycle is divided into four phases: 'G₁', 'S', 'G₂' and 'M' phase. The first three phases taken together are termed Interphase. Mitosis and cytokinesis are called M-phase. Figure adapted from 'Biologie' 1st edition by Neil A. Campbell, (German version).

1.1.2. The stages of mitosis

Mitosis is the phase in which the chromosomes are segregated and then the cell divides into two daughters (cytokinesis). The process of mitosis is by necessity a highly regulated procedure, which itself divided into distinct sequential stages (Fig. 1.2), to ensure that throughout the separation of chromosomes the integrity of the genome and of the cell as a whole is maintained. During S-phase, each chromosome is replicated once, but remains attached at the centromere to its identical sister chromatid. The first stage of mitosis, *prophase* is characterised by one of the most striking phenomena in cell biology: chromosome condensation. The replicated chromosomes undergo extensive condensation (*i.e.* coiling), cells compact their amorphous chromatin into highly compacted threads which are greatly thickened and shortened as mitosis progresses, but are still contained within the nuclear envelope. Pairs of sister chromatids can eventually be visually distinguished. Late in

prophase, the duplicated centrosomes separate and start to form the mitotic spindle. The final event of prophase is the breakdown of the nuclear envelope into small vesicles, caused by dissolution of the nuclear lamina filaments, the meshwork of proteins which covers and stabilises the nucleus. Once the nuclear envelope has broken down, *prometaphase* starts. The microtubules emanating from the centrosomes capture chromosomes at their kinetochores, special proteinaceous structures which assemble near the primary constriction of chromosomes (Cleveland et al., 2003). Once sister chromatids are thus attached in an amphitelic manner (adjusted by microtubule motors and tension sensors), to opposite poles, chromosomes undergo what is known as congressional movement, where they ultimately end up aligned on a 'metaphase plate'. This alignment represents essential prerequisites for the proper separation of the replicated genome into two equal parts. The mechanisms underlying congression are under intense scrutiny. When all chromosomes are thus aligned, the cell is in *metaphase*. Metaphase is followed by *anaphase*, which commences with the initial separation of sister chromatids at their centromeres. These daughter chromosomes then begin to separate from each other, each moving away from the metaphase plate, towards opposite spindle pole regions. The mechanisms that control chromosome separation clearly involve the interactions between microtubules and components near or inside the kinetochore. In *telophase*, the condensed chromosomes become bound by vesicles of the nuclear membrane, which then fuse to form a mini-nucleus, or karyomere. Chromosomes decondense and karyomeres fuse to form one interphase nucleus. The final stage of 'M-phase' is called *cytokinesis* which is initiated by forming of a contractile ring, this separates the two daughter cells by ingression of the cell membrane. Each of the daughter cells now contains one set of chromosomes and one spindle pole, also the microtubule network undergoes reorganisation and returns to its interphase state.

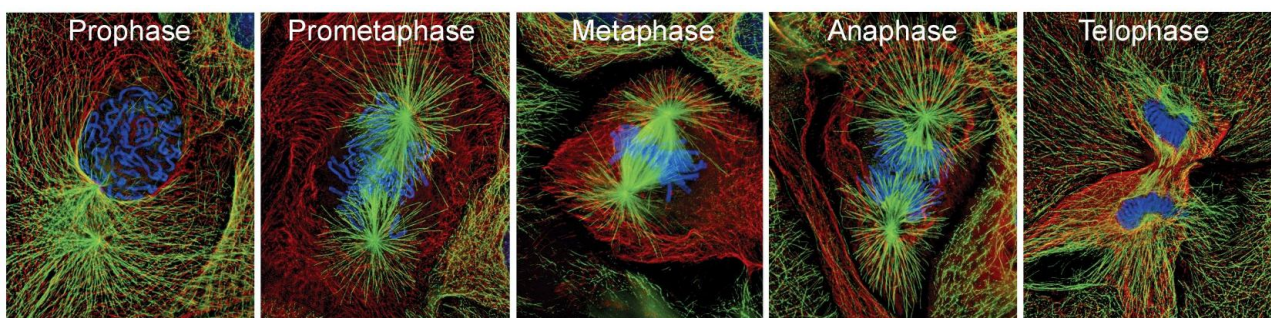


Figure 1.2. Stages of mitosis. Immunofluorescence microscopy is used here to illustrate the five distinct stages of mitosis (M-phase) in animal cells: prophase, prometaphase, anaphase and telophase, which is subsequently followed by cytokinesis (not shown). In these confocal images of fixed newt lung cells, microtubules are shown in green, intermediate filaments are in red, and chromosomes are stained in blue. Figure adapted from "The Biology of Cancer", by Robert A. Weinberg.

1.1.3. Chromosome segregation, instability and cancer

All genetic information required to form a differentiated organism is contained within chromosomes. To ensure the correct inheritance of this information, the two key events of the cell cycle, DNA replication and sister chromatid segregation, have to be precisely controlled. The molecular mechanisms which ensure accurate chromosome segregation during mitosis are critical to the conservation of euploidy in eukaryotic cells. Errors in this process, such as chromosome loss or disjunction, result in aneuploidy and phenotypic consequences for these imbalances in chromosome number are usually severe (Friedlander et al., 1984; Hassold et al., 2001). In humans, failure in mitotic chromosome segregation may play a crucial role in the onset of neoplasia by reducing tumor suppressor gene dosage or by amplifying oncogenes. Mutations causing genomic instability are being recognised as being predisposing conditions for cancer (Lengauer et al., 1998; Cahill et al., 1999; Rajagopalan et al., 2004). Genomic instability in colon cancer, for example, arises by one of two mechanisms: microsatellite instability, where defects in mismatch repair lead to increased mutation rates; or chromosome instability, where improper sister chromatid segregation leads to aneuploidy (Lengauer et al., 1997; Orr-Weaver et al., 1998). Missing or extra chromosomes in germ-line cells, due to missegregation during meiosis, usually result in premature abortion of the fetus (Griffin, 1996) or generation of offspring with birth defects such as Patau syndrome, Edwards syndrome, Down syndrome or Klinefelter's syndrome, which are characterised by the presence of an extra copy of chromosome 13, 18, 21 or the X chromosome respectively (Sluder et al., 2000). Thus the precise regulation of DNA replication and sister chromatid segregation is crucial, since cells and the replicated genome are irreversibly separated after each cell cycle.

1.1.4. Molecular mechanisms controlling cell cycle progression

During cell cycle there are several points at which the progression to the next phase can be halted or delayed until certain criteria are fulfilled. These points are referred to as cell cycle checkpoints. There is for example one checkpoint at the G1 to S transition, which monitors the size of the cell, the supply of nutrients and growth factors; one at the G2 to M transition ensures that all chromosomes have been replicated properly and that there is no DNA damage and another one in M-phase, which is required for delaying cells until all chromosomes are attached properly to the mitotic spindle in an amphitelic fashion. These checkpoints contribute to the fidelity of the cell cycle by ensuring that both internal and external conditions are favourable for cell division (Hartwell et al., 1989). Another mechanism, which controls the unidirectional progression through the cell cycle, is fulfilled by phosphorylation of effector proteins that initiate or regulate DNA replication, mitosis or

cytokinesis. The phosphorylation reactions are carried out by a specific family of protein kinases called cyclin dependent kinases (Cdks), which are the main cell cycle kinases. The activation of those enzymes critically depend on their association with proteins called cyclins, which are accumulated and degraded in a cyclical manner during the cell cycle (Evans et al., 1983; Lee et al., 1987). The degradation of cyclins by ubiquitination and subsequent proteolyses represents an irreversible step in the cell cycle, which drives the cell in one direction (Lee et al., 1987; Morgan, 1997; Murray, 2004).

1.1.5. Mitotic kinases

The regulation of M-phase, the faithful progression through mitosis and cytokinesis, relies predominantly on two post-translational mechanisms, phosphorylation and proteolysis. These processes are intimately connected in that the proteolytic machinery is controlled by phosphorylation, whereas several mitotic kinases are downregulated by degradation (Nigg, 2001). Three best characterised classes of kinases are the cyclin-dependent kinases (Cdk), Polo-like kinases (Plk) and Aurora kinases (A and B). Cdk1 is one of the key-regulators of the M-phase, its activity critically depends on the association with Cyclin A and B (Murray, 2004). High Cdk1 activity is required for mitotic entry and chromosome condensation but Cdk1 activity must be low to allow cells to exit mitosis. This is accomplished by degradation of Cyclin B by ubiquitination, catalysed by the anaphase-promoting complex or cyclosome (APC/C), (Peters, 2006). The APC/C is kept inactive towards cyclin B until chromosomes are aligned on a proper metaphase plate and are attached to opposite poles of the mitotic spindle. The Plk1 kinase is required for stable interactions between microtubules and the kinetochores (Sumara et al., 2004) and for the activation of Cdk-cyclin complexes. Furthermore Plk1 helps to remove Cohesin from chromosomes (Sumara et al., 2002) – the “molecular glue” which prevents premature sister chromatid separation before anaphase (Nasmyth et al., 2000). Aurora B is known to be needed for the correction of irregular attachment of the mitotic spindle to the kinetochore and subsequently to support the alignment of correct spindle attached chromosomes in the metaphase plate (Tanaka et al., 2002; Hauf et al., 2003).

1.2. The Kinetochore

The kinetochore is a macromolecular, multilayered complex, consisting of centromeric DNA and associated proteins, which is tightly connected with the process of chromosome segregation. There are two kinetochores on each pair of replicated chromosomes, one on each chromatid. The highly complex machine of a kinetochore is responsible for mediating the attachment of mitotic spindle (microtubules) to the centromere of sister chromatids and

for guiding chromosome movement during mitosis and meiosis (Nasmyth et al., 2000; Nasmyth, 2002). Remarkably, the kinetochore supervises microtubule attachment in mitosis and is essential in sensing the completion of metaphase (amphitelic, bi-polar attachment of all chromosomes) before allowing the onset of anaphase (Tanaka, 2002; Lew et al., 2003). This quality-control mechanism, intimately linked to kinetochores, is known as the spindle-assembly checkpoint, or SAC (Musacchio et al., 2007), it is an ubiquitous safety device preventing chromosome mis-segregation and aneuploidy. When the SAC senses unattached kinetochores, it blocks the activation of the APC/C towards cyclin B and securin and inhibits therefore the separation of sister chromatids i.e. the initiation of anaphase.

To fulfil these ambitious tasks, the kinetochore acts as a kind of a central hub where kinetochore proteins, centromeric chromatin, cohesions and spindle checkpoints and microtubule-associated proteins accumulate to coordinate sister chromatid segregation. The budding yeast kinetochore, which is considered to be the simplest one, contains a single microtubule-binding unit on a short, well defined centromeric DNA sequence; roughly 60 kinetochore proteins have been identified in budding yeast (McAinsh et al., 2003). The animal kinetochore in contrast binds 20-40 microtubules each on a large array of centromeric DNA repeats. The number of functioning proteins, which this multilayered protein complex consist of, is predict to be more than 100 (Fukagawa, 2004).

Nevertheless, animal and yeast kinetochore have basic similarities in structure and function, and contain related protein complexes forming the microtubule-binding units, whose basic design is the same in all species. On the basis of their spatial proximity to the centromeric DNA, kinetochore components can be classified as inner, central and outer kinetochore proteins. Further proteins, such as spindle checkpoint proteins, microtubule-associated proteins, motor proteins and regulatory proteins (for example kinases like Aurora B and Cdk1), are of outstanding importance to regulate spindle-kinetochore attachments, generate and govern the forces that move chromosomes on the spindle, monitor local tension and use this information to coordinate and control cell cycle progression (Biggins et al., 2003; McAinsh et al., 2003).

1.2.1. Organisational model of the human kinetochores

The observation of the sub-cellular body which leads mitotic chromosomes, termed 'Leitkörper' was first made by W. Flemming in 1891 (Flemming, 1891). This structure, which is situated on the centromeric heterochromatin was subsequently characterised by transmission electron microscopy (TEM) studies using conventional staining and fixation methods (Brinkley et al., 1966; Jokelainen, 1967; Comings et al., 1971) and more recently by fast freezing substitution (McEwen et al., 1998). In these studies the kinetochores, in higher

eukaryotes, appear to be composed of several distinct layers, seen as a trilaminar stack of plates, with an electron-dense inner domain containing centromeric heterochromatin, a less dense middle domain, and a diffuse outer domain containing microtubule binding activities (Fig. 1.3). In some images, in the absence of MT attachment, a diffuse fibrous region, known as the corona is visible. It is unclear whether these structures observed by EM in fixed specimens represent the kinetochores in living mitotic cells. The assembly of the kinetochore and the recruitment of the different kinetochore complexes occurs in a hierarchical manner. A result of which some components localise more to the inner and some more to the outer kinetochore as it is represented in a current organisational model Fig. 1.4 (Musacchio et al., 2007).

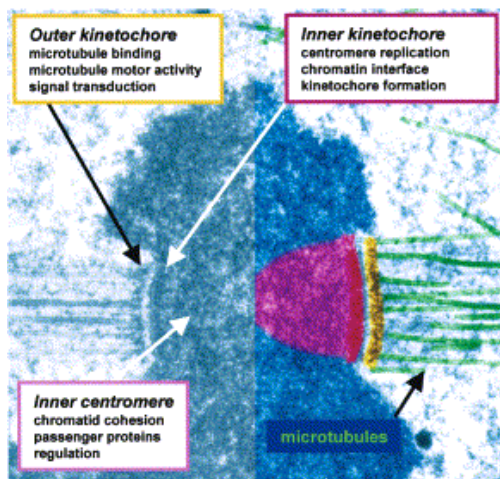


Figure 1.3. The centromere-kinetochore region – the overall organisation. A mitotic chromosome has been sectioned along the plane of the spindle axis, according to its symmetric bipolar organisation, completely attached to the microtubules and visualised by electron microscopy. The key elements have been pseudo-coloured (right). The inner centromere (purple), a heterochromatin domain that is a focus for cohesins and regulatory proteins such as Aurora B and Kin I. The inner kinetochore (red), a region of distinctive chromatin composition attached to the primary constriction. The outer kinetochore (yellow), the site of microtubule binding, is comprised of a diverse group of microtubule motor proteins, regulatory kinases, microtubule binding proteins, and mitotic checkpoint proteins. Figure adapted from (Cleveland et al., 2003).

In all eukaryotes the kinetochore is assembled on specialised nucleosomes containing at least one specialised histone H3 variant of CENP-A (Warburton et al., 1997; Cleveland et al., 2003). CENP-A nucleosomes together with other proteins characteristic for heterochromatin, are found in large numbers in human centromeric DNA. The CENP-A nucleosomes associate directly with a conserved protein CENP-C. Numerous other proteins termed CENP-H to T (Foltz et al., 2006) bind to the CENP-A nucleosome and form the *inner* kinetochore (blue and purple ovals in Figure 1.4), which exists as a discrete heterochromatin domain throughout the entire cell cycle (Cimini et al., 2006; Knowlton et al., 2006). The inner kinetochore makes contacts with complexes such as Mis12, Hec1 (described later), which in turn contact outer kinetochore proteins and ultimately to the kinetochore-microtubules. Electron microscopy pictures show a very low electron density region between inner and outer kinetochore plates, termed the *inter zone*. What the inter zone is made of is unclear, but it is implicated in tension sensing and checkpoint signalling. In this region a phospho-

antigen called 3F3/2 is situated, known to be dependent on Plk1 (Ahonen et al., 2005). The *outer* kinetochore is composed of proteins whose primary function is to link the inner kinetochore to the microtubule to mediate and regulate the attachment. Many other proteins, including those organised in multiprotein complexes that contain Hec1, Mis12, Mcm21 and KNL1 (Af15q14) proteins, are recruited to the outer kinetochore specifically in mitosis. They present a landing platform for the SAC proteins (Chan et al., 2005). The Hec1 complex, an assembly of four proteins with conserved relatives in yeast and animal cells, seems to be directly involved in microtubule binding (Cheeseman et al., 2006; DeLuca et al., 2006). The region of the kinetochore extending from the surface of the outer plate forms a *fibrous corona*, which is usually only visible in the absence of attached microtubules (Ris et al., 1981). This corona is composed of a dynamic meshwork of resident and transient components that are involved in the SAC and the regulation of the microtubule attachment. It contains most of the proteins known to interact with microtubules (i.e. CENP-E, dynein, TIPs) as well as checkpoint proteins (Bub1, BubR1, Bub3, Mad1, Mad2, Mps1, Zwint-1, ZW10, ROD) which monitor the integrity of kinetochore attachments. The microtubule-plus-end-binding proteins (+TIPs) are important for microtubule-kinetochore attachment (Tanaka et al., 2005). Several subunits of the nuclear pore complex (NPC) also localise to mitotic kinetochores, but their detailed function on the kinetochore remains uncertain. The APC/C is recruited to mitotic kinetochores in a SAC dependent manner (Acquaviva et al., 2004; Vigneron et al., 2004). The RZZ complex regulates the recruitment of Mad1 and Mad2 to the kinetochore (Karess, 2005). Large cytosolic pools of Mad2 and Cdc20 exist besides the proteins that are recruited to the fibrous corona. This is also the case for other SAC proteins, including BubR1 and Bub3, and for the APC/C itself. Mad2 adopts two conformational versions, O-Mad2 (open Mad2) and C-Mad2 (closed Mad2), which are depicted as red and yellow circles respectively in Fig. 1.4 (Sironi et al., 2002; De Antoni et al., 2005).

Also, in the centromere-kinetochore region Aurora-B, Borealin, Survivin, INCENP - together known as the chromosome passenger complex, 'CPC' (Ruchaud et al., 2007) - and MCAK are located, found to be predominantly involved in microtubule attachment error correction (Tanaka et al., 2002; Cimini et al., 2005).

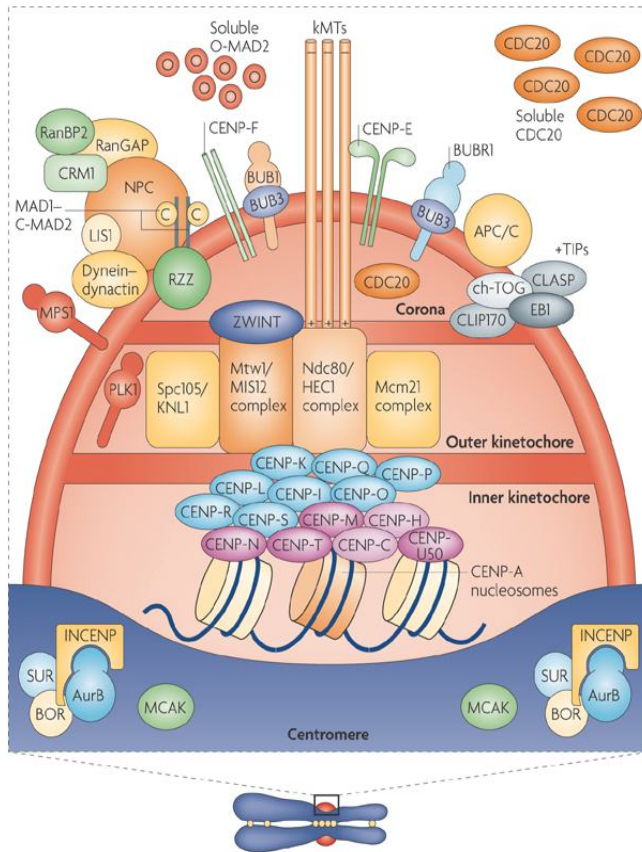


Figure 1.4. The centromere-kinetochore region – a model. Depicted is a model of organisation and location of components and complexes within the kinetochore. Most proteins indicating in this drawing are present at kinetochores in all metazoans. BOR, Borealin; BUB, budding uninhibited by benzimidazole; CENP, centromere protein; CLASP, CLIP-associating-1; CLIP170, cytoplasmic linker protein-170; EB1, end-binding protein-1; HEC, highly expressed in cancer, INCENP, inner centromere protein; kMTs, kinetochore microtubules; LIS1, lissencephaly-1; MAD, mitotic-arrested deficient; MCAK, mitotic centromere-associated kinesin; Mcm21, minichromosome maintenance protein-21; MPS1, multipolar spindle-1; PLK1, polo-like kinase-1; RanBP2, Ran-binding protein-2; RanGAP, Ran-GTPase-activating protein; ROD (rough deal)-ZW 10 (zeste white-10)-ZWILCH (RZZ); SUR, Surviving; +TIP, microtubule-plus-end-binding protein; ZWINT, ZW10 interactor. Figure from NATURE REVIEWS I MOLECULAR CELL BIOLOGY (Musacchio et al., 2007).

1.3. Specific kinetochore complexes

1.3.1. Features of the Hec1 complex

The Hec1 complex is a constituent of the outer kinetochore and plays an essential role in establishing stable kinetochore-microtubule interactions, which are required for chromosome segregation in mitosis. The Hec1 complex is evolutionarily conserved from yeast to human. It contains four protein subunits, known as Hec1 (whose yeast homologue is termed Ndc80) Nuf2, Spc24 and Spc25 (Chen et al., 1997; Janke et al., 2001; Wigge et al., 2001). These four subunits exist in a 1:1:1:1 stoichiometry and each contain a globular domain and an extensive coiled-coil region. Two tight Hec1/Nuf2 and Spc24/Spc25 sub-complexes, each stabilised by a parallel heterodimeric coiled-coil formation, maintain this organisation. These subcomplexes tetramerise via an interaction between the C- and N-terminal regions of the Hec1/Nuf2 and Spc24/Spc25 coiled-coils, respectively (Ciferri et al., 2005), depicted in Fig. 1.5.

The Hec1 complex localises at centrosomes during interphase (Hori et al., 2003), but it is unknown yet whether this localisation has a functional significance. From late G2 phase, the Hec1 complex relocates to the outer kinetochore, where it remains stably bound until late

anaphase (McClelland et al., 2004). Recent studies have shown that the Hec1 complex is directly involved in stabilising the kinetochore-microtubule interface and sustain tension in metaphase (Desai et al., 2003). It directly interacts, although at low affinity, with the microtubule lattice (Cheeseman et al., 2006; Kotwaliwale et al., 2006; Wei et al., 2007). At the kinetochore, Hec1 complex interacts with a subset of proteins and protein complexes, including the Mis12 complex, the Mcm21 complex, the KNL1 (Af15q14) protein, Zwint polypeptides, SAC proteins and motor proteins such as dynein-dynactin (De Wulf et al., 2003; Desai et al., 2003; Westermann et al., 2003; Cheeseman et al., 2004; Obuse et al., 2004; Cheeseman et al., 2006; Lin et al., 2006). All these proteins and complexes, with the exception of Zwint, are conserved in eukaryotes. The interaction of the Hec1 (Ndc80) complex, Mis12 complex and KNL1 (Af15q14) is especially important – those form a stoichiometric super complex, known as the KMN (KNL1, Mis12, Ndc80) network (Cheeseman et al., 2006; Dong et al., 2007). KNL1(Af15q14) also contains a microtubule-binding region, and the binding interaction with the Hec1 complex is crucial to generate a high-affinity microtubule-binding site (Cheeseman et al., 2006).

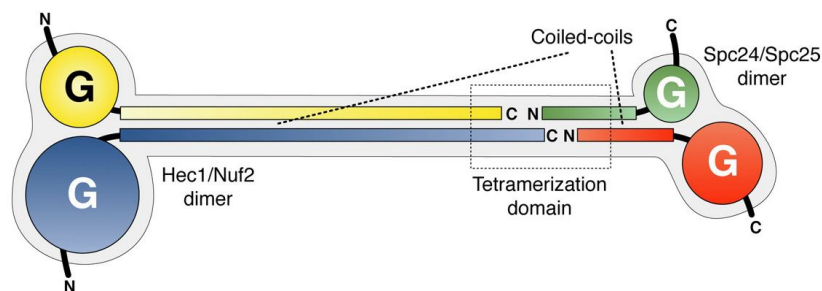


Figure 1.5. Features of the Hec1 complex. The elongated Hec1 complex contains globular regions at each end of a central shaft containing the coiled coils of the Hec1-Nuf2 and Spc24-Spc5 subcomplexes. The tetramerisation domain is proposed to involve the C termini of the Hec1-Nuf2 coiled coil and the N termini of the Spc24-Spc25 coiled coils. The bridge between subcomplexes might consist of overlapping C- and N-terminal segments of Hec1 and Spc24, respectively, as these may be unpaired to the Nuf2 and Spc25 chains, respectively. (Figure adapted from (Ciferri et al., 2005))

1.3.2. Features of the Mis12 complex

Mis12 is one of the core kinetochore-protein complexes that together with the KNL1 and the Hec1 complex form the KMN network, which has been shown in recent studies on yeast, worm and human (Cheeseman et al., 2004; Obuse et al., 2004; Liu et al., 2005) and is presumably situated in the outer kinetochore (Musacchio et al., 2007). The Mis12 complex has been identified to be crucial for kinetochore assembly, kinetochore fibre stability, chromosomal biorientation, segregation and it is thought to control the rate and extent of

formation of the attachment site (Goshima et al., 2003; Cheeseman et al., 2004). Subunits and the formation of the Mis12 complex is not known in detail yet. So far four subunits, with unknown function, conserved from yeast to human, have been identified to be in a complex with the Mis12-protein - Q9H410, DC8, PMF1 and AF15q14 (Obuse et al., 2004; Kline et al., 2006). The function of those proteins still remains unknown. Further interaction partners of the Mis12 complex have been found, e.g. proteins HP1-alpha, HP1-gamma and the kinetochore protein Zwint. Mis12 also forms a stable complex with the centromeric heterochromatin components HP1-alpha and HP-gamma. Centromeric HP1 has been suggested to be the base to anchor the Mis12 core complex, which then extends as far as Zwint in the outer kinetochore during mitosis (Obuse et al., 2004). One of the Mis12 associated proteins, AF15q14/KNL1, has recently been reported to functionally link the Mis12 complex to the spindle-checkpoint proteins Bub1 and BubR1, and has been given the name 'Blinkin' (Kiyomitsu et al., 2007).

1.3.3. Features of the RZZ complex

The proteins Rod, Zw10 and Zwilch forming the RZZ complex, are key players in the spindle assembly checkpoint regulation. The RZZ components were first identified in *Drosophila* (Smith et al., 1985; Karess et al., 1989) and orthologues were identified in worm, chicken, mouse and human (Smith et al., 1985; Starr et al., 1997; Chan et al., 2000; Okamura et al., 2001). However, no orthologues of these components have been found in yeast. The role and function of the RZZ complex is poorly understood yet, but it is known that RZZ is required for the recruitment of the dynein-dynactin complex to the kinetochore (Starr et al., 1998). Furthermore RZZ is also responsible for Mad1-Mad2 recruitment to unattached kinetochores and its subsequent shedding from kinetochores following microtubule attachment (Buffin et al., 2005; Kops et al., 2005). Therefore RZZ is involved in activation and inactivation of the checkpoint (Karess, 2005). Another protein functional associated with Zw10 is Zwint1, Zw10-interactor (Starr et al., 2000), which is part of a separate complex of structural kinetochore components including the Mis12 complex, the Hec1 complex and the protein KNL1 (KMN supercomplex). Zwint is critical for recruiting RZZ to unattached kinetochores, where it is also essential for the stable binding of the Mad1-Mad2 complex. Thus, RZZ functions as a linker between the core structural elements of the outer kinetochore and components that catalyse generation of the mitotic checkpoint-derived "stop anaphase" inhibitor (Kops et al., 2005).

The kinetochore is a very complex mini-organelle, consisting of many sub-complexes; not all of their constituents are fully identified yet. Many kinetochore proteins were initially found by genetic studies (Hoyt et al., 1991; Li et al., 1991; Winey et al., 1991; Takahashi et al., 1994; Desai et al., 2003). To obtain a complete description of the kinetochore proteomic studies are additionally required, ideally combining the purification of sub-complexes with using the analytical power of mass-spectrometry. The Kinetochore is very likely to be regulated by mechanisms including phosphorylation, consistent with this several kinetochore proteins were reported to be phosphorylated, including BubR1 (Elowe et al., 2007; King et al., 2007; Wong et al., 2007) and APC/C (Kraft et al., 2003) also several mitotic kinases (Cdc2, AuroraB, Plk1, Cdk1, Bub1, BubR1) are localised to the centromere-kinetochore region. To understand the mechanism of the phospho-regulation of the kinetochore is a very active and promising area of research and requires the latest high-tech proteomic approaches in combination with molecular cell biology.

1.4. Aims of the study

This study is part of the European Commission Sixth Framework Programme, Integrated Project 'MitoCheck' (www.mitocheck.org). This is a phospho-proteomic project to characterise protein complexes required for mitosis. In this thesis project, I am particularly interested in studying the kinetochore protein complexes Mis12, Hec1 and RZZ (Table 1.1). Most of these complexes were discovered in yeast or fly, recent studies in human cells showed that they are required for chromosome alignment, proper kinetochore-microtubule attachment, chromosome segregation and control of spindle checkpoint proteins. So far, very little is known about the regulation and the detailed functional mechanisms of these complexes and their constituent proteins. This project aims to purify kinetochore protein complexes, and to use mass spectrometry to identify protein interaction partners and map phosphorylation sites, enabling these complexes to be characterised in greater detail. My specific aims in this thesis project are:

- 1) To generate HeLa cell lines stably expressing myc-tagged kinetochore components.
- 2) To raise antibodies against selected kinetochore proteins in rabbits for immunoprecipitation (IP) and immunofluorescence (IF) experiments.
- 3) To purify, using tagged cell lines or antibodies, kinetochore complexes from HeLa cells.
- 4) To identify the components of the purified kinetochore complexes.
- 5) To identify phospho-sites on the purified kinetochore proteins and to characterise them in terms of mitotic specificity.

Table 1.1. Previously reported subunits of the three kinetochore complexes studied in this project.

Protein	Gene	Synonyms	size [kDa]	Uniprot #
Hec1 complex				
Hec1	NDC80	KNTC2, kinetochore associated 2, highly enhanced in cr, Ndc80 ^{SC}	74	O14777
Nuf2	NUF2	NUF2, CDCA1, Cell division cycle-associated protein 1, Q9BZD4	54	Q9BZD4
Spc24	SPBC24	Hypothetical protein FLJ90806	22	Q8NBT2
Spc25	SPBC25	2600017H08Rik, AD024, AD024, MGC22228	26	Q9HBM1
RZZ complex				
Rod	KNTC1	Kinetochore associated 1, FLJ36151	251	P50748
ZW10	ZW10	KNTC1AP, Kinetochore associated homolog	89	O43264
Zwilch	ZWILCH	FLJ10036, KNTC1AP, MGC111034, Zwilch	67	Q8N404
Zwint	ZWINT	ZWINT-1, ZW10 interacting protein-1, KNTC2AP*	31	O95229
Mis12 complex				
Mis12	MIS12	Q9H081, 2510025F08Rik, MGC2488, Mtw1 ^{SC} , KNTC2AP*	24	Q9H081
DC8	NSL1	DC8, DC31, DKFZP566O1646, Protein C1orf48, Mis14, Nsl1 ^{SC}	32	Q96IY1
PMF1	PMF1	Polyamine-modulated factor 1, Nnf ^{SC}	23	Q6P1K2
Q9H410	DSN1	C20orf172, Mis13, dJ469A13.2, FLJ13346, Dsn1 ^{SC}	40	Q9H410
AF15q14	CASC5	CASC5, D40, KIAA1570, KNL1, Blinkin, Spc105 ^{SC}	265	Q8NG31

Legend: Kinetochore protein complexes (gold) and complex partners (yellow); * gene name now defunct.

1.5. Experimental approach

To achieve the specific aims of this thesis I will take the experimental approach as depicted in Fig. 1.6. In order to immuno-purify the kinetochore protein complexes Mis12, Ndc80 and RZZ, two different strategies will be used: (1) generating HeLa cell lines stably expressing myc-tagged constructs encoding the desired proteins, and (2) raising antibodies in rabbits against selected kinetochore proteins. Antibodies that recognise the correct proteins in HeLa cell lysates, by western blotting (WB), will be affinity-purified on peptide-coupled columns and analysed in immunoprecipitation (IP) and immunofluorescence (IF) experiments.

The next step is to identify *in vivo* mitotic phosphorylation sites, which involves: (1) isolation of protein complexes, by IP from extracts of mitotic HeLa cells, using conditions in which phosphorylation should be maintained; (2) proteolytic in-solution digestion of purified complexes to yield peptides suitable for analysis by mass spectrometry (MS); (3) chromatographic separation, MS, MS² and MS³ data generation; (4) computational analysis and manual interpretation of spectra to identify phospho-sites. Finally the phospho-site data will be made available online, published by our MitoCheck colleagues at the Sanger Institute, on the mtcPTM database site <http://www.mitocheck.org/cgi-bin/mtcPTM/search> (Jimenez et al., 2007).

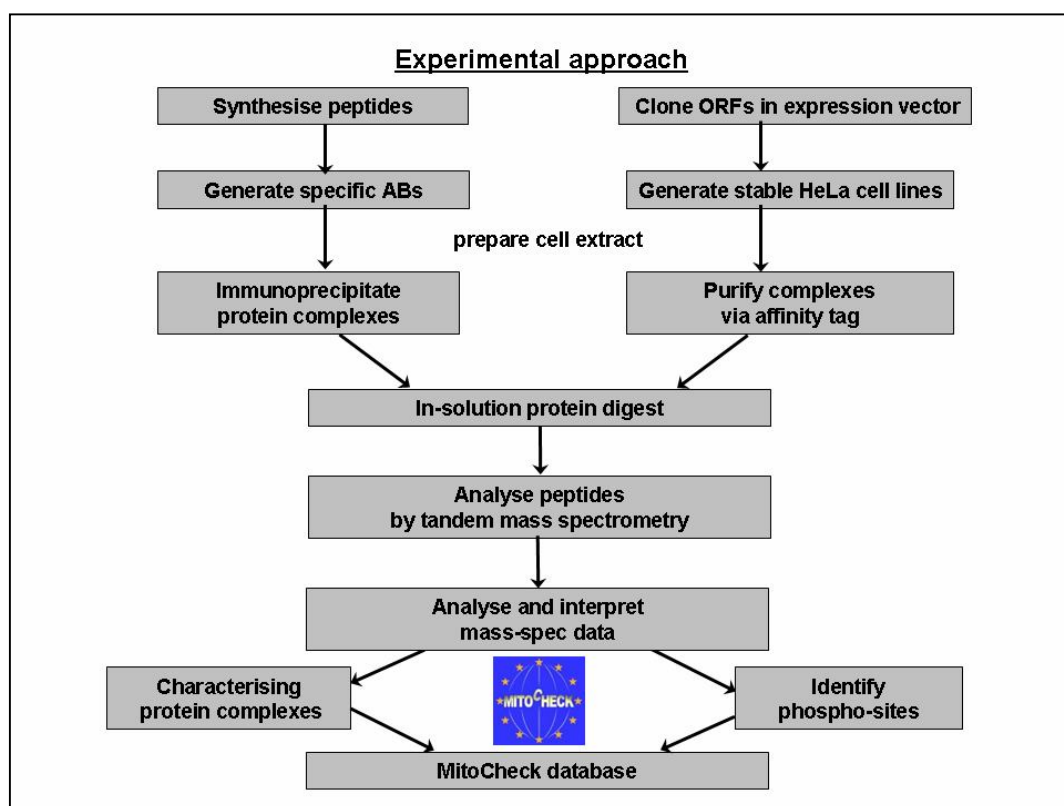


Figure 1.6. Scheme of the experimental approach for this project.

2. Results

2.1. Generation of cell lines stably expressing 9myc-tagged human kinetochore proteins

2.1.1. Generation of expression constructs

In order to express myc-tagged recombinant proteins in human cells, open reading frame (ORF) sequences of human kinetochore cDNAs (the Hec1 complex with bait proteins Hec1, Nuf2, Spc24 and Spc25; the RZZ complex with bait proteins Zwilch and ZW10; the Mis12 complex with baits DC8, Q9H410 and Mis12) were amplified by PCR (for details, see methods section) from their original vectors and cloned, in frame, into pcDNA3.1_9myc, a plasmid vector which allows expression in bacterial and mammalian cells. This vector, derived from the commercial pcDNA3.1/myc-His (V866-20, Invitrogen) adds 9 myc epitopes (Waizenegger et al., 2000; Hauf et al., 2001) to the N- or C-terminus of the protein, enabling detection of the tagged protein by anti-myc antibodies in immunofluorescence, western blotting and immunoprecipitation of the protein. The 9 myc gives an enhanced signal of the tagged proteins and this is particularly advantageous for the recognition of kinetochore proteins, which are generally of low abundance in the cell.

It is important that the affinity tag be added to a terminus of the protein that is unlikely to destabilise the complex. This is only possible for complexes where structural information is known. The recently proposed model of the Hec1 complex (Ciferri et al., 2005) suggests that the C-termini of Hec1 and Nuf2 interact with the N-termini of Spc24 and Spc25, leaving the N-termini of Hec1 and Nuf2 and the C-termini of Spc24 and Spc25 free for affinity tagging. In the case of the RZZ and Mis12 complexes, little is known about the stoichiometry and arrangement of their subunits, and the decision was made to 9myc-tag the kinetochore proteins DC8, Q9H410, Mis12, ZW10 and Zwilch on one terminus. Here, the C-terminus was chosen for tagging, so that only those proteins which were expressed as full-length peptides would contain the 9myc-tag and would be detected or affinity-purified.

Eight human kinetochore ORF sequences were amplified by PCR using primers containing flanking restriction sites. PCR products were digested with the appropriate restriction enzymes and ligated into the pcDNA3.1_9myc C or N target vector. This cloning procedure is summarised in Table 2.1. Correct orientation and sequence of the inserts and junctions were assessed by DNA sequencing. Sequencing of the two N-terminal tagged clones Hec1 and Nuf2 showed numerous insertions and deletions. After three unsuccessful attempts, I decided not to continue cloning Hec1 and Nuf2 and to focus on the six C-terminal tagged clones DC8, Q9H410, Mis12, Spc24, Spc25 and Zwilch, for which sequencing showed that the cloning had been successful.

Table 2.1. Summary of cloning procedure for human kinetochore ORFs into pcDNA3.1_9myc construct.

Insert (ORF size)	Donor vector	Resistance	Acceptor vector	5'	3'	Resistance
DC8 (846 bp)	pBluescriptR	Amp	pcDNA3.1 9mycC	<i>Xho</i> I	<i>Nhe</i> I	Amp
Q9H410 (1071 bp)	pcMV-Sport6	Amp	pcDNA3.1 9mycC	<i>Xho</i> I	<i>Nhe</i> I	Amp
Mis12 (618 bp)	pOTB7	Cam	pcDNA3.1 9mycC	<i>Xho</i> I	<i>Nhe</i> I	Amp
Spc24 (594 bp)	pET28(+)	Kan	pcDNA3.1 9mycC	<i>Xho</i> I	<i>Nhe</i> I	Amp
Spc25 (675 bp)	pET28(+)	Kan	pcDNA3.1 9mycC	<i>Xho</i> I	<i>Nhe</i> I	Amp
Hec1 (1929 bp)	pcMV-Sport6	Amp	pcDNA3.1 9mycN	<i>Kpn</i> I	<i>Hind</i> III	Amp
Nuf2 (1395 bp)	pDNR-LIB	Cam	pcDNA3.1 9mycN	<i>Kpn</i> I	<i>Kpn</i> I	Amp
Zwilch (1434 bp)	pWS4stopEGFP	Amp	pcDNA3.1 9mycC	<i>Nhe</i> I	<i>Not</i> I	Amp

2.1.2. Test expression of myc-tagged proteins by IVT

Before starting to generate stable cell lines (constitutively-expressing the myc tagged recombinant kinetochore proteins). Small-scale expression experiments were performed using the 'IVT' (in vitro transcription / translation) system. The reasons for this were: (1) to test whether proteins of the correct size can be expressed in a eukaryotic system from these constructs, and (2) to generate recombinant proteins to test the specificities of new kinetochore antibodies.

The IVT system ('TnT', Promega) allows radioactively-labelled proteins to be generated via integration of ³⁵S-methionine. Those radioactive labelled proteins were visualised on a Phosphorimager (PI) and by western blotting (WB) with anti-myc (9E10) antibody.

Six kinetochore proteins, 9myc tagged on their C-termini, and myc-tagged Cyclin B, used as a positive control, were successfully expressed in the IVT system. The pattern of the resulting bands is similar in both, PI and WB (Fig. 2.1). Due to the 9myc-tag, proteins have an additional molecular weight of roughly 14 kDa. Nevertheless, for all IVT recombinant kinetochore proteins the major band was observed to migrate at approximately 10 kDa higher than the expected size of the bait protein plus the tag. Furthermore, additional bands below the major signal were observed, which might arise from internal start codons or might be due to proteolysis of the expressed proteins.

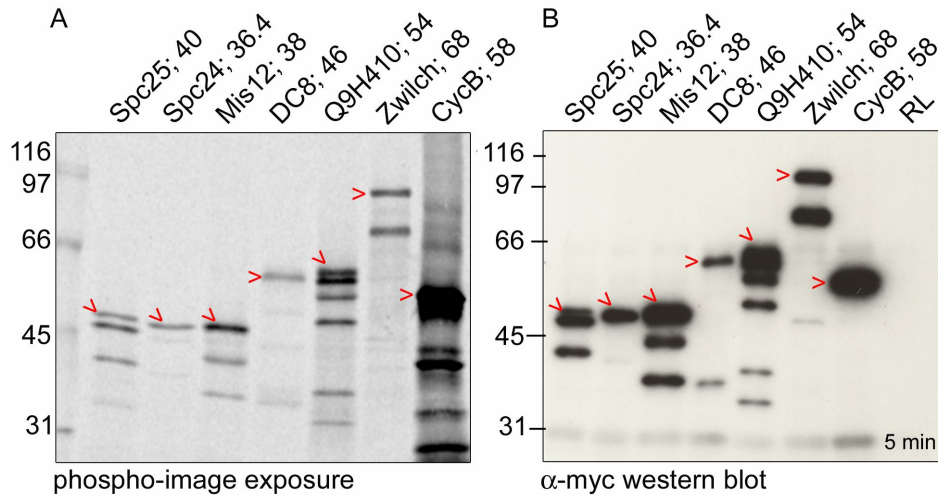


Figure 2.1. Test expression of myc-tagged recombinant kinetochore proteins. 2 μ l of each IVT reaction, i.e. reticulocyte lysate (RL) incubated with myc-tagged kinetochore construct and 35 S-methionine, were separated by SDS-PAGE (8-12% gradient gel). Cyclin-B-myc was used as a positive control. Signals were visualised by either using **(A)** phospho-imaging (35 S) or **(B)** anti-myc western blotting (9E10; 1:5000), RL-only was used as a negative control. The arrows indicate the presumed full-length expressed proteins. Numbers after the protein names indicate the size of the recombinant proteins, including the 9myc tag. Protein marker bands are marked in kDa.

2.1.3. Creating and testing stably expressing HeLa cells

To be able to identify interaction partners and phospho-sites, I wanted to stably and constitutively express the myc-tagged kinetochore proteins in HeLa cells and to purify these proteins and their bound complex partners by myc-immunoprecipitation (IP). Mammalian expression constructs for Mis12, Q9H410, DC8, Spc24, Spc25, Zwilch kinetochore proteins had been generated and were tested positive for expression in the IVT system.

In order to create stable cell lines, these constructs (except DC8) were used to transfect adherent HeLa cells. After three weeks of Geneticin (G418) selection, exponentially grown cells (log) were obtained and analysed by immunofluorescence (IF) and western blot (WB), to test the localisation and expression levels of the 9myc-tagged proteins. Small-scale anti-myc immunoprecipitations were performed to test the ability of the proteins to be purified for mass-spectrometry analysis.

2.1.3.1. Immunofluorescence microscopy

For each cell pool IF experiments were performed in two ways: firstly, cells were grown on coverslips before being fixed and stained; and secondly, cells were spun onto slides (cytospins) to provide a clearer image of protein localisation at mitotic kinetochores. Cells grown on coverslips were fixed with PFA without any pre-extraction, then stained for the 9myc-tagged construct (red) and for DNA (blue), as described in Fig. 2.2. For the cytospins pre-extraction was performed to remove cytoplasmic proteins, before fixation with paraformaldehyde (PFA) and staining for DNA (blue), 9myc-tagged constructs (red) and centromeres (green). IF microscopy showed that typically only 3-10% of cells within an antibiotic-resistant pool displayed a visible signal of expressed 9myc-tagged protein, allowing fluorescence micrographs to be taken and the localisation patterns of these proteins to be described. These images (Fig. 2.2) show the localisation of myc-tagged protein in interphase cells grown on coverslips (left panel), and in mitotic cells as cytospins (right panels).

In mitotic cells (displaying condensed chromosomes) which were positive for the myc signal, all myc-tagged proteins were observed to localise to the kinetochores (consistent with their physiological roles), as indicated by a pair of myc signals distal to the centromeric marker CREST (Fig. 2.2). Spc25 localisation is indicated by the arrow heads in the enlarged image. Zwilch protein was additionally associated with the mitotic spindle (Fig. 2.2) as indicated by the arrow heads, in the merged image.

In myc-positive interphase cells, proteins Q9H410 and Mis12, both constituents of the Mis12-complex, were found predominantly in the nucleus, whereas Spc24 and Spc25 showed an almost exclusively cytoplasmic localisation. Zwilch was found to be equally distributed between the cytoplasm and the nucleus, in interphase. In the case of Spc24 a high proportion of the myc-positive cells were observed to be multinucleated, suggesting that the level of this protein is critical for correct chromosome segregation.

A large fraction of cells highly expressing 9myc-tagged Spc24, Spc25 or Zwilch displayed apoptotic morphology. This is a possible explanation for the rather low number of myc-positive cells in these pools (approximately 3%). To summarise, these IF experiments showed that all five stable cell pools expressed their tagged kinetochore proteins, albeit at variable levels, and that they localised to the kinetochores in mitosis.

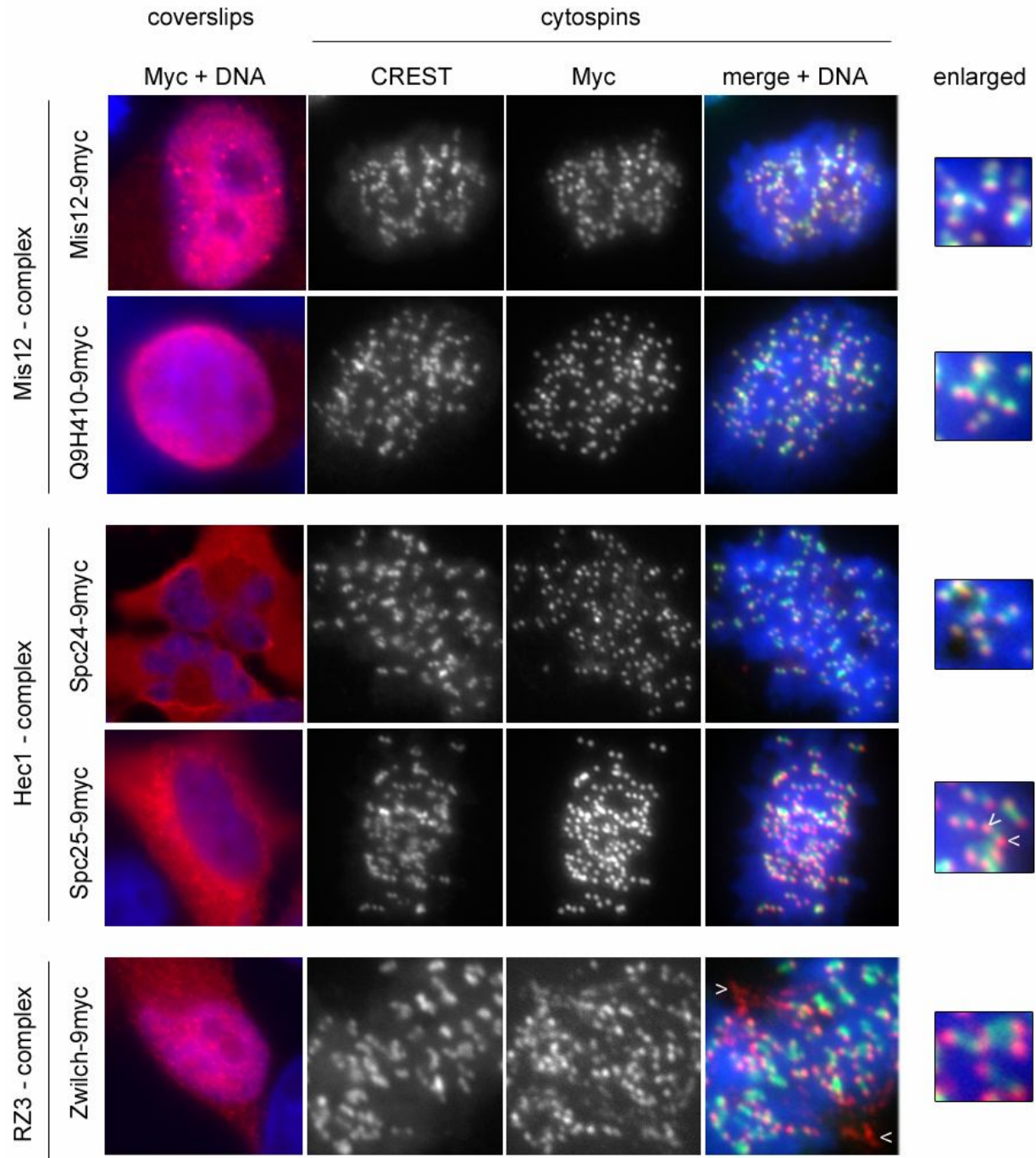


Figure 2.2. IF images of HeLa cells stably expressing myc-tagged kinetochore proteins. HeLa cells stably expressing Mis12-9myc, Q9H419-9myc, Spc24-9myc, Spc25-9myc or Zwilch-9myc were exponentially grown on coverslips or were spun onto slides by performing cytospins. Pre-extraction was performed for cytospins only. Primary antibodies mouse-anti-myc (9E10, red) and human-CREST antiserum (green), which stains centromeric domains, were each used at a 1:1000 dilution and incubated for 1 h. As secondary antibodies, goat anti-mouse Alexa 568 (red) or goat anti-human Alexa 488 (green) were used at a 1:500 dilution. DNA was stained with 1 µg/ml Hoechst 33342 (blue). Images show myc-tagged proteins in red, CREST in green and DNA in blue.

2.1.4.2. Western blot and immunoprecipitation

As shown in the IF microscopy above, the myc-tagged kinetochore proteins stably expressed in HeLa cell pools were localised appropriately to the kinetochores. Next, I wanted to determine whether these myc-tagged proteins could be detected in a western blot, and if they could be immunoprecipitated using an anti-myc antibody.

For WB, exponentially grown HeLa cell pools, stably expressing Mis12-9myc, Q9H410-9myc, Zwilch-9myc, Spc24-9myc and Spc25-9myc, were lysed, the soluble fractions (S14) were separated on an SDS-PAGE gel and western blotted against anti-myc (9E10). As a negative control, a cell pool transfected with the pcDNA3.1 9myc C-terminal construct, with no insert, was also analysed. As depicted in Fig. 2.3.A each cell pool showed a myc-signal at the size where the tagged protein was expected, consistent with the IVT test-expression pattern shown in Fig. 2.1. This shows that a myc-tagged protein of the correct size is expressed for each cell pool.

Next we wanted to test whether the myc-tagged kinetochore proteins from these cell pools can be affinity purified by anti-myc IP. For this experiment, a mouse monoclonal anti-myc (9E10) antibody, covalently crosslinked to G-protein beads was used. Due to the low expression of the desired kinetochore proteins, it was decided to load 2.5 times more protein onto the beads, than under standard conditions, i.e. 10 mg protein onto 20 µl beads. Apart from that, the IP was performed under standard conditions and proteins were eluted from the cross-linked beads using glycine. In all cases, except for Zwilch, the anti-myc IP was successful, as indicated by the presence of a band in the eluate lane, shown in Fig. 2.3.B. The intensity of the bands in the eluate lanes varies considerably between the different cell-pools, reflecting in part the amount of tagged protein loaded onto the IP (as shown in the S14 lane).

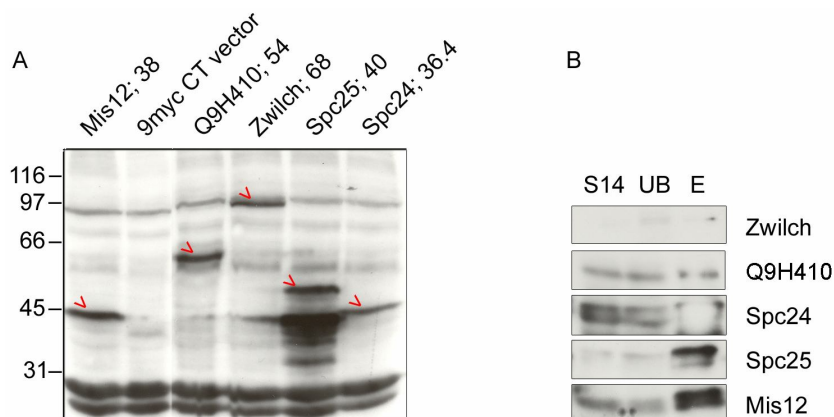


Figure 2.3. Western blot and Myc-IP of stable expressing HeLa cell pools. Generated HeLa log cell pools were lysed, spun at 14000 g and the supernatant (S14) was used to perform either WB (A) or a Myc-IP (B). **(A)** For WB 50 µg protein (S14) of each cell pools Mis12-9myc, Q9H410-9myc, Zwilch-9myc, Spc24-9myc, Spc25-9myc and C-terminal 9myc tagged pcDNA3.1 vector (negative control) were separated on an 8-12% gradient SDS-PAGE gel and western blotted with anti-myc (9E10; 1:1000). **(B)** For Myc-IP 10 mg of protein (S14) were loaded each to 20 µl protein-G beads, covalently cross linked with myc-antibody (mouse, 9E10). Purified proteins were eluted twice with 20 µl 0.1 M glycine. For analysis, 100 µg of S14, 100 µg of unbound protein (UB) and 20 µl of the eluates (E), which is a fraction of 2/3 of the starting material, were separated on a 10% SDS-PAGE and proteins were detected by western blot with anti-myc (9E10; 1:1000). The eluate lane of the Spc24 shows a bleached spot which is sometimes produced from a very intense ECL signal.

2.1.5. Result summary of the first strategy

To summarise the results of the first strategy (Table 2.2), six out of the eight kinetochore proteins that were initially proposed to be 9myc-tagged were cloned successfully into an expression vector and were observed to be positive in expressing the appropriate 9myc-tagged kinetochore protein in IVT. The constructs for Q9H410, Mis12, Spc24, Spc25 and Zwilch were used to generate stable, constitutively-expressing cell pools. For DC8, cloning difficulties delayed production of a tagged construct, and therefore a cell transformation with this construct was not performed. In all five generated cell pools, 9myc-tagged kinetochore proteins were observed to express the proteins, to localise as expected from the literature to the kinetochores in mitosis, and furthermore could be immunoprecipitated by anti-myc antibody, as shown in the IF and WB experiments above.

Table 2.2. Summary of results achieved by the first experimental strategy.

Protein Incl. 9myc tag	Cloned into expression vector pcDNA3.1_9myc	IVT	α -myc WB	stably expressing cell pools generated	IF localisation on kinetochores	α -myc-IP pull-down
<i>Mis12 complex</i>						
DC8	Yes, C-terminus	Yes	-	-	-	-
Q9H410	Yes, C-terminus	Yes	Yes	Yes	Yes	Yes
Mis12	Yes, C-terminus	Yes	Yes	Yes	Yes	Yes
<i>Hec1 complex</i>						
Spc24	Yes, C-terminus	Yes	Yes	Yes	Yes	Yes
Spc25	Yes, C-terminus	Yes	Yes	Yes	Yes	Yes
Hec1	No, N-terminus	-	-	-	-	-
Nuf2	No, N-terminus	-	-	-	-	-
<i>RZZ complex</i>						
Zwilch	Yes, C-terminus	Yes	Yes	Yes	Yes	No

Legend: Yes, successfully done; No, unsuccessfully done; “-“, not done

Despite the apparent success in generating stable cell pools, these cells showed very poor viability, often accompanied by gross cell morphology defects, such as a multinucleate phenotype. One solution to this situation could be to isolate and test multiple cell clones from each pool; however, as this requires about two months of additional work, due to time constraints it was decided to pursue the alternative second strategy of immunoprecipitating kinetochore proteins using custom-made specific antibodies.

2.2. Generation and characterisation of kinetochore antibodies

To enable the immunoprecipitation of human kinetochore proteins for phospho-mass-spectrometry analysis, a second experimental approach was to raise polyclonal antibodies against these proteins in rabbits. It was decided to generate antibodies against six human kinetochore proteins: Spc24, Spc25, DC8, Q9H410, ZW10 and Zwilch.

2.2.1 Preparation of peptides and proteins for immunisation

Where possible, it is preferable to raise antibodies against full-length proteins, as this provides the maximum number of epitopes for antibody generation. In the case of Spc24 and Spc25, plasmid vectors containing the cDNAs for these proteins were available (courtesy of Dr. P.T. Stukenberg), allowing the bacterial expression of full-length proteins with a C-terminal His₆ tag. These proteins were over-expressed in *E.coli* BL21 (DE3) cells and purified via their His₆ tags by Ni-NTA chromatography under denaturing conditions, as shown in Fig. 2.4. The yields of purified Spc24-His₆ and Spc25-His₆ were 10.0 mg and 8.8 mg, respectively. 1.6 mg of the first elution (E1) of each protein was dialysed against 3 M urea, TCA precipitated and used for rabbit immunisation.

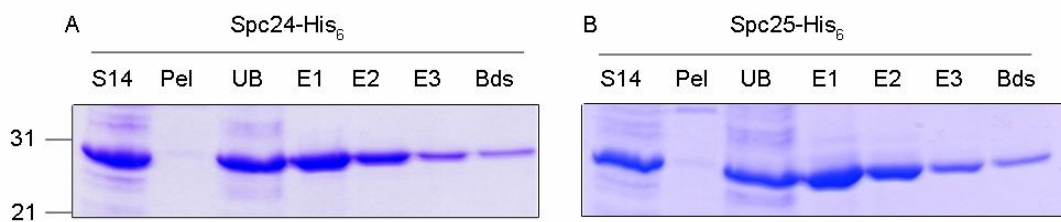


Figure 2.4. Coomassie-stained SDS-PAGE showing the purification of (A) Spc24-His₆ and (B) Spc25-His₆, indicated by the intense bands. 25 ml bacterial cell lysate were spun at 14000g, the supernatant (S14) was used for binding to the Ni-NTA beads, 5 µl of S14 were kept for analysis on SDS-PAGE. The pellet (Pel) was resuspended in 25 ml lysis buffer and 5 µl loaded onto the gel. After binding to beads, 5 µl of the supernatant (unbound = UB) were kept for analysis. Purified proteins were eluted in three steps, each with 1 ml elution buffer, containing 300 mM imidazole and 8M urea. For the eluates E1-E3, 5 µl (1/5000 of the starting material) were analysed.

For the kinetochore proteins ZW10, Zwilch, DC8 and Q9H410, no expression plasmids were available, and therefore synthetic peptides were generated in order to raise antibodies against these proteins. Computational sequence analysis for each of these proteins predicted a C-terminal region, of around 20 amino acid residues, to be highly antigenic (Table 2.3). A cysteine residue was added to the C-terminus of each antigenic sequence, to enable the corresponding peptides to be coupled to keyhole limpet hemocyanin (KLH). These peptides were synthesised, and 1 mg of each was conjugated to KLH and used for rabbit immunisation.

Table 2.3. Polyclonal antibodies generated against human kinetochore proteins.

Complex	Protein	Antibody	Rabbit no. (peptide)	Immunogenic region
RZZ	ZW10	Ab1619	854 (kpep 1619)	601-621, C-LERLSSARNFSNMDDEENYS
RZZ	Zwilch	Ab1620	844 (kpep 1620)	515-537, C-RPTAVKNLYQSEKPKWRVEIY
Mis12	DC8	Ab1621	842 (kpep 1621)	265-282, C-PQRKWYPLRPKKINLDT
Mis12	Q9H410	Ab1622	838 (kpep 1622)	317-337, C-VQLGKRSMQQLDPSPARKLL
Hec1	Spc24	Ab 889	889	Full length protein plus C-term. His ₆ tag
Hec1	Spc25	Ab 887	887	Full length protein plus C-term. His ₆ tag

2.2.2. Characterisation of kinetochore anti-sera by western blot

The affinity and specificity of the antibodies raised against full-length kinetochore proteins or peptides (Table 2.3) were characterised by: (1) their recognition of endogenous proteins in HeLa-cell extracts by western blotting; (2) the loss of the western-blot signal in extracts of HeLa cells subjected to RNAi against these proteins; (3) their ability to immunoprecipitate their target proteins, and complex partners, as detected by western blotting and mass spectrometry analysis. These criteria enable us to judge whether the antibodies are suitable for use in phospho-site mapping experiments.

Rabbit immune sera raised against DC8, Q9H410, Zw10 and Zwilch peptides were affinity purified on an immobilised antigenic peptide column, and antibodies were eluted first using MgCl₂, then with glycine. Eluates were dialysed and concentrated to about 1 mg/ml as described in section 4.3.2.1. The purified antibodies, as well as their corresponding pre-immune (PI) and immune sera (IS) were tested for their ability to specifically recognise their endogenous target proteins in HeLa log cell extracts by western blotting. As shown in Fig. 2.6 the immune sera against ZW10, Zwilch, DC8 and Q9H410 detected a major band at the predicted size for the endogenous protein in HeLa cell extracts (89 kDa, 54 kDa, 32 kDa and 40 kDa, respectively), which was not recognised by the pre-immune sera. For DC8 the glycine-eluted antibody (1621-G#1) and for Q9H410 the MgCl₂-eluted antibody (1622-M#1) gave the most specific signal, while background signals (seen with the immune serum) were abolished. Purified antibodies against ZW10 (Ab1619) and Zwilch (Ab1620) failed to recognise the bands of interest, therefore for further western blot experiments using these antibodies, the immune sera instead of the purified antibodies were used.

Antisera raised against full-length Spc24-His₆ and Spc25-His₆ proteins were then passed through a His₆-peptide coupled column to deplete His₆-binding antibodies. Immunoglobulins recognising Spc24 and Spc25 were affinity purified on a column of recombinant protein covalently coupled to Sepharose beads (described in section 4.3.2.2). MgCl₂- and glycine-eluted antibodies were dialysed and then concentrated to about 1 mg/ml. Testing the

antibody eluates by WB (Fig. 2.7) showed immune sera Ab889-IS#1 and purified antibodies (Ab889-M#1 and Ab889-G#1) detected both, endogenous Spc24 (23 kDa) and recombinant Spc24-His₆. Also, the Spc25 antisera and purified antibody (Ab887) recognised bands at the size of its target protein, Spc25 (26 kDa) in the log cell extract and recombinant protein lanes.

For Spc25, the background signal in the HeLa log extract was high with the IS (Ab887-IS#1), and this was greatly reduced following purification. In contrast, for Spc24 the background was not very strong with the IS (Ab889-IS#1), and this did not change significantly after purification. For both Spc24 and Spc25, purified antibodies were obtained that showed a signal for the endogenous proteins in HeLa log extract (Spc24: Ab889-M#1 and -G#1; Spc25: Ab887-G#1).

When comparing recognition of recombinant proteins, Spc24 and Spc25 antibodies show reciprocal cross-reactions, to different extents: faint bands are detected in the Spc25-His₆ lanes when probed with the Spc24 antibodies, whereas strong bands are detected by the Spc25 antibodies in the Spc24-His₆ lanes. These cross-reactions might be due to recognition of the His₆-tag, which both recombinant proteins have in common. By contrast, the native sequences of Spc24 and Spc25 show very little sequence identity (Fig. 2.5), and are therefore unlikely to share identical epitopes.

CLUSTAL W (1.83) multiple sequence alignment

```

Spc24      --MAAFRDIEEVSQGLSLLGANRAEAQRRLLGRHEQVVERLLETQDGAEKQLREILTM 58
Spc25      MVEDELALFDKSINEFWNFKSTDTSCQMAGLRDTYKDSIKAFAEKLSVKLKEEERMVEM 60
           :  :::  :  :  .  :  :  :  :  *  *  .  :::  :  :  *  .  .  *:  .::  *

Spc24      EKEVAQSLNNAKEQVHGGGVELQQLEAGLQEAGEEDTRLKASLLQLTRELEELKEIEADL 118
Spc25      FLEYQNQISRQNKLIQEKKNLLKLIAEVKGKKQELEVLTANIQDLKEEYSRKKETISTA 120
           *  :.  .  :  :  :  :  :  *  *  *  :  :  *  *.  .:  :  *.  .  **  :

Spc24      ERQEKE-----VDEDTTVTIPSAVYVAQLYHQVSKIEWDYCEPGMVKGIIHGGPS 168
Spc25      NKANAERLRLQKSADLYKDRGLGLEIRKIYGEKLQFIFTNIDPKNPESPFMFS-LHLNEA 179
           ::  :  *          :  :  *          :  *  :  *  .  :  :  :  .  .  *  *.  :  *  .  :

Spc24      VAQPIHLDSTQLS-----RKFISDYLSLVDTEW- 197
Spc25      RDYEVSDSAPHLEGLAEFQENVRKTNNFSAFLANVRKAFTATVYN 224
           :  .::  *.          *:::  :  .  *  :

```

Figure 2.5. Clustal W alignment of human Spc24 (UniProt AC: Q8NBT2) and Spc25 (UniProt AC: Q9HBM1) sequences shows no significant similarity.

For the most promising antibodies anti-DC8 (Ab1621), anti-Q9H419 (Ab1622), anti-Spc24 (Ab889) and anti-Spc25 (Ab887), different bleeds (immune sera) were tested by western blotting. As shown in Fig. 2.8, bleeds 1 to 5 (part A), or 4 (B) detected a band in the size of their target protein in HeLa cell log extract. For DC8 and Q9H410 WB was additionally performed with purified antibodies, showing that anti-DC8 (Ab1621-G#1) and anti-Q9H410 (Ab1622-M#1) recognised the presumed band for their respective proteins DC8 (32 kDa) and Q9H410 (40 kDa).

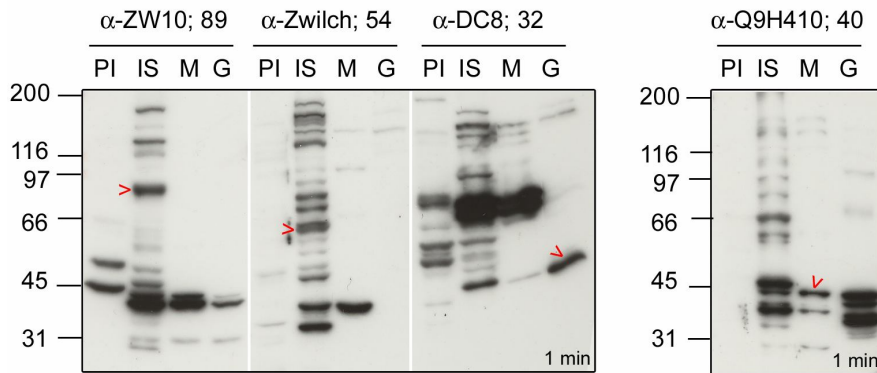


Figure 2.6. Characterisation of antisera and purified antibodies raised against kinetochore protein derived peptides. Antisera against four kinetochore proteins Zw10, Zwilch, DC8 and Q9H410 were analysed by western blotting. HeLa log cell lysate (50 µg per lane) was separated by SDS-PAGE (8-12% gradient) and transferred onto a PVDF membrane. For western blotting each membrane was cut vertically to separate the lanes into strips, which were then probed with pre-immune (PI) or immune sera (IS), each at 1:1000 dilution, or MgCl₂ (M) or Glycine (G) antibody eluates, each at a concentration of 2 µg/ml. The arrows are presumed to be the endogenous kinetochore proteins recognised by the antibodies. Numbers after the protein name indicate the size [kDa] of the recombinant proteins.

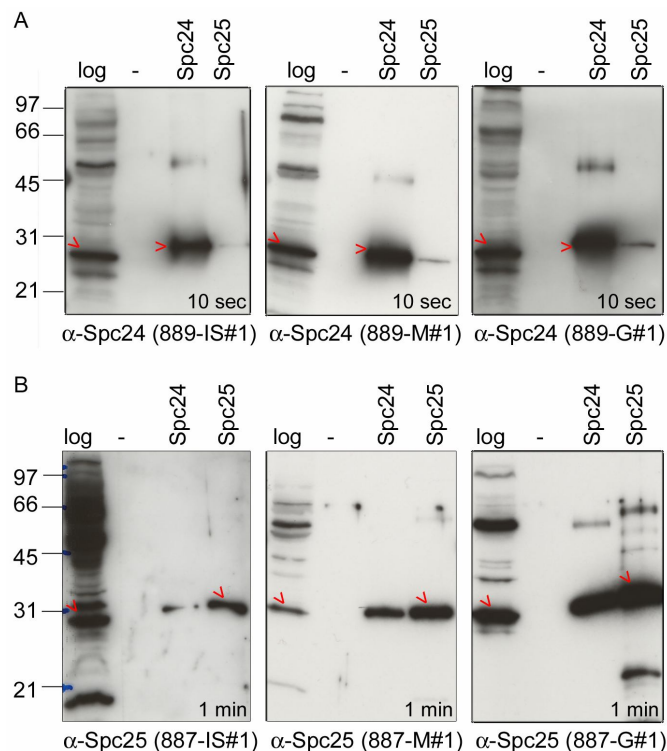


Figure 2.7. Characterisation of antisera and purified antibodies raised against full length kinetochore proteins Spc24 (A) and Spc25 (B). Antisera against two kinetochore proteins Spc24-His₆ and Spc25-His₆ were analysed by western blotting. HeLa log cell lysate (50 µg per lane) and 100 ng of the recombinant Spc24-His₆ and Spc25-His₆ were separated each by SDS-PAGE (8-12% gradient) and transferred onto a PVDF membrane. For western blotting each membrane was probed separately with immune sera (IS), at dilution 1:1000, or MgCl₂ (M) or Glycine (G) antibody eluates, each at a concentration of 2 µg/ml. The arrows are presumed to be the endogenous or recombinant kinetochore proteins recognised by the antibodies.

2.2.3. Testing the specificity of the kinetochore antibodies by western blot

To further examine if the antibodies specifically detect the correct proteins, RNAi was used to knock down endogenous protein levels. HeLa cells were transfected with siRNA oligonucleotides (oligos) and cell extracts were analysed by western blotting with the kinetochore antibodies to examine whether the signal intensities of the correlating bands were abolished or reduced. RNAi transfection was performed (as described in section 4.6.2) with two different siRNA oligos for each of the six kinetochore proteins of interest. The antibody signal over time was clearly reduced for the DC8 protein using siRNA “52” (Fig. 2.8.C, upper panel), this indicates the antibody recognises the correct protein. As shown in Fig. 2.8.C (lower panel) the antibody signal for Q9H410 was not reduced by RNAi treatment. For Spc24, Spc25, ZW10 and Zwilch there was also no obvious reduction in antibody signal after RNAi treatment (data not shown).

Assuming the antibodies do recognise the correct proteins, the absence of silencing could mean that either the RNAi transfection was not efficient or the oligonucleotides were not effective in directing the RNAi machinery to destroy the corresponding mRNAs, thus silencing the protein. To further validate the specificity of the antibodies, which could not be confirmed with RNAi experiments, it was decided to test whether these antibodies are able to detect the IVT signals of the appropriate proteins. The antibodies anti-DC8 (Ab1621-G#1) and anti-Spc24 (Ab889-IS#1) clearly detected the correct band in the appropriate IVTs of DC8 (Fig. 2.8.E) and Spc24 (Fig. 2.8.D upper panel), whereas α -Spc25 (Ab887-IS#1) did not clearly recognise the IVT of Spc25-His₆ (Fig. 2.8.D, lower panel), but it did recognise the recombinant Spc25-His₆.

The antibody against Q9H410 (Ab1622-M#1) did not give a clear signal in IVT either (data not shown). Zwilch and ZW10 antibodies did not recognise their correct target proteins, neither in IVT nor in RNAi experiments (data not shown). Therefore, it was decided not to use these antibodies further for purifying the kinetochore proteins of the RZZ complex, but instead to focus on the remaining four better validated antibodies, against DC8, Q9H410, Spc24 and Spc25.

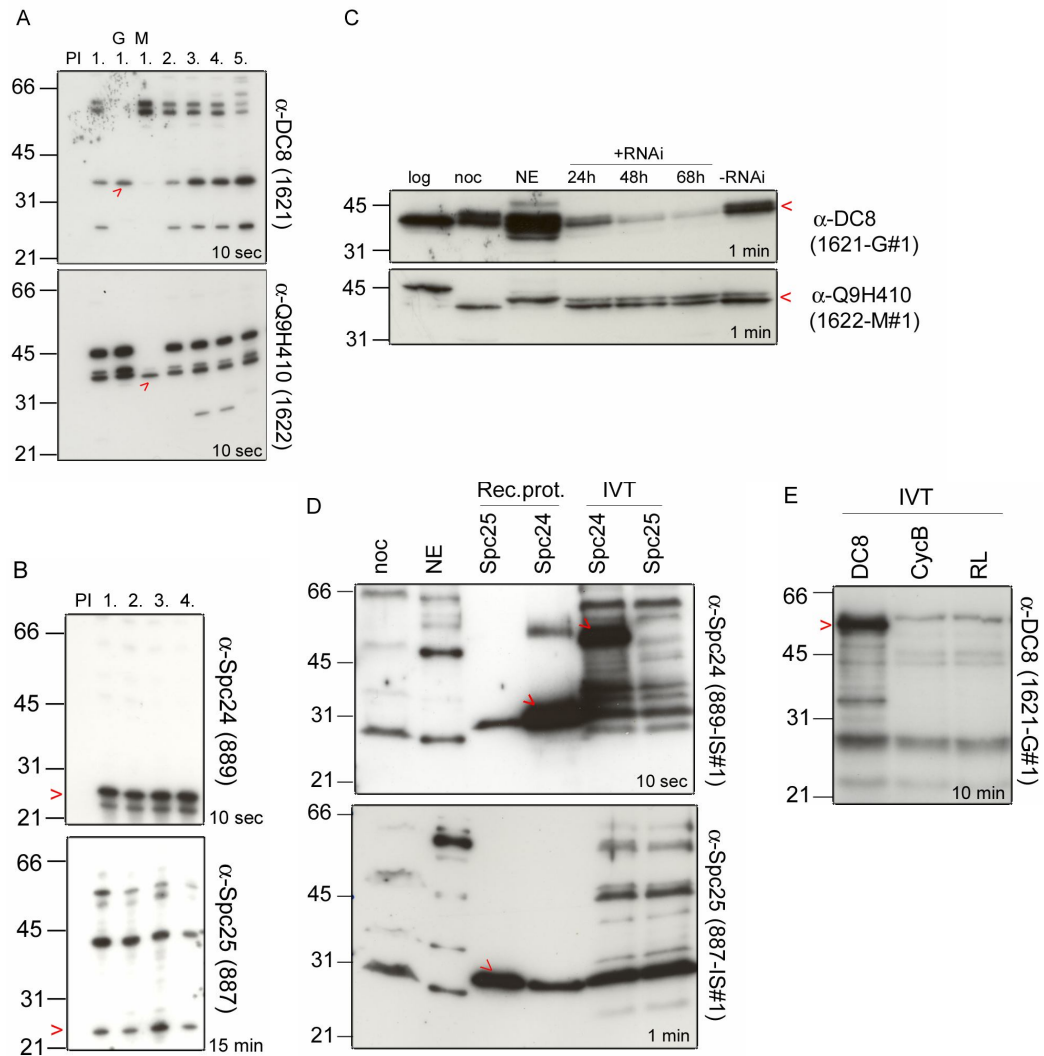


Figure 2.8. Testing the specificity of immune sera and purified antibodies (A, B) 50 μ g of HeLa log cell lysate were loaded onto each lane and separated by SDS-PAGE, transferred onto a PVDF membrane, then each lane was probed with a different immune serum (numbers shown refer to bleeds), PI or purified antibody. Recognition of endogenous proteins **(A)** DC8 (by Ab1621) and Q9H410 (by Ab1622), and **(B)** Spc24 (by Ab889) and Spc25 (by Ab887), as indicated by the arrows. **(C)** 50 μ g of HeLa nuclear (NE), noc, log and siRNA transfected (24, 48 and 68 hours) log cell extracts were each separated on an 8-12% SDS-PAGE gel and analysed by western blotting, either against anti-DC8 (Ab1621-G#1) or anti-Q9H410 (Ab1622-M#1). **(D)** Recognition of Spc24 and Spc25 proteins in HeLa noc extract (50 μ g), HeLa nuclear extract (NE, 50 μ g), of recombinant Spc24 and Spc25 proteins (100 ng each) and 2 μ l each of RL from an IVT reaction, as indicated by the red arrow. **(E)** Recognition of 9myc-tagged DC8 protein from an IVT reaction (2 μ l of RL loaded) by DC8 antibody Ab1621-G#1.

2.2.4. Testing the kinetochore antibodies for immunoprecipitation

Kinetochore antibodies, which had been purified and either MgCl_2 - or glycine-eluted, were tested for their ability to immunoprecipitate (IP). Specifically, the following questions were asked for each antibody:

- 1) Can the antibody immunoprecipitate its target protein so that it can be detected on a western blot?
- 2) Is the ability of the antibody to IP the target protein preserved when the antibody is covalently crosslinked to beads?
- 3) Can the crosslinked antibody co-IP proteins known to be in a complex with the target (as detected by western blotting)?
- 4) Can the immunoprecipitated protein complex be visualised on a silver-stained gel?
- 5) Following in-solution digestion of the immunoprecipitated complex, can the target protein be identified by LC-MS/MS?
- 6) Can LC-MS/MS identify proteins known to be complex partners of the immunoprecipitated target protein?

To address these questions, IP experiments were set up using antibodies bound to protein A beads, either without crosslinking (- x-link) or with crosslinking between the immobilised antibodies and the beads (+ x-link), using the crosslinking reagent dimethylpimelimidate (DMP). These antibody-bound beads were then used to immunoprecipitate proteins from HeLa log cell extracts. The crosslinking of antibodies to the beads prevents the bound antibody from being co-eluted from the beads together with the complex of interest and interfering with the identification of the proteins of interest by mass spectrometry. The IPs were performed under standard conditions (section 4.5.1) then analysed by western blotting with antibodies against DC8, Q9H410, Spc24 or Spc25 and additionally tested by western blot, whether it is possible to co-immunoprecipitate other complex partners (Fig. 2.9). Furthermore, all eluates obtained from IPs with crosslinked antibodies were separated on an 8-12% gradient SDS-PAGE gel and silver stained (Fig. 2.10) to determine the purity of the samples and judge whether it is possible to excise bands from the gel for identification by mass spectrometry.

For DC8-IPs using anti-DC8 antibodies Ab1621-M#1 and Ab1621-G#1, either crosslinked (Fig. 2.9.C) or not (Fig. 2.9.A), the immunoprecipitation of DC8 protein from HeLa cell log was successful. Co-IP of Mis12 protein, a complex-partner of the DC8 protein, was successful for both antibodies, crosslinked or not. Co-IP of Q9H410 was tested for non-crosslinked antibodies and was successful with anti-DC8 (Ab1621-G#1).

Using non-crosslinked anti-Q9H410 antibodies Ab1622-M#1 or Ab1622-G#, Q9H410 protein could be immunoprecipitated but not eluted with glycine, only boiling the beads in SDS-PAGE sample buffer eluted the protein off the beads (Fig. 2.9.B). Co-IP of complex-partner Mis12 protein was successful with both antibodies, whereas co-IP of complex-partner DC8 was successful only with anti-Q9H410 (Ab1622-G#1). For the Q9H410-IP carried out with crosslinked antibodies (Fig. 2.9.D), Q9H410 protein was immunoprecipitated from HeLa log cell extract with both antibodies (M and G). Co-IP of Mis12 was only obtained with anti-Q9H410 (Ab1622-G#1) and co-IP of DC8 was not tested here.

For Spc24-IP, shown in Fig. 2.9.E, using anti-Spc24 antibodies Ab889-M#1 and Ab889-G#1, with and without crosslinking, Spc24 protein was immunoprecipitated from HeLa log cell extract. Spc25-IP (Fig. 2.9.F) was performed by using anti-Spc25 antibodies Ab887-M#1 and Ab887-G#1, with and without crosslinking. Spc25 protein was successfully immunoprecipitated from HeLa log cell extract in all cases, whereby Ab887-G#1 gave a higher yield of immunoprecipitated Spc25 protein than Ab887-M#1 (as estimated from the intensity of the western blot signal). Hec1 and Nuf2, both complex partners of Spc24 and Spc25 did not co-IP, neither with anti-Spc24 (Ab889-M#1 and Ab889-G#1) nor anti-Spc25 antibodies (Ab887-M#1 and Ab887-G#1).

2. Results

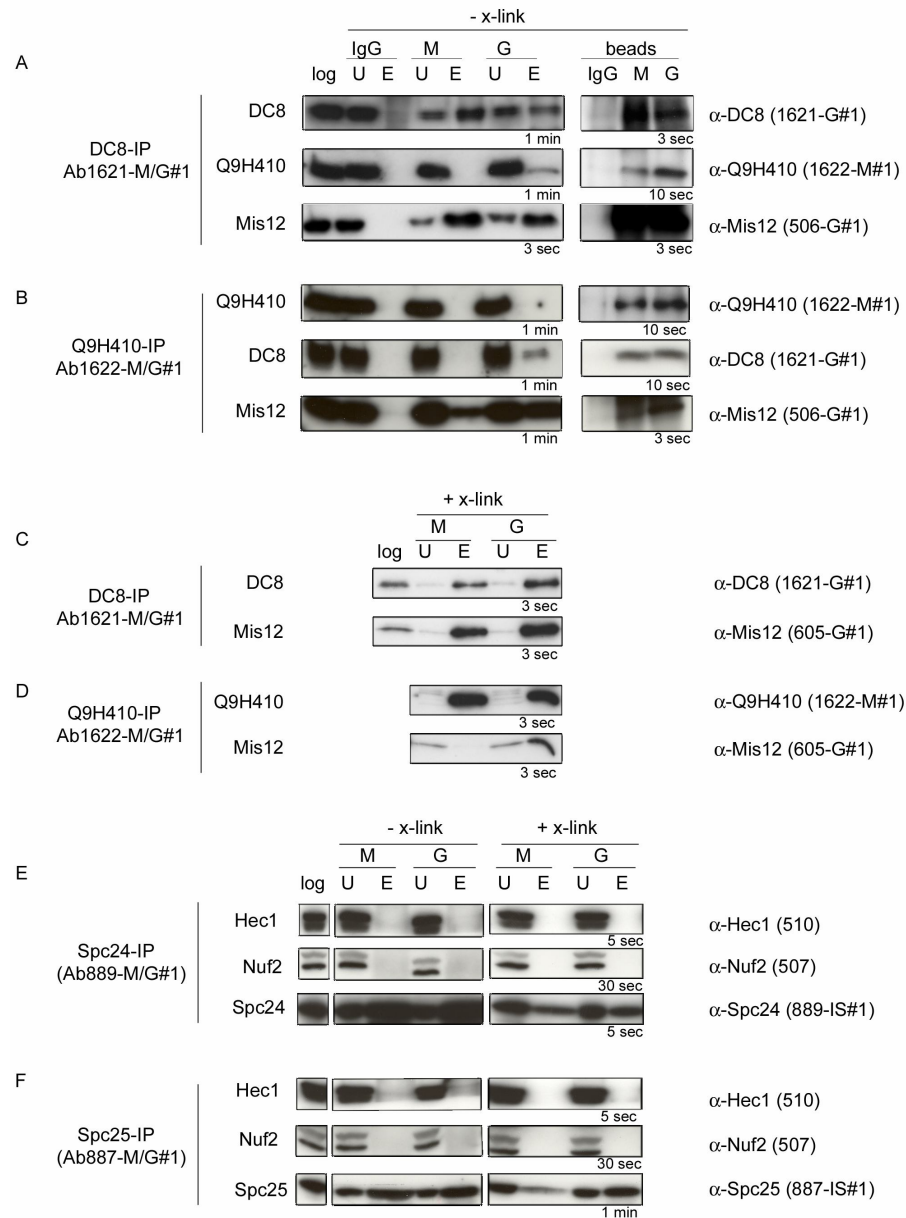


Figure 2.9. Test immunoprecipitation of kinetochore proteins by generated antibodies, with and without crosslinking. Antibodies Ab1621-M#1, Ab1621-G#1, Ab1622-M#1, Ab1622-G#1, Ab889-M#1, Ab889-G#1, Ab887-M#1 and Ab887-G#1 were tested for their ability to immunoprecipitate their target proteins. Immunoprecipitation experiments were performed under standard conditions from HeLa cell log extract (log), with crosslinking (+ x-link) or without crosslinking (- x-link) the antibodies to Affi-Prep Protein-A beads. For analysis, 60 µg of extract (log), 60 µg of unbound protein (U) and half of the total eluate were separated on an 8-12% gradient SDS-PAGE gel and probed with the appropriate antibodies. Anti-DC8 Ab1621-M#1 and Ab1621-G#1 without (A) or with (C) crosslinking to the beads were used to perform a DC8-IP. Anti-Q9H410 Ab1622-M#1 and Ab1622-G#1 without (B) or with (D) crosslinking were used for a Q9H410-IP. For non-crosslinked DC8- (A) and Q9H410-IPs (B), an additional control IP (IgG-only) was carried out. Half of the total elution volume was separated on the SDS-PAGE gel. Proteins were subsequently analysed by western blotting, using anti-DC8 (Ab1621-G#1), anti-Q9H410 (Ab1621-M#1) and Mis12 (Ab506-G#1). For Spc24-IP (E) and Spc25-IP (F) antibodies Ab889-M#1 and Ab889-G#1 or Ab887-M#1 and Ab887-G#1, each with and without crosslinking were used. Additionally, antibodies against Hec1 (Ab510) and Nuf2 (Ab507) were used to detect co-IPed complex partners by WB. Primary antibodies were used at a concentration of 2 µg/ml and were recognised using HRP-conjugated anti-rabbit antibody (1:5000) and visualised by the ECL system. For the IPs performed with non-crosslinked antibodies, 'Trueblot' secondary HRP-coupled anti-rabbit antibody was used (1:7500).

The silver gel in Fig. 2.10 shows eluates of the IPs, performed with crosslinked antibodies. For Spc24 and Spc25, at the size of 25 kDa, there is no promising band visible, neither for MgCl_2 - nor for glycine-eluted antibody. For DC8 there is an intense band just above 31 kDa in the eluate of the DC8-IP performed with anti-DC8 (Ab1621-G#1). For Q9H410 three promising bands at a size around 40 kDa are visible in the eluate from the IP obtained with the anti-Q9H410 (Ab1622-G#1) antibody and additionally a band can be seen at 21 kDa, which possibly could be co-IPed Mis12 protein. Although these IPs show specific and promising bands, all still have a strong background of non-specific bands. Under these conditions, the specific bands were not sufficiently 'clean' for excising and identifying by MS. Also, for phospho-site mapping, it is important to have a clean prep to obtain a high signal-to-noise ratio for the phospho-peptides. Therefore, before phospho-site mapping it was essential to increase the purity of the sample by optimising the IP conditions.

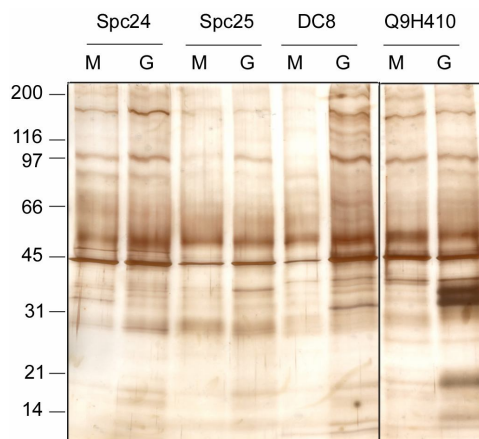


Figure 2.10. Test IP-silver with crosslinked kinetochore antibodies. Half of the volume (i.e. 15 μl) of the total eluates from the test-IP with crosslinked antibodies (Fig. 2.9) were separated on an 8-12% gradient SDS-PAGE gel then silver stained in order to assess the quality of the purification, in terms of purity and yield.

In summary, at least one of the two antibodies against each of the four kinetochore proteins was able to immunoprecipitate their target proteins. Additionally, the antibodies anti-DC8 (Ab1621-G#1) and anti-Q9H410 (Ab1622-G#1) could co-immunoprecipitate their complex-partner protein Mis12 in IP-WB and possibly also in IP-silver. The antibodies which worked best in IP pull-down experiments (anti-DC8 [Ab1621-G#1], anti-Q9H410 [Ab1622-G#1], anti-Spc24 [Ab889-G#1] and anti-Spc25 [Ab887-G#1]) were used to ask the question: can immunoprecipitation followed by mass spec be used to identify the target proteins and known complex partners?

To address this, IPs were carried out under standard conditions from HeLa log cell extracts, using antibodies anti-DC8 (Ab1621-G#1), anti-Q9H410 (Ab1622-G#1), anti-Spc24 (Ab889-G#1) and anti-Spc25 (Ab887-G#1). The IPed proteins were eluted from the beads,

proteolytically digested in solution using trypsin and subsequently analysed by liquid chromatography-tandem mass spectrometry (LC-MS/MS). The principles behind this technique are described in section 2.3, and procedural details can be found in sections 4.5.3 and 4.5.4. The output of this analysis yielded MS/MS spectrum files, which were searched against a human genome-wide protein database (KBMS) generating a list of protein hits. Results of MS/MS analysis of DC8, Q9H410, Spc24 and Spc25 – IPs are shown in Table 2.4. Proteins are sorted by MASCOT score, which is a measure of confidence in protein detection, furthermore common contaminants (keratin, IgG, HSP70, trypsin) were filtered out.

Table 2.4. Analysis of DC8, Q9H410, Spc24 and Spc25 - IPs by mass spectrometry (MS/MS).

DC8-IP (Ab1621-G#1),			Spc24-IP (Ab889-G#1)		
Protein	MS score	seq. cov.	Protein	MS score	seq. cov.
SPAG5	904,7	20%	RUN and FYVE domain containing protein 1	604,3	19%
TRAP3	797,8	18%	Fibroblast growth factor receptor 1	352,9	17%
Q9H410	720,7	55%	MKLP1	350,1	10%
GAPCenA	675,7	19%	dihydrolipoyl transacylase	332,9	17%
Chromodomain helicase-DNA-binding protein 4	498,5	9%	SH2-domain binding protein	291,9	9%
DC8	168,3	22%	Clathrin heavy chain 1	264,4	4%
PMF1	160,5	19%	Spc25	222,9	17%
Hec1	155,6	8%	Spc24	180,9	29%
Mis12	75,3	10%	Mis12	52,2	5%
→ 5 out of 10 complex partners found → AF15q14, Nuf2, Spc24, Spc25, Zwint not found			→ 2 out of 4 complex partners, additionally Mis12 found → Hec1, Nuf2 not found		

Q9-IP (Ab1622-G#1)			Spc25-IP (Ab887-G#1)		
Protein	MS score	seq. cov.	Protein	MS score	seq. cov.
Dedicator of cytokinesis 7	405,5	5%	Heat shock protein 8 isoform 1	397,6	16%
Bloom syndrome protein	238,2	3%	Spc24	369,1	15%
Q9H410	69,6	9%	Tubulin, beta	311,7	20%
PMF1	55,3	9%	Actin, beta	303,9	26%
Mis12	41,2	5%	Spc25	168,6	24%
→ 3 out of 10 found → AF15q14, DC8, Hec1, Nuf2, Spc24, Spc25, Zwint not found			→ 2 out of 4 found → Hec1, Nuf2 not found		

Legend: Target proteins are indicated in gold, kinetochore complex partners in yellow and kinetochore proteins of other complexes in grey.

As listed in Table 2.4, for the Mis12 complex, which is reported to comprise ten proteins (Obuse et al., 2004), five complex-partners (Q9H410, DC8, PMF1, Hec1, Mis12) could be purified by anti-DC8-IP (Ab1621-G#1) and three (Q9H410, PMF1, Mis12) by Q9H410-IP (Ab1622-G#1). For the Hec1 complex, consisting of four core proteins (Bharadwaj et al., 2004; McClelland et al., 2004; Ciferri et al., 2005), two proteins (Spc24, Spc25) could be purified by both anti-Spc24-IP (Ab889-G#1) and anti-Spc25-IP (Ab887-G#1). Interestingly, in the Spc24-IP Mis12 could additionally be identified and in the DC8-IP another interesting

protein SPAG5 (also known as Astrin, Deepest, Mitotic spindle associated protein p126; UniProt code Q96R06) was co-purified. Based on this identification-analysis we decided to predominantly concentrate on optimising the IP conditions for anti-DC8-IP (Ab1621-G#1) and anti-Spc24-IP (Ab889-G#1). A summary of the results for characterisation of the kinetochore antibodies, generated during this thesis is listed in Table 2.5.

Table 2.5. Summary of kinetochore antibody characterisation.

Antibody name	western blot - HeLa	western blot - IVT or rec.p.	band silenced by RNAi	IP + x-link	co-IP of complex proteins
anti-DC8 (Ab1621)					
Ab1621-IS#1-5	well	well	very well	-	-
Ab1621-M#1	weak	weak		very well	-
Ab1621-G#1	very well	very well		very well	yes
anti-Q9H410 (Ab1622)					
Ab1622-IS#1-6	well	not well	no	-	-
Ab1622-M#1	well	not well		very well	-
Ab1622-G#1	well	not well		very well	yes
anti-ZW10 (Ab1619)					
Ab1619-IS#1-6	ok	no	no	-	-
Ab1619-M#1	No	no		-	-
Ab1619-G#1	No	no		-	-
anti-Zwilch (Ab1620)					
Ab1620-IS#1-6	ok	no	no	-	-
Ab1620-M#1	no	no		-	-
Ab1620-G#1	no	no		-	-
anti-Spc24 (Ab889)					
Ab889-IS#1-7	well	well	not well	-	-
Ab889-M#1	well	well		very well	-
Ab889-G#1	well	well		very well	yes
anti-Spc25 (Ab887)					
Ab887-IS#1-7	ok	ok	not well	-	-
Ab887-M#1	ok	ok		ok	-
Ab887-G#1	ok	ok		very well	yes

Legend: -, not performed; no, negative result; not well; very weak; ok; well; very well.

2.2.5. Optimising IP conditions (IP-WB, IP-silver, IP-MS)

In order to make the IPs suitable for MS analysis, especially for phospho-mapping, the yield and the purity of the IPed kinetochore proteins and their interaction partners have to be increased by optimising IP conditions. To optimise the purification conditions (focusing on Spc24- and DC8-IPs), IPs were performed and the yield and purity of their products assessed by SDS-PAGE and silver-staining. The variation of the following parameters was tested:

- 1) Antibody concentration: increasing the concentration of antibodies crosslinked to the protein-A beads to achieve a higher yield of purified target proteins (1 µg, 3 µg and 5 µg Ab per 1 µl beads).
- 2) Ionic strength of the wash buffer: increasing the stringency of the washing step (e.g. by using a higher salt concentration) reduces the probability of proteins binding non-specifically to the antibodies. Washes were performed with increasing salt concentration: NaCl at 0.15 M, 0.3 M or 0.5 M, or KCL at 0.3 M.
- 3) Including a pre-clearing step: this procedure removes proteins that bind non-specifically to IgG-coupled beads, thus reducing the background signal in IPs. HeLa cell extracts were incubated with beads conjugated with non-specific IgG, then centrifuged. The supernatant (the pre-cleared extract) was then used to perform the IP with specific kinetochore antibodies crosslinked to the beads.
- 4) Increasing the protein concentration of extracts used for IPs could result in an increased yield of specific protein, as long as the beads are not saturated. The amount of protein loaded onto beads was varied: 4 mg, 20 mg, 50 mg protein per 20 µl beads.
- 5) Changing the time of incubating the extracts with the beads: reducing the IP time (60 min, 30 min, 10 min) is known to decrease the binding of non-specific proteins to the beads, therefore reducing the background – but this may also result in a reduction in the binding of the specific protein.
- 6) Using a larger wash-volume: increasing the volume of buffer (from 20 to 200 bv) in which the beads were washed after incubation with the extracts can result in the removal of a larger fraction of the unbound or weakly-bound protein from the beads.
- 7) Up-scaling the entire IP: once the optimum IP parameters have been established, the volume of beads and of extract can be increased proportionately, in order to yield sufficient product for phospho-mass spectrometry analysis.

As shown in Fig. 2.11.A, the increased concentration of antibodies crosslinked to the beads did not have an effect on the purity of the samples, neither in Spc24- nor in DC8-IPs. The yield of the purified target proteins was hard to judge, due to several bands migrating at a size similar to the proteins of interest. Under these conditions, the specific bands are not sufficiently 'clean' for excising and identifying by MS. Generally, candidate bands in Spc24- (just below 31 kDa) and DC8- (between 31 kDa and 45 kDa) IPs performed with 3 μ g and 5 μ g antibody look slightly more intense compared to IPs using 1 μ g Ab/ μ l beads. Due to limitations in the amount of antibody available, we decided to continue using 1 μ g Ab/ μ l beads and to further optimise IP conditions by changing the other parameters listed above.

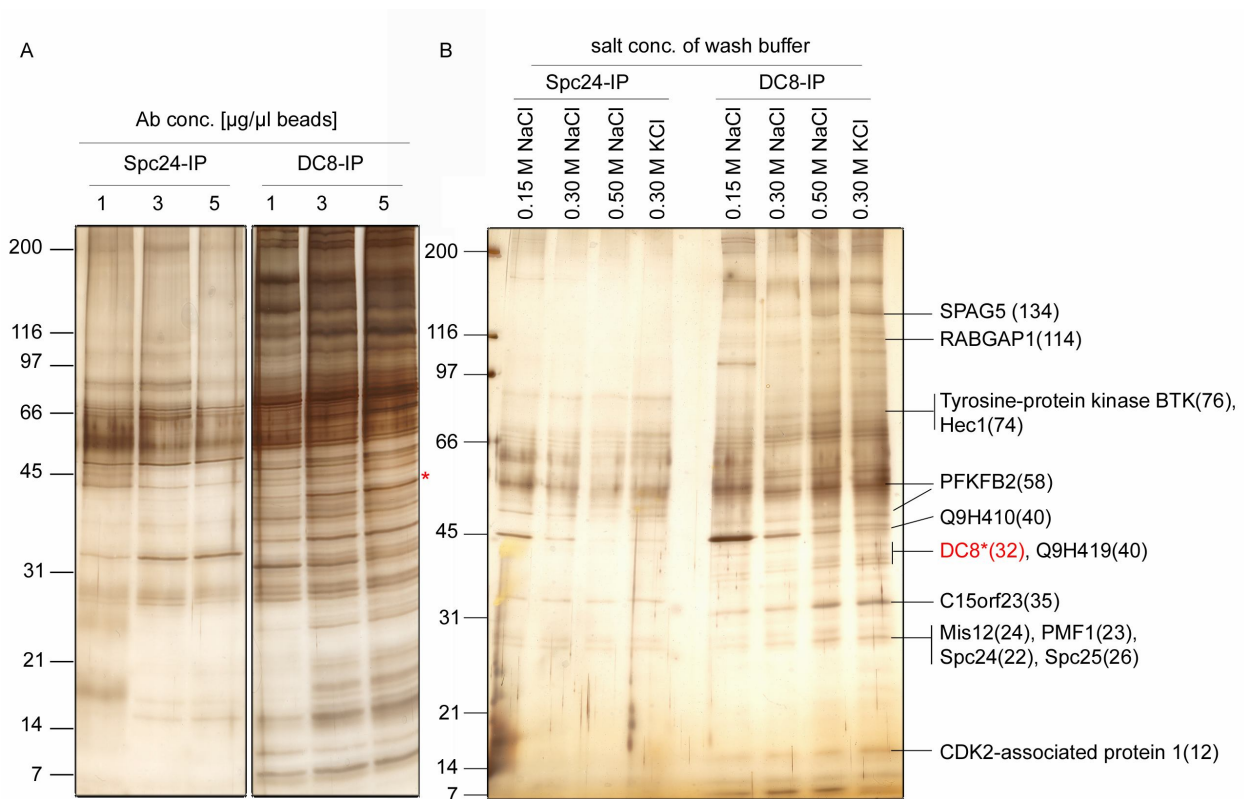


Figure 2.11. Optimising IP conditions: variations in (A) Ab concentration and (B) wash stringency. Except for these variations, IPs from HeLa log cell extract were performed under standard conditions using antibodies Ab889-G#1 (Spc24-IP) and Ab1621-G#1 (DC8-IP). Half the volume (i.e. 15 μ l) of the total glycine eluates was separated on an 8-12% gradient SDS-PAGE gel then silver stained in order to assess the quality of the purification in terms of purity and yield. **A:** The concentration of antibodies crosslinked to protein-A beads (μ g Ab/ μ l beads) was increased from 1 μ g/ μ l to 3 μ g/ μ l and 5 μ g/ μ l, for both the Spc24- and the DC8-IP. **B:** The stringency of washing was changed by varying the salt concentrations of the wash buffer from 0.15 M NaCl to 0.3 M NaCl, 0.5 M NaCl or 0.3 M KCl, for both Spc24- and DC8-IP. Selected bands from the DC8-IP (0.3 M NaCl) were excised from the gel, trypsin digested and identified by MS analysis. High Mascot-scoring protein hits are indicated on the silver gel (numbers after protein names mark the size in kDa). Common contaminants (keratin, IgG, HSP70, trypsin) were filtered out. The bait protein DC8 is highlighted in red and its position in panel A is marked by an asterisk (*).

Next, the stringency of washing the beads after IP was increased by using higher salt concentrations in the wash buffer. As shown in Fig. 2.11.B, there was no striking effect in the reduction of the background signal for the Spc24-IP. For the DC8-IP the “clearest” sample was obtained by using 0.3 M NaCl washes. Candidate bands of DC8-IP (in the range of 31 to 45 kDa) looked most intense with 0.5 M NaCl and 0.3 M KCl washes, but due to the better reduction of background signal we decided to use 0.3 M NaCl for further IPs. Bands of DC8-IP (0.3 M NaCl) were excised from the gel and analysed by MS. DC8 protein was identified in a band migrating at ~40 kDa. For Q9H410 protein, several hits were found at different molecular weights, i.e. at 45 kDa and in several bands at ~40 kDa, which could possibly be splicing variants (Table 2.6) or degradation products of the protein. Besides DC8 and Q9H410, additional Mis12-complex partners, including Mis12, Spc24, Spc25, PMF1 and Hec1 were identified in excised bands of the DC8-IP (Fig 2.11.B). The bands on the silver gel for Spc24-IP were not sufficiently intense or resolved to be excised from the gel for MS identification analysis, therefore it was decided to perform the optimising steps only for the DC8-IP.

Table 2.6. Predicted splicing variants of proteins Q9H410 and DC8, website: www.ensembl.org

Ensembl mRNA	Ensembl protein	Uniprot name	Mass [Da]
Q9H410			
ENST00000373750	ENSP00000362855	CT172_HUMAN	40 067.08
ENST00000373752	ENSP00000362857	Q4G1A1_HUMAN	38 323.09
ENST00000373733	ENSP00000362838	Q5JW57_HUMAN	33 151.58
ENST00000373745	ENSP00000362850	Q9H410-2	32 927.42
ENST00000373740	ENSP00000362845	Q5JW54_HUMAN	3 2219.35
ENST00000373743	ENSP00000362848	Q5JW55_HUMAN	27 997.68
DC8			
ENST00000366977	ENSP00000355944	CA048_HUMAN	32 161.82
ENST00000366976	ENSP00000355943	NP_001036014.1	19 511.28
ENST00000366975	ENSP00000355942	novel transcript	19 471.13
ENST00000366978	ENSP00000355945	Q5SY76_HUMAN	8 454.89

Next, DC8- IPs and a Cdc27-IP (as control) were performed including a pre-clearing step (described above) and additionally an upscale of the volume of the entire IP, from 20 µl to 40 µl IP-bead volume. Comparing IPs with and without pre-clearing (Fig. 2.12.A, lane 2 and 3), IPs with pre-clearing did not show an improvement in terms of reduction in the background signal, therefore we decided not to include a pre-clearing step in further IPs. Upscaling the IP-volume resulted in an overall stronger signal of background and candidate bands. In Fig. 2.12.B, DC8-IPs are shown with variations in IP-time (the time of incubating extracts with antibody-bound beads) and concentration of the cell extract. The silver-stained SDS-PAGE gel of the eluates from all conditions looked very clean and showed a distinct pattern of bands. The bands were excised from the gel, analysed by MS and proteins were

identified as indicated in Fig. 2.12.B. In parallel, an IP using an anti-Cdc27 antibody, which reliably and reproducibly pulls down the Anaphase-Promoting Complex (Gieffers et al., 2001; Kraft et al., 2003) was performed, as a positive control for the IP technique, and to identify background bands, i.e. those not specific for the DC8-IP. This IP showed the typical migration pattern of APC subunits, and only minor amounts of contaminating proteins.

Summarising the results for optimising the DC8-IP, we found the following conditions to be suitable for our purposes: using 1 µg Ab per 1 µl beads, incubating the IP at the proportions of 4 mg extract per 20 µl beads, for 60 minutes (IP-time), and performing washes using 50 bead-volumes and salt strength of 0.3 M NaCl.

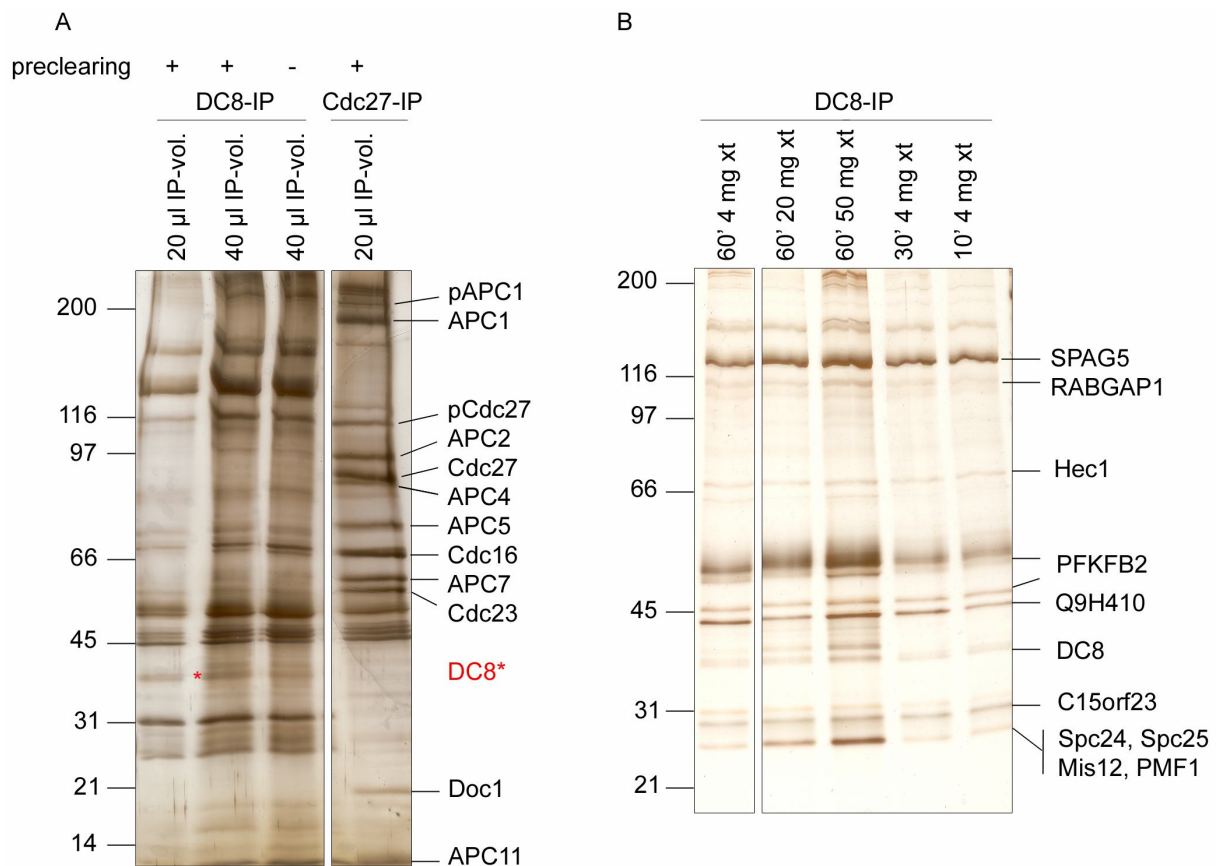


Figure 2.12. Optimising IP conditions: variations in (A) scale and pre-clearing, (B) protein concentration and IP-time. Except for these variations and an increased salt concentration of 0.3 M NaCl in wash-steps, IPs from HeLa log cell extract were performed under standard conditions using antibodies Ab1621-G#1 (DC8-IP) and anti-Cdc27. Half the volume of the total glycine eluates was separated on an 8-12% gradient SDS-PAGE gel then silver stained in order to assess the quality of the purification in terms of purity and yield. **(A)** For the pre-clearing step, 4 mg extract were loaded onto 20 µl protein-A-beads, crosslinked with unspecific IgG (e.g. pre-IS) and incubated 1 h rotating at 4°C. After centrifugation, the supernatant was applied to beads crosslinked with DC8-Ab or Cdc27-Ab. The pre-cleared IPs (+) for DC8 were performed in two different volumes, either with 20 µl or 40 µl beads (IP-vol.). Pre-cleared Cdc27-IP was carried out with 20 µl and non pre-cleared DC8-IP with 40 µl beads. The bait protein DC8 is highlighted in red and its position in panel A is marked by an asterisk. **(B)** DC8-IPs with different protein concentrations (4 mg, 20 mg, 50 mg), were incubated with 20 µl beads for a varying time (60 min, 30 min, 10 min). Bands were excised from DC8-IP eluates from both silver gels, from lane three (A) and lane one (B), trypsin digested and identified by MS analysis. High Mascot-scoring protein hits are indicated on the silver gel. Common contaminants (keratin, IgG, HSP70, trypsin) were filtered out. Annotation of proteins in the Cdc27-IP is based on published data (Gieffers et al., 2001; Kraft et al., 2003).

2.3. Identification of interaction partners and phospho-sites by liquid chromatography-tandem mass-spectrometry (LC-MS/MS)

Mass spectrometry is a very powerful technique to obtain information about the primary sequence of proteins and their post-translational modifications. For analysis by tandem mass spectrometry, proteins must first be digested into peptides. Peptide mixtures with high complexity have to undergo separation, which is usually achieved by reversed-phase liquid chromatography (LC). Separated peptides have to be ionised before introduction into the mass-spectrometer. This can be achieved online with the separation by electrospray ionisation (ESI). Peptides in a solvent are forced through a needle kept at high voltage, resulting in a spray of droplets containing positively-charged peptides. Evaporation of the solvent results in charged peptides in the gaseous phase entering the mass spectrometer. Here, the charged peptides (precursor ions) are separated according to their mass-to-charge ratio (m/z) in an ion trap, or cyclotron, depending on the type of machine. The ion intensities are measured by a detector, resulting in an MS spectrum, which shows the m/z ratio and intensities of the detected peptides. Precursor ions displaying a high intensity signal are isolated in the ion trap and then bombarded with inert gas particles, causing them to break apart at their weakest bonds, usually the peptide bonds between the amino acid residues. The resulting charged particles (fragment ions) are separated by m/z , generating an MS/MS (or MS^2) spectrum. Analysis of a typical protein digest in this way yields thousands of MS and MS/MS spectra.

To obtain sequence information from these data, a computer algorithm such as Mascot (Perkins et al., 1999) is used. Mascot works by matching MS^2 spectra with *in silico* digested peptide sequences derived from a protein database. Identified peptides are given an 'Ions Score', and are then matched onto their proteins of origin, allowing these to be identified. Proteins are assigned a 'Mascot Protein Score' based on the ions scores of the peptides which match onto them. This protein score is a measure of confidence in protein identification. However, as larger proteins generate more peptides than smaller ones, ranking proteins by Mascot score alone may generate a distorted view of the contribution of each protein to a sample. To compensate for this, I choose to rank proteins by Mascot protein score divided by mass, a quantity I refer to as the 'Specific Mascot Score' (SMS). An additional quality criterion for each protein hit is sequence coverage, i.e. the percentage of the amino acid residues of the full-length protein that are matched by the peptides detected by MS.

Post-translational modifications such as phosphorylation sites on peptides can also be identified by mass spectrometry analysis. When precursor ions containing phospho-serine or

phospho-threonine residues are fragmented, the major event is a 'neutral loss' (NL) of the phosphate group (as phosphoric acid, H_3PO_4), rather than the breakage of the peptide bond, resulting in an MS^2 spectrum dominated by one peak (the 'NL'-peak). From this neutral-loss ion, sequence information can be generated by further fragmenting it and recording the m/z of its fragment in an MS^3 spectrum. Identification of phospho-sites from these MS^2 and MS^3 spectra is performed by specialised algorithms and manual interpretation. Details on the exact procedures used in this study are described in section 4.5.3 and 4.5.4.

2.3.1. Identification of interaction partners from DC8-IP

In the case of the kinetochore protein complexes, I performed DC8-IPs in up-scaled volumes, using the established optimum IP parameters (section 2.2.5), in order to yield sufficient product for phospho-mass spectrometry analysis. To be able to identify mitosis-specific phospho-sites HeLa cell log extracts (with more than 90% interphase cell stages) and HeLa cell noc extracts (more than 90% of cells arrested in mitosis) were used to purify DC8 kinetochore protein and its complex partners. As a positive control a fraction of eluates (~1-2%) were separated on an SDS-PAGE gel which showed the same pattern of bands (Fig. 2.13), compared to previous DC8-IPs. For mass-spectrometry analysis the major fraction of the DC8-IP-eluates were directly protease digested in solution, which allows the investigation of all the subunits of the protein complex simultaneously within a single mass-spectrometric analysis. The DC8-eluates were split into three equal aliquots and digested in parallel using a different protease in each aliquot (trypsin, chymotrypsin and GluC), which increases the sequence coverage for the proteins. The generated peptide mixtures were separated by reversed phase liquid chromatography (LC) and mass-spectrometry analysis was performed as described above and in section 4.5.4.

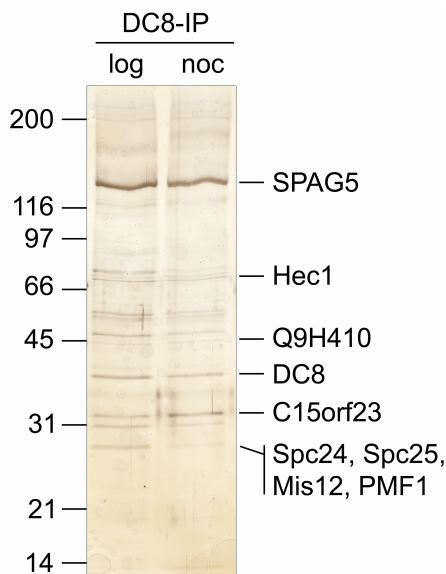


Figure 2.13. DC8-IP for MS protein identification and p-site mapping. IP was performed under the following conditions: 1 μg Ab (Ab1621-G#1) per 1 μl beads, incubated the IP with 100 mg HeLa cell log (> 90% of cells in S-phase, interphase) or noc (mitotic) extract with 500 μl protein-A-beads (4 mg extract per 20 μl beads), for 60 minutes and performing washes using 50 bead-volumes and salt strength of 0.3 M NaCl. The complex was eluted with 1.5 bv glycine (low pH) and 10 μl of 750 μl ($1/75^{\text{th}}$) was separated on an 8-12% gradient SDS-PAGE gel and silver stained. The major fraction of the eluate was in-solution digested with three different proteases and analysed for interaction partners and phospho-sites by LC-MS/MS.

All tandem mass spectra from this analysis were searched against the human KBMS database, using the algorithm included in the MASCOT 2.1 program to identify proteins in the sample. The list of proteins identified in the trypsin-digested sample is shown in Table 2.7. Trypsin is usually the most efficient protease, yielding the largest number of peptides. This results in the greatest possible number of proteins identified and the highest sequence coverage, and thus best represents the protein components of the sample (Olsen et al., 2004).

Eight proteins (Q9H410, PMF1, Mis12, Spc24, Hec1, HP1-gamma, Spc25 and Nuf2) known to be kinetochore components and recently found to be complex-partners of DC8 in the Mis12-complex (Obuse et al., 2004), were identified as co-purifying with DC8 from interphase and four (Q9H410, PMF1, Mis12, Hec1) from mitotic extracts (Table 2.7). This difference might be due to the overall slightly lower concentration of proteins in the mitotic sample, as apparent in Fig. 2.13. However, when combining the three digests, all kinetochore proteins (except Spc25), identified in the interphase sample (experiment 1) were also present in the mitotic sample. The combined sequence coverages of two DC8-IP experiments, using the same antibody and the same IP-conditions are shown in Table 2.8. To examine the reproducibility of the protein-identification and phospho-site mapping results, a second DC8-IP was performed under similar conditions (experiment 2). The results of this experiment were comparable to experiment 1, in terms of kinetochore proteins identified by MS² (Table 2.8).

In the analysis of experiment 1, additional proteins (SPAG5, RABGAP1, C15orf23, ELP4, HSPC002, 6-phosphofructo-2-kinase, MYCBP and TMEM103) not reported to be members of the Mis12 complex were identified in mitotic and interphase samples, with high Mascot-score over mass (SMS) values. SPAG5 and RABGAP1 have previously been implicated to play a role in microtubule dynamics (paragraph A). The function of the remaining proteins is either unknown or not related to mitosis (paragraph B).

(A) SPAG5, also called Astrin or Mitotic spindle associated protein p126, is associated with spindle microtubules in early prophase where it concentrates at spindle poles. It localises to the spindle in metaphase and anaphase, and associates with midzone microtubules in anaphase and telophase. Astrin also localises to kinetochores but only on congressed chromosomes (Abend et al., 1995; Mack et al., 2001; Gruber et al., 2002).

(A) RABGAP1 (also named human GAPCenA) is a GTPase activating protein for Rab6. Rab6 GTPase regulates intracellular transport at the level of the Golgi apparatus. RABGAP1 was reported to mainly localise in the cytosol, but a minor fraction is associated with the centrosome. Moreover, GAPCenA was found to form complexes with cytosolic gamma-

tubulin and to play a role in microtubule nucleation. Therefore, RABGAP1 might be involved in the coordination of microtubule and Golgi dynamics during the cell cycle (Cuif et al., 1999).

(B) C15orf23 (TRAF4-associated factor 1, or TRAF4AF1) is a protein for which little is known except that it binds MPP6 (membrane protein, palmitoylated 6) and MPHOSPH6 (M-phase phosphoprotein 6), (Gandhi et al., 2006).

(B) ELP4 (Elongator complex protein 4) acts as subunit of the RNA polymerase II elongator complex, which is a histone acetyltransferase component of the RNA polymerase II (Pol II) holoenzyme and is involved in transcriptional elongation. ELP4 may play a role in chromatin remodeling and is involved in acetylation of histones H3 and probably H4. (Hawkes et al., 2002; Kim et al., 2002).

(B) HSPC002 (DERP6) is reported to be involved in p53-mediated transcription (Yuan et al., 2006).

(B) The protein PFKFB2 (6-phosphofructo-2-kinase) is involved in both the synthesis and degradation of fructose-2,6-bisphosphate, a regulatory molecule that controls glycolysis in eukaryotes. The encoded protein has a 6-phosphofructo-2-kinase activity that catalyses the phosphorylation of F6P to generate fructose-2,6-bisphosphate, and a fructose-2,6-biphosphatase activity that catalyses the reverse reaction. This protein regulates fructose-2,6-bisphosphate levels in the heart, while a related enzyme encoded by a different gene regulates fructose-2,6-bisphosphate levels in the liver and muscle. This enzyme functions as a homodimer. Two transcript variants encoding two different isoforms have been found for this gene (Hilliker et al., 1991).

(B) TMEM103, called transmembrane protein 103 for which nothing has been reported in the literature. MYCBP (AMY1) is a novel C-MYC binding protein which stimulates the transcriptional activity of C-MYC (Taira et al., 1998).

All proteins, immunopurified by DC8 antibody and identified by MS² analysis, can be grouped into different categories (see section 3.2.1, Discussion). Some of these proteins, which from experience are known to be background proteins (keratins, IgG, proteases, HSP70, actins, myosins, albumin, tubulins, ribosomal proteins and cytochrome c), were removed from the lists (Table 2.7). All protein hits comprises at least two peptides, each of a Mascot ion score of at least 30. Overall it is not possible to tell from this DC8-IPs which proteins, besides the known complex-partners, are pulled down specifically by their interaction with the Mis12 complex. To further address this question, further control IPs using different antibodies, against the DC8 protein or different Mis12-subunits (e.g. Q9H410, PMF1 or Mis12) could be performed.

Table 2.7. Proteins identified by mass spectrometry from a DC8-IP from interphase or mitotic cell extracts.

Experiment 1:			Interphase		Mitosis	
Rank	ID	Protein	Mass [kDa]	Score	Seq-Cov [%]	SMS
1	itm Q9Y448	C15orf23 protein, FLJ14502, HSD11, chromosome 15 open reading frame 23	30.6	1041.9	63.4	34.89
2	spt Q96R06	SPAG5, Astrin, Mitotic spindle associated protein p126, Deepest	135.7	3777.7	66.4	30.10
3	itm Q9Y204	HSPC002, Dermal papilla derived protein 6 (DERP6)	18.4	533.9	49.1	29.01
4	itm Q9NX11	ELP4 elongation protein 4 homolog (S. cerevisiae)	47.0	1315.4	59.2	27.98
5	itm Q9Y3P9	RAB GTPase activating protein 1, RABGAP1	114.0	3037.1	49.5	27.18
6	itm Q9BW57	TMEM103, transmembrane protein 103	30.6	578.1	39.9	23.49
7	spt P62269	40S ribosomal protein S18, Ke3, RPS18	17.7	414.9	39.5	23.43
8	itm Q6IB68	MYCBP protein	11.9	265.6	54.4	22.24
9	pdb P63167	Dynein light chain 1 (fragment)	10.0	220.6	48.2	22.13
10	emb Q60825	6-phosphofructo-2-kinase, MGC138308, PFK-2/FBPase-2, PFKFB2	58.8	1216.1	50.2	21.53
11	spt Q9H410	Q9H410, C20orf172 protein	40.4	821.4	52.0	20.34
12	itm Q6PIK2	PMF1, Polyamine-modulated factor 1 (RP11-54H19.4-001)	23.5	460.8	59.5	19.61
13	itm Q9H081	Mis12 kinetochore protein	24.5	464.5	36.6	18.98
14	itm Q961Y1	DC8/DC31 protein	32.5	562.1	46.6	17.27
15	spt Q00571	DEAD-box protein 3, Helicase-like protein 2, HLP2, DBX, DDX3	73.5	1230.6	38.6	16.75
16	plr R5HU23	ribosomal protein L23 - human	15.1	242.3	35.0	16.00
17	itm Q8NBT2	Kinetochore protein Spc24	22.5	344.1	45.2	15.30
18	itm Q9NWB6	ERCC5	33.2	278.5	17.9	14.25
19	itm Q8WX16	KCTD3, Potassium channel tetramerisation domain containing 3	89.6	1145.4	39.3	12.78
20	rf NP_001264	chromodomain helicase DNA binding protein 4	219.4	2684.7	35.9	12.24
21	itm Q96EX0	Arg/Abi-interacting protein 2 isoform 2	71.9	854.6	40.6	11.88
22	spt Q9UMS4	PRP19/PSO4 homolog, Nuclear matrix protein 200, hPso4, NIMP200	55.6	622.8	45.2	11.87
23	itm Q86SF8	HNRPC heterogeneous nuclear ribonucleoprotein C	32.4			11.27
24	itm Q5W095	OTTHUMP0000039784 (GD-RP11-328M4.1-001)	75.6	741.4	38.6	9.81
25	sp Q14777	Hec1, hNdc80 'cmere/kchore' (KNTC2)	74.4	698.6	32.2	9.39
26	itm Q96PE2	Tumor endocytosis marker 4 (TEM4)	223.6	1576.8	22.7	9.39
27	sp Q13185	HP1-gamma 'cmere/kchore' (CBX3)	21.0	188.6	30.1	8.99
28	itm Q9UGM4	Nuclear LIM interactor (Fragment) (NLI)	46.2	413.2	27.6	8.94
29	itm Q9HEM1	Kinetochore protein Spc25	26.2	230.7	31.3	8.81
30	spt Q86YP4	Transcriptional repressor p66 alpha (Hp66alpha)	68.4	587.8	28.0	8.81
31	gb AAH09359	Heterogeneous nuclear ribonucleoprotein AB, isoform b	30.7	261.4	21.2	8.52
32	dbj BAA36707	metastasis-associated gene family, member 2	75.7	476.9	16.8	8.28
33	itm Q5VTK6	Thyroid hormone receptor-associated protein, 150 kDa subunit (TRAP150)	108.7	737.7	19.0	8.06
34	cra hCP38365	NRAA Best Hit: similar to KIAA0870 protein	146.2	1027.8	23.1	7.03
35	gb AAA35750	DNA-binding protein B	40.0	273.5	28.8	6.84
36	itm Q6PIR7	RelA-associated inhibitor (RelA-associated inhibitor)	89.4	533.7	20.0	5.97
37	spt Q13151	Heterogeneous nuclear ribonucleoprotein A0, hNRNP A0, HNRPA0	31.0	183.0	9.8	5.90
38	spt P60842	Eukaryotic initiation factor 4A-1, eIF4A-1, DDX2A, EIF4A	46.4	402.7	18.2	5.75
39	spt Q9Y8K6	CD2-associated protein (Cas ligand with multiple SH3 domains)	71.6	402.7	18.2	5.62
40	spt Q9NYF8	Bcl-2-associated transcription factor 1, BTF, KIAA0164	106.2	214.0	8.5	5.49
41	itm Q9BZD4	Kinetochore protein Nuf2, NUF2, NUF2R	54.6	298.9	16.2	5.47
42	itm Q6IBM8	EFTUD2 elongation factor Tu GTP binding domain containing 2	110.4	211.0	5.0	5.41
43	spt Q16576	Histone acetyltransferase type B subunit 2, RBBP-7, RBAP46	48.1	246.1	14.6	5.11
44	plr DNHLPA	Polyadenylate-binding protein - human	70.5			4.88
45	sp Q9HAW4	Caspin (CLSPN)	151.6	685.7	15.8	4.52
46	spt P38159	Heterogeneous nuclear ribonucleoprotein G, hNRNP G, HNRPG, RBMXP1	42.3	181.8	12.8	4.30
47	emb CAC01407	Double stranded RNA binding nuclear protein, ILF3	61.9	245.5	17.9	3.96
48	itm Q9BQ09	Heterogeneous nuclear ribonucleoprotein U, isoform b	89.7			3.43
49	itm Q5SO29	HLA-B associated transcript 2 (DAQB-195H10.7-001, XXbac-BCX270M2.7-001)	247.3	613.5	8.1	3.23
50	itm Q6NZY0	ASCC3L1 activating signal co-receptor 1 complex subunit 3-like 1	246.0			3.06
51	spt Q96JJ3	Engulfment and cell motility protein 2, CED-12 homolog A, hCED-12A	83.0	207.2	9.7	2.50
52	spt Q9NQ7	Ubiquitin-specific processing protease CYLD, Deubiquitinating enzyme CYLD	109.0	158.2	3.2	1.45

Legend: Target protein is indicated in gold; kinetochore complex partners in yellow and other proteins, chosen for further analysis in grey. Protein hits are ranked by SMS.

Table 2.8. Total Sequence coverage of in-solution digested DC8-IPs.

Seq.-cov. (3 digests) Mascot	exp. 1	exp. 1	exp. 2	exp. 2
Protein	Interphase	Mitotic	Interphase	Mitotic
SPAG5	94%	93%	95%	94%
RABGAP1	87%	86%	84%	81%
Q9H410	85%	62%	94%	74%
PMF1	82%	61%	87%	68%
DC8	80%	62%	90%	62%
PFKFB2	61%	57%	80%	70%
Spc25	63%	-	63%	-
Mis12	61%	54%	59%	40%
C15orf23	47%	53%	60%	52%
Spc24	67%	20%	62%	-
Hec1	54%	14%	36%	-
Nuf2	44%	7%	22%	-

Legend: Target protein (bait) is indicated in gold; kinetochore complex partners in yellow and other proteins of chosen for further analysis in grey. Sequence coverage [%]; proteins ranked by SMS.

2.3.2. Phosphorylation-site mapping of interaction partners from DC8-IP

As the DC8-IP was performed under conditions designed to preserve phospho-sites, the same data were subjected to p-site mapping. Given that it was not feasible to phospho-map all 52 proteins identified in the DC8-IP (Table 2.7), it was necessary to be selective about the proteins that were considered for phospho-site analysis. In addition to the Mis12 complex and other kinetochore-associated proteins, I decided to phospho-map one example protein from 4 categories: (1) a protein known to associate with a mitotic structure (SPAG5); (2) a protein that may have an indirect role in regulating some feature of mitosis (RABGAP1); (3) a protein of known function, considered unlikely to be involved in mitosis (PFKFB2); and (4) a protein of completely unknown function (c15orf23). All proteins, chosen to identify phospho-sites, are listed with their combined sequence coverages in Table 2.8. The sequence coverage is the percentage of the amino acid residues of the full-length protein that are matched by the peptides found in the sample and therefore an additional quality criterion for each protein hit. Two sets of DC-IP experiments (exp.1 and exp.2) were performed, using the DC8 antibody (Ab1621-G#1) and the same IP conditions. The sequence coverage was generated by the Mascot program and proteins were ranked by decreasing average sequence coverage.

To identify phosphorylation-sites in the kinetochore proteins pulled down by the DC8-IP, the mass spectrometry data (MS, MS² and MS³ spectra) from both experiments (exp.1 and exp. 2) were subjected to phospho-site analysis using the Mascot program (Perkins et al., 1999;

Mann et al., 2002). This algorithm searches for phosphoserine (pSer), phosphothreonine (pThr) and neutral loss peaks in MS² spectra, and post-neutral loss products dehydroalanine and dehydroaminobutyric acid, of pSer and pThr, respectively, in the MS³ spectra. MS search algorithms tend to generate many false-positive phospho-site assignments, and so we have opted to subject the spectra to additional manual validation. The phospho-peptide spectra for the proteins listed above (Table 2.8) were rated by our colleague Otto Hudcz (IMP – Vienna) according to the following criteria (Table 2.9):

Table 2.9. Quality criteria for rating MS-spectra, used for phospho-site mapping in this study

<i>Rating</i>	<i>Criteria</i>
3	Fragment ions equally distributed over m/z range, all distinct peaks are assigned.
2	Fragment ions equally distributed over m/z range, few peaks are not assigned.
1	Peak suppression, low signal to noise ratio.
0	No distinct peaks assigned, high noise level.

I decided to reject phospho-peptides where the spectra were given a rating of '0'. Phosphopeptides with a rating of 1-3 were included. These phospho-peptides are shown in Table 2.10 and summarised as a bar diagram in Fig. 2.14.

Phospho-site information was extracted manually from the list of p-peptides and evaluations. In many cases a peptide is known to be phosphorylated, but the exact position of the phospho-site within this peptide cannot be determined exactly from the spectrum, therefore it is appropriate to list the number of possible positions and the number of phosphorylations. Where two or more phospho-peptides had the same sequence, the peptide with the highest rating was chosen to be listed in the Table 2.10. Where two or more peptides overlapped in sequence, they were combined into one cluster of peptides and the number of possible positions and the number of phosphorylations was considered for that cluster. The data were further manually interpreted to determine which sites are mitosis specific, which are interphase specific and which are present under both cell cycle states. Sites considered to be mitosis-specific, have to be present in the noc sample, but not in the log sample, i.e. an unmodified (UM) peptide has to be in the log sample.

Twelve proteins (listed in Table 2.8), were analysed in the data from both experiments, and six were found to be phosphorylated. In total, 44 phosphorylations were detected, corresponding to 63 possible positions (Table 2.10). Of the 44 sites, 27 could be unambiguously assigned to a specific amino acid residue, whereas in 16 peptides the modified residue could not be identified with certainty. Among the clearly identified sites, 23 were phosphorylated on serine, four on threonine and none on tyrosine residues. In my

study, 18 sites were exclusively found in mitotic stage, four only in interphase and 17 were found in both (Table 2.11).

The kinetochore-proteins DC8 and Q9H410 were found to be phosphorylated, DC8 on T242 and Q9H410 on S27/28, S30, S58, S68, S77/81 and S331. No phospho-sites were found for the remaining six kinetochore proteins identified in the sample (PMF1, Spc25, Mis12, Spc24, Hec1, Nuf2). Interestingly the SPAG5 protein was found to be highly phosphorylated, many of these sites being mitosis-specific.

It is possible that some of these newly discovered sites already have been found in previous studies. To examine this I searched two public phospho-databases: PhosphoELM (Diella et al., 2004), www.phospho.elm.eu.org and PhosphoSite (Hornbeck et al., 2004), www.phosphosite.org.

From this search I found that several of the sites were contained within these databases, many of them originating from one recent publication, which identified p-sites on components of the mitotic spindle (Nousiainen et al., 2006). These sites have also been listed in Table 2.10 and in Fig. 2.14.

Table 2.10. Phospho-residues of selected proteins identified by mass-spectrometry analysis from DC8-IP.

Protein	Site	Sequence	Interphase		Mitosis		Rating	Presence	Possible positions	Number of Phosphorylation	Published sites
			exp.1	exp.2	exp.1	exp.2					
Q60825											
PFKFB2	S466	RNSFTPL	-	+	-	+	1	I	M	1	S461, S466
PFKFB2	S483	NYVSGSR	-	+	-	+	1	I	M	1	T475, S483
PFKFB2	S493	LKPLPLRA	-	+	-	+	1	I	M	1	S493
Q9Y448											
C15orf23	S171	SKQKSEEL	48%	60%	53%	52%	1	I	M	1	
C15orf23	S241/T242/T243 (2p)	QE ST TDHMD 2p	-	+	-	1p	1	I	M	2	
Q961Y1											
DC8	T242	TQIEITPTET	81%	90%	62%	62%	2		M	1	T242
Q9H410											
c20orf172	S27/S28+S30 (2p)	HQLE SL SPVEV 2p	85%	94%	62%	74%	1	I	M	2	S28+S30
c20orf172	S58	RIHLGSPKKG	+	+	-	30	1	I*	M*	1	S58
c20orf172	S68	GNCDLSHQER	+	-	+	-	1	I	M	1	S68
c20orf172	S77/S81	SLHLSPQEQ	+	81	81	UM	1	I	M	2	
c20orf172	S331	QLDPSPARK	-	+	-	-	1	I		1	
Q9Y3P9											
RABGAP1	T38/S42/T47	ETPTNNNGSDDEK T GL	87%	84%	86%	81%	2	I*	M*		
RABGAP1	T35+S42 (2p)	QGDPTSTNNGSDDEK T GL 2p	+	38/42	+	42	2	I*	M*	3	
RABGAP1	T284/S287	AAQ T PDSDIF	+	-	UM	-	1	I		1	
RABGAP1	S360	NNDMHL	-	+	-	UM	2	I	M	1	
RABGAP1	S419	KTTA S PSVR	UM	UM	+	+	2		M*	1	
RABGAP1	S508	SVIP S PPED	UM	-	+	-	1		M	1	
RABGAP1	T924	LDED T DEEK	+	+	+	+	3	I*	M*	1	
Q96R06											
SPAG 5	S10/S12	LSLS L SPSPQ	94%	95%	93%	94%	3	I	M		
SPAG 5	S12+S14 (2p)	LSLS L SPQGTG 2p	+	-	+	-	2	I	M	2	S12+S14
SPAG 5	S39 + S43 (2p)	PGALTN SG KRSPACS 2p	-	UM	+	39	1		M*	2	
SPAG 5	S62/S65/S66 (2p)	LOEG NN SPVDF 2p	UM	UM	+	+	1		M*	2	S62+S66
SPAG 5	S66	SNNSPVDF	UM	UM	62/65/66	+	1		M*	2	
SPAG 5	S79/S80	RTDL SE EHF	UM	UM	+	79	2		M*	2	
SPAG 5	S76/S80	TDLS SE HFS	UM	UM	+	79	1		M*	2	
SPAG 5	S109/S110/T111	IPQI ST PK	-	UM	+	+	2		M*	1	T111
SPAG 5	S135	VLVP PL GQ	+	+	+	+	1	I*	M*	1	S135
SPAG 5	S157/S159	AETN I SLNGP	UM	UM	+	159	3		M*	1	
SPAG 5	S197/S199	IFQ SP SHLE	-	UM	+	197	1		M*	2	
SPAG 5	S217 + S220 (2p)	QLHC SK SLSSR 2p	UM	-	+	-	1		M	2	
SPAG 5	S249/S251/S252	VLWL SP TALAA	UM	249	+	249	1	I	M*	3	S249
SPAG 5	S341	ESWM SL PLAW	+	+	+	+	3	I*	M*	1	S334 + S341
SPAG 5	T352/S353/S362/S364 (2p)	GVNT SV MLENLRQ SL LPMLR 2p	UM	-	353+362	+	2		M*	2	S353+S362+S364
SPAG 5	T376+S391 (2p)	DAAIG TT PFSTGCVGWFT TS APQEK 2p	-	UM	-	+	2		M*	2	T377 + S389
SPAG 5	S397/T398/T400/S401	STN TS QTGL	UM	UM	+	400/01/03	1		M*		S401
SPAG 5	T400/S401/T403	STN TS QTGLVGTK	UM	UM	+	+	1		M*	2	
SPAG 5	S944	PLLGS DK	-	UM	-	+	2		M*	1	T937
Σ											63
Σ											44

"+" Corresponding peptide was found with the same modification

"-" Corresponding peptide was not found with the same modification

UM Corresponding peptide was present, but not modified

red Unambiguous p-site position

blue Uncertain p-site position

* Site found in 2 experiments

I Site in Interphase cells

M Site in Mitotic cells

2p Two phospho-residues

Legend: Protein names are indicated with their Swiss-prot-ID (in bold). Percentages are given for the combined sequence coverages for each IP sample. Sites which are published but not found in this study are indicated in italic and underlined.

Table 2.11. How many mitosis-specific p-sites were found?

<i>Categories of p-sites / positions</i>	<i>Number of p-sites / positions</i>
P-sites only found in interphase cells	4
P-sites only found in mitotic cells	18
P-sites found in both, interphase and mitotic cells	17
P-positions unambiguous	27
P-positions uncertain	16

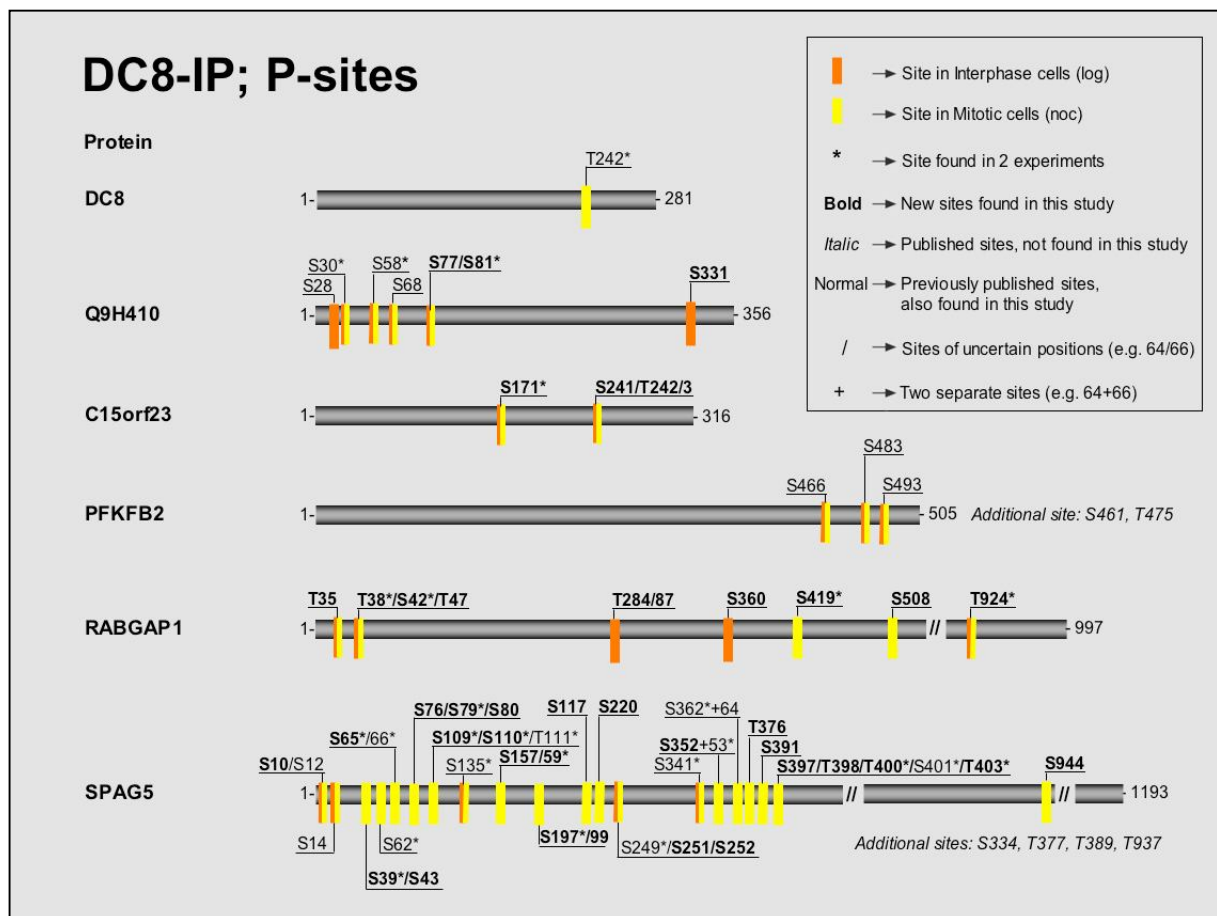


Figure 2.14. Summary of phosphorylation sites of selected proteins identified by mass-spectrometry analysis from DC8-IP.

3. Discussion

3.1. Expressing tagged kinetochore proteins

My initial strategy to express tagged kinetochore proteins involved the expression of tagged cDNAs in HeLa cells. This is a straightforward approach due to the availability of human cDNAs and of tagged expression vectors. On choosing an approach one has to decide whether to employ a constitutive or inducible expression system. Constitutive expression systems are well established for the expression of mitotic proteins (Waizenegger et al., 2000; Kunitoku et al., 2003) and have the advantage of consistency. With inducible systems, the expression of the tagged gene can be titrated by the addition of an inducing agent and therefore it needs to be constantly monitored.

The plan was to select clonal cell lines of HeLa cells constitutively expressing the tagged kinetochore proteins near endogenous levels. However, the propagation and selection of clones proved to be a huge technical challenge with many of the cells showing morphological defects and high rates of apoptosis. One explanation for this could be the expression level of the kinetochore cDNA was not in the range of that of the endogenous gene. As kinetochore complex subunits are typically low abundant proteins, their over-expression could disrupt the structure of the kinetochore and interfere with accurate chromosome segregation. An alternative approach that could prevent these problems could be the use of tagged Bacterial Artificial Chromosome (BAC) constructs. Here whole genes, in BACs, are tagged and stably expressed in HeLa cells. In most cases the tagged BAC gene (e.g. from mouse) is expressed at an endogenous level and can complement (rescue) the knock-down of the endogenous gene by RNAi (Kittler et al., 2005). This strategy has recently been adopted by the I.M.P. MitoCheck team, for the large-scale purification of mitotic complexes.

3.2. Interpretation of interaction results

When kinetochore protein complexes were immuno-precipitated by specific antibodies, I found that DC8-IP worked best in terms of the isolation of kinetochore complexes. Mass spectrometry and Mascot searching enabled us to identify 275 proteins, including nearly all Mis12 complex components and many other kinetochore proteins.

Each of the MS results takes the form of a table of proteins, each with a confidence score generated by the search software (Mascot). The two main issues at this stage are a) to determine which proteins are genuine components of the complex (categorisation) and b) to rank confident protein hits by a meaningful score.

3.2.1. Categorisation of protein hits

To determine which proteins are genuine complex members, I have chosen to categorise these proteins as follows:

All proteins we found must belong to at least one of the following categories

- (1) The bait protein.
- (2) Known complex partners - previously reported to be in a complex with the bait.
- (3) All other physiologically mitosis relevant proteins - includes all proteins reported to be involved in mitosis or localised to the kinetochore.
- (4) Proteins neither previously reported to be associated with the bait nor directly involved in mitosis.
- (5) Proteins not interacting with the bait but cross-reacting specifically with the particular antibody used for the IP.
- (6) Proteins known to arise from contamination during sample preparation - e.g. keratins.
- (7) Proteins resulting from a carry-over from the purification procedure - e.g. IgG, proteases.
- (8) Proteins (often highly abundant) which from experience are known to associate non-specifically with baits during IP experiments - e.g. HSP70, actin, myosin, albumin, tubulin, ribosomal proteins, cytochrome c.

To ensure only relevant proteins are in the list, members of categories 6 to 8 should be deleted. Many novel proteins could possibly fit in categories 4 and 5 - this could be further discriminated by additional experiments (see below).

For the DC8 IP, after the proteins listed as examples in categories 6 to 8 (background, contaminant, or non-specific hits) were removed, 52 proteins remained. How could these proteins be categorised as described above? For category 1 (the bait, i.e. DC8), the UniProt accession code is known, allowing it to be unambiguously identified among the list of protein hits. DC8 is a known component of the Mis12 complex, and other subunits of this complex (category 2) have been previously reported, see Table 3.1, (Cheeseman et al., 2004; Obuse et al., 2004). To identify other physiologically relevant proteins (category 3) it requires a systematic investigation of each Mascot-identified hit by accessing online bioinformatics databases e.g. via the Bioinformatic Harvester: harvester.embl.de (Liebel et al., 2004) and published literature. The remaining proteins, in categories 4 and 5, are not known to be directly involved in mitosis or kinetochore function, and therefore it is not possible for us to discriminate between these two categories from this experiment alone. How could we distinguish between these sets of proteins experimentally? To address this, further

experiments could be performed to control for the specificity and cross-reactivity of the antibody used for the IP. The use of at least one other additional antibody, targeting either the same bait (preferably raised against a different peptide, or the full-length protein), or another known complex component, in a similar IP experiment would enable true interacting proteins to be distinguished from artefacts arising from the antibody used in the IP. Another approach would be to affinity tag one or more components of the complex, then to identify the bait and interacting proteins by affinity-purification followed by mass-spectrometry.

Table 3.1. How many Mis12 components were found?

This study	(Obuse et al., 2004)	(Cheeseman et al., 2004)	category
Proteins purified with 9MYC-hDC8	Proteins purified with GFP-hMis12	Proteins purified with LAP-hMis12	
Mis12-complex			
Mis12	Mis12	Mis12	2
Q9H410	Q9H410	Q9H410	2
DC8	DC8	-	1
PMF1	PMF1	PMF1	2
-	AF15q14 (KIAA1570)	AF15q14	-
Hec1-complex			
Hec1	Hec1	Hec1	2
Nuf2	-	Nuf2	2
Spc24	-	Spc24	2
Spc25	-	Spc25	2
Other kinetochore or mitosis relevant proteins			
-	Zwint	Zwint	-
-	HP1 α	-	-
HP1 γ	HP1 γ	-	2
SPAG5	-	-	3
RABGAP1	-	-	3
Other proteins			
TRAF4AF1	-	-	4 or 5
ELP4	-	-	4 or 5
PFKFB1	-	-	4 or 5
DERP6	-	-	4 or 5
MYCBP	-	-	4 or 5
TMEM103	-	-	4 or 5

3.2.2. Ranking and confidence of MS protein hits

In general, proteins identified by the Mascot program are ranked by decreasing Mascot protein score, a measure of confidence in protein identification. As the Mascot protein score approximates to the sum of peptide scores, then larger proteins (which generate a greater number of distinct proteolytic peptides) will generate higher Mascot protein scores, even if their relative abundance is the same as that of a smaller protein. This feature limits Mascot score alone as a suitable ranking method, especially when dealing with heterogeneous protein complexes. In order to compensate for disproportionately high scores of the large proteins I decided to use the 'SMS' ranking, which is the Mascot score divided by the molecular weight in kDa. For the results in the DC8 IP, for the Mascot score alone DC8 has a position of 25 whereas with SMS ranking its position is raised to 14 (Table 2.7).

The standard procedure ("rule of thumb", employed by the IMP mass spec facility) to be confident that a protein is an MS hit and not a false positive, is that it should be recognised by two peptides, each with a peptide Mascot score of 30 or above. This means that proteins with a Mascot score of lower than 60 should be marked as "low confidence" or removed from the list. In the case of the DC8 IP, all proteins identified by Mascot satisfied this confidence criterion. The lowest Mascot score in my table is 145 (Table 2.7).

A newly introduced analysis program, to give a greater confidence in protein detection by Mass-spec, is 'Scaffold'. This program imports Mascot results and assigns a statistical confidence score for each peptide, based on the 'Peptide Prophet' algorithm (Keller et al., 2002); (Nesvizhskii et al., 2003). Protein hits are then ranked according to the number of high-scoring peptides matching onto each protein. In this way false positive peptides (and thus proteins) are eliminated. Scaffold analysis of DC8-IP results showed that all Mis12 components found by Mascot also passed the Scaffold "quality" filter (i.e. each matches two or more peptides, each with a probability score of 95% or more) and thus are genuine hits. Table 5.1 (Appendix) shows proteins identified on the basis of peptides, which have a Scaffold-peptide-probability score of over 95%, calculated by the 'Peptide Prophet algorithm'.

3.2.3. Possible improvement of IP-MS quality

For a possible improvement in purifying the Mis12 complex, further antibodies targeting subunits in addition to DC8 (e.g. Q9H410, Mis12 or PMF1) could be used for IP. Where novel proteins are found following pull down with one antibody, it is important to know if they are also pulled down with another antibody for the same complex. This would give us confidence that this result is not an artefact. Where a novel protein is found I suggest to raise antibodies against it and to perform IP experiments to examine whether a reciprocal

interaction (i.e. protein X pulls down Y and vice versa) can be identified. This would strengthen the evidence for a real, physiological interaction.

Limitations: The general strategy used here is a 'shotgun approach', in which a complex sample was digested and all the resultant peptides were analysed in one LC-MS/MS run. The advantage of this is that hundreds of proteins could be analysed in a single experiment. One significant limitation is that not every peptide will be identified, due to the sensitivity of the mass spectrometry detector and due to masking of low abundant peptides (which may include some kinetochore proteins) by high abundant peptides. Variations in separation and detection of peptides mean that this type of experiment is not always completely reproducible. One way of partially overcoming this limitation, is that the analysis could be repeated and the total set of proteins from both analyses would give a more complete picture of the proteins in the purified complex.

3.2.3. Follow-up experiments for interaction analysis

In IP-MS experiments several proteins had been identified, which were not known to be kinetochore components (e.g. SPAG5, C15orf23). Could these proteins be part of the kinetochore or involved in its function? To address this and to characterise novel proteins in general, several follow-up experiments could be performed.

a) IF-experiments would help to determine the localisation of those "unknown" proteins. High resolution experiments using LAP (GFP) tagging in BACs enables us to identify kinetochore proteins, as intensely-stained pairwise dots, in close proximity to the centromere of the condensed mitotic chromosomes. Furthermore these tagged proteins could be observed using time-lapse experiments, during mitotic cell cycle. This will tell us when the proteins become localised to the kinetochore and could give information about eventual degradation.

Using high resolution fluorescence microscopy the position of this tagged protein between inner centromere and the outer kinetochore can be judged relative to the position of specific markers, such as CREST for centromeres and Mis12 for the outer kinetochore.

b) Furthermore, roles for these proteins can be inferred from the phenotype observed in RNAi screens, by silencing the genes of candidate proteins and examining their effect on mitosis. In addition to that, mouse-LAP cell pools could be established and rescue experiments performed to discover if the LAP-tagged mouse genes rescue the depletion of the human mRNA by RNAi. These data could be used to look for similarities in phenotypes with known kinetochore components, e.g. the DC8/Mis12 complex. If knockdown of a novel protein phenocopies that of a known protein, e.g. a kinetochore protein such as Mis12, then it supports the evidence that this novel protein is involved in a related process. Such RNAi

screens for mitotic relevant proteins are performed in a genome-wide scale as part of the MitoCheck-project, at the EMBL Heidelberg (Neumann et al., 2006). The final result of this screen will be a comprehensive list of genes required for mitosis in human cells. It will enable scientists, for the first time, to know exactly which genes are active during mitosis and what happens in the cell when these genes are suppressed.

c) Fluorescence Recovery after Photo-bleaching (FRAP) experiments could be used to assess the dynamics of a fluorescently tagged protein on the kinetochore, giving us a measure of its rate of turnover in a living cell, during mitosis. These experiments would tell us whether the proteins are stably or rather transiently bound to the kinetochore. Such experiments were performed by (Andrews et al., 2003) and (Howell et al., 2004), observing that Mad1 is stably bound to the kinetochore, whereas for Mad2 there is a stable and a highly dynamic pool.

d) Similarity of a protein of interest to other proteins could be assessed using the BLAST algorithm (www.ncbi.nlm.nih.gov/BLAST). If nothing is known about the protein apart from its sequence, possible functional domains can be predicted using bioinformatics prediction programs such as the IMP-Annotator (Annotator.org) or NCBI's Conserved Domain Database (www.ncbi.nlm.nih.gov/sites/entrez?db=cdd). This kind of analysis could reveal motifs such as WD40-repeat domains, which mediates protein-protein interactions (Smith et al., 1999). Domain deletion experiments could be performed, to understand which part of the protein is involved in binding with the complex and targets it to the kinetochore. Ideally, one could knock down the endogenous protein whilst expressing mutated or truncated fluorescent tagged recombinant forms and assessing their localisation within the cell during mitosis.

e) Other interesting questions are: in what hierarchy do the components bind to each other, and how are they organised? In an approach similar to that of (Cheeseman et al., 2004) this could be addressed using a series of RNAi experiments to silence the expression of kinetochore proteins. To assess whether other kinetochore proteins still bind under these conditions, fluorescently tagged candidate proteins could be visualised by fluorescence microscopy, to determine whether they still bind to the kinetochore. Alternatively, kinetochore complexes could be purified under these conditions and analysed by mass spectrometry to determine which subunits are still present.

3.3. Interpretation of phospho-site mapping results

In phospho-site mapping experiments of interaction partners from DC8-IP, six proteins (PFKB2, C15orf23, DC8, Q9H410, RABGAP1 and SPAG5) were observed to be phosphorylated.

We expected to find more p-sites in kinetochore proteins in mitosis than in interphase, because there is a significant increase of total phosphorylation of proteins in mitosis relative to interphase, a fact which is been known for more than 20 years (Karsenti et al., 1987), and now known to be due to the action of mitotic kinases (Nigg, 2001). Furthermore the mitotic kinases, such as Plk1 and Aurora-B, as well as spindle-checkpoint kinases such as Bub1, BubR1 and Mps1 are localised in the centromere/kinetochore region in mitosis and so kinetochore proteins are prime candidates to be phosphorylated. Unexpectedly I found more sites phosphorylated in interphase than in mitosis, amongst the six proteins of interest that were mapped. One explanation for this could be that although I used the same amount of starting material (cell extract) for the IP from interphase and mitosis, the final yield of protein complex could have been higher for interphase than for mitosis. As shown in Fig 2.13, the bands of the interphase complex are slightly more intense than those of the mitotic complex; this is also reflected in sequence coverage which is for most proteins greater in the interphase than in the mitotic complex. For the mitotic complex less material was purified and therefore fewer phospho-peptides would have been generated and therefore fewer phospho-sites would have been detected.

As SPAG5 was not previously reported to be a component of the Mis12 complex, it was somewhat unexpected to find SPAG5 with the highest number of phospho-sites out of all those proteins found. Most the phospho-sites for this protein were mitosis specific and had not been previously reported. Conspicuously most of the phospho-sites were found within the N-terminal third of the protein (between residues S10 and T403, shown in Fig. 2.14). As SPAG5 is known to associate with spindle microtubules in early prophase (Abend et al., 1995; Mack et al., 2001; Gruber et al., 2002) this N-terminal region, specifically phosphorylated in mitosis, might be a functional domain which mediates the binding of SPAG5 to microtubules.

For phospho-site mapping, the sample was digested with three different proteolytic enzymes, allowing as many peptides as possible to be recovered and therefore the identification of as many phospho-sites as possible, amongst the entire amino acid-sequence of a protein. This helps to identify peptides which have not been found in a trypsin digest alone. For example, the phospho-serine 66 residue of SPAG5 was found in the GluC, but not in the trypsin digest.

The greatest limitation in phospho-site mapping is the ambiguity of the actual position of a specific p-site. The reason for this ambiguity is that the quality of the MS² and MS³ spectra is not sufficient to distinguish the residue which is phosphorylated. In Table 2.9, these sites are indicated in blue and counted as “possible positions”.

As mentioned previously, the method which was used in this study was a shotgun approach, meaning the peptides and phospho-peptides were analysed together and that could cause the problem that low abundant p-peptides could be masked by higher abundant unphosphorylated peptides. One strategy to overcome this problem is to use a phospho-peptide enrichment step before the HPLC separation. Two common ways of doing that are 1) Metal Oxide Chromatography (MOC), most often using titanium dioxide (Mazanek et al., 2007; Zhang et al., 2007) and 2) immobilized metal ion affinity chromatography (IMAC) (Corthals et al., 2005). Future studies investigating kinetochore protein phosphorylation may benefit from these approaches.

One important issue when studying protein phosphorylation is the stoichiometry of phosphorylation at a particular site. If a method could show that the phosphorylation of a site has a high stoichiometry, this would increase our confidence that this site is of physiological relevance. Two methods to obtain stoichiometry data are 1) phospho-peptide peak area quantification (PAQ) and 2) stable isotope labelling of amino acids in cell culture (SILAC). In PAQ, the integrated area under the HPLC UV-chromatogram trace corresponding to a known (phospho-) peptide can be used as a measure of the abundance of that peptide. By calibrating the HPLC with known amounts of standard peptides, semi-quantification can be obtained. In SILAC (Ong et al., 2002; Mann, 2006), cells grown in media with either heavy or light isotopes are treated in two different conditions (e.g. log growth vs. mitotic arrest with nocodazole). Differences in peak heights of the heavy and light forms can indicate the relative abundance of (phospho-) peptides under these two conditions.

When phospho-sites have been found, one immediate question could be: which protein kinase is responsible for this phosphorylation. One way of addressing this question could be to inhibit the action of particular kinases by RNAi. Alternatively, potent and specific kinase inhibitors could be used (Davies et al., 2000; Bain et al., 2003). If a phospho-site were lost under these conditions, this would indicate that the inhibited kinase is required for this phosphorylation, but this may not necessarily be direct (the inhibitor could be targeting an up-stream kinase).

For three well characterised mitotic protein kinases, potent and specific inhibitors have been developed. Two of these compounds, hesperadin and BI 2536 were discovered by Boehringer Ingelheim. Hesperadin inhibits Aurora kinases and its action can be explained entirely by the inhibition of Aurora-B (Hauf, 2003). BI 2536 is a potent Plk1 inhibitor and

currently is under clinical trials as an anti-cancer drug (Lenart et al., 2007; Steegmaier et al., 2007). If one adds these drugs to mitotic cells they still stay in mitosis with certain defects whereas addition to a mitotic cell of a Cdk inhibitor such as Roscovitine (Meijer et al., 1997) would cause cells to exit mitosis. The use of these inhibitors, especially of BI 2536 and hesperadin can be used in conjunction with IP mass spectrometry to characterise the kinase dependences of mitotic phospho-sites. Such studies could be used to enhance the DC8 data set and to discover potential Aurora and Plk1 dependent phospho-sites in kinetochore proteins.

3.3.1. Kinase consensus sequences

Phospho-sites found in this study (section 2.3.2 and Table 2.10) and their surrounding sequences were compared to published kinase consensus sequence motifs, to give an idea of the kinase required for a particular phosphorylation event. Out of the total 44 phosphorylations, five possible Aurora-sites, six possible Cdk-sites and five possible Plk1-sites were discovered in this comparison (Table 3.2).

Table 3.2. Possible P-sites found in this study.

Kinase	Consensus sequence (Reference)	Protein	p-sites found matching this consensus (this study)
Aurora	R/K-X- <u>S/T</u> -I/L/V (Cheeseman et al., 2002)	PFKFB2	S466
		RABGAP1	T47
			S76, S240, S362/364
CDK	<u>S/T</u> -P-X-R/K (Nigg, 1993)	PFKFB2	S493
		Q9H410	S28, S331
		RABGAP1	S419
		SPAG5	S43, S109
PLK1	D/E-X- <u>S/T</u> -Φ-X-D/E (Nakajima et al., 2003)	C15orf23	T242
		Q9H410	S68
		RABGAP1	S287, T924
		SPAG5	S10/12

Φ, hydrophobic amino acid; X, any amino acid.

3.3.2. Conservation of phospho-sites across species

If a phospho-site is widely conserved through evolution this suggests the site is important for the regulation of that protein. For the phospho-proteins DC8, Q9H410 and SPAG5, the sequences of the human (*Homo sapiens*), dog (*Canis familiaris*), chicken (*Gallus gallus*) and mouse (*Mus musculus*) orthologues were aligned by using the ClustaW algorithm. Positions of the mapped human phospho-sites were compared to the equivalent positions in the other

species, to assess their evolutionary conservation (Fig. 5.1, Appendix). For summary this comparison is shown in Table 3.3.

Table 3.3. Summary of conserved phospho-site residues, amongst three vertebrate species.

Protein	Number of p-sites in Human	Number of conserved sites in:					
		Dog	Seq.-identity to human	Mouse	Seq.-identity to human	Chicken	Seq.-identity to human
DC8	1	1	74%	1	67%	1	45%
Q9H1410	6	4	78%	4	70%	3	45%
SPAG5	24	21	70%	13	64%	No seq.	No seq.
Total no. of p-sites	31	26		18		4	

For DC8 the one threonine residue found phosphorylated in human, was found to be conserved in dog, mouse and chicken. This site is followed by proline, which is also conserved across all four species and forming a “TP”-site. As Cdks require “TP” or “SP”-sites as targets, a Cdk would be an attractive candidate kinase for phosphorylating this residue. For Q9H410 six phospho-sites were found in human, the exact position for two of them remains uncertain (serine 27/28 and serine S77/81). The S27/28 is conserved across all four species, whereas S331 is conserved in dog, and mouse; but conservation in chicken can not be determined because the chicken sequence is C-terminally truncated.

For SPAG5, 24 phospho-sites were found in human, eleven of those were found to be conserved amongst all three species (human, dog, mouse), the exact position for five of them remains uncertain (Fig. 5.1). One of these phospho-sites is S362/364. Here, the position (S362 or S364) is uncertain, these residues lie within a region of eight amino acids, which is conserved amongst all three species.

In the sequence comparison I found a total of 31 phospho-sites in human. Out of those 31 human sites, 26 (84%) are conserved in dog, whereas 18 sites (58%) are conserved in mouse and 57% are conserved in chicken. For all of these proteins considered for our analysis, there is a high sequence identity in mammalian proteins of at least 64%. This would suggest that the more conserved the overall protein sequence the greater the number of phospho-sites which also would be conserved.

This dataset is too small to make a generalisation about conservation of phospho-sites in eukaryotic proteins. A recent study (Jimenez et al., 2007) using a much larger number, of thousands of protein sequences across different species, shows that a general correlation between conservation of phospho-sites and conserved regions does exist (the more conserved the region, the more conserved the phospho-site).

Although the conservation of a phospho-site in other species strengthens the argument that this is a biologically important site, but formally speaking it does not demonstrate that: (a) the

site is also phosphorylated in other species nor, (b) that it is essential for the function or regulation of the protein.

3.3.3. Follow-up experiments for phospho-site analysis

In this study several phospho-sites had been found on kinetochore proteins and on other proteins which may play a crucial role in progressing mitosis (see above). To obtain a closer insight into the functional role of particular phosphorylation events further experiments could be interesting to follow up:

a) To study spatiotemporal regulation of these sites, phospho-specific antibodies could be generated. To identify in which phase of the cell cycle the phosphorylation appears, the cells can be synchronised and analysed for the phosphorylation state by using WB. Furthermore IF experiments could be performed to see where in the cell the phospho-epitope is localised during interphase and mitosis.

b) To discover the importance of the phospho-site, mutants could be expressed from cDNA or BACs, in which the relevant sites are either non-phosphorylatable (Ser or Thr to Ala; or Tyr to Phe) or which may mimic constitutive phosphorylation (for example Ser or Thr to Glu). The effects of these mutations on the cell cycle can be assessed by video-microscopy.

Ideally these mutants could be expressed with a background of knocking down the endogenous gene by RNAi. This could be performed by expressing a) mouse orthologues in BACs or cDNAs or b) RNAi resistant forms of the human sequence.

c) To identify the dependency of the phospho-sites on different kinases, phospho-mapping could be performed from complexes, following IPs from extracts of cells treated with specific kinase inhibitors such as BI2536, which inhibits Plks (Lenart et al., 2007) or Hesperadin which inhibits Aurora-kinases (Hauf et al., 2003). Although potentially very informative, results of these kinase inhibitor experiments should be treated with caution, because these effects could be indirect, i.e. the Aurora or Plk which is inhibited may act upstream of the kinase targeting the site (also see end of section 3.3).

3.4. Outlook: Kinetochore regulation by phosphorylation

Protein phosphorylation is one of the most widely studied regulatory mechanisms in biology, which has essential functions in signalling, metabolism and cell cycle control. How does phosphorylation regulate kinetochore proteins? This is not yet known, but by analogy with known phosphorylated proteins and enzymes, mechanisms could include:

Phospho-dependent inhibition of catalytic ability of an enzyme by adding a phosphate group to the catalytic site, e.g. protein kinase Cdc2 is inhibited by phosphorylation of the Tyr-15 residue, in its ATP-binding site (Gould et al., 1989).

Phospho-dependent conformational/structural change which for some enzymes can be key for regulating their activity, e.g. activation loop of protein kinases (Johnson et al., 1996).

Phospho-dependent protein-protein binding interaction, e.g. phosphatidylinositol-3-kinase (PI3K) binding to insulin receptor substrate-1 (IRS-1), (Backer et al., 1992) or SH3-domain and 14-3-3 proteins (Yaffe et al., 2001; Yaffe, 2002).

Phospho-dependent targeting of proteins to specific compartments within the cell, e.g. extracellular signalling-regulated kinase Erk2, which is upon phosphorylation by and upstream kinase translocated to the nucleus where it is targeting transcription factors, modulating gene expression (Khokhlatchev et al., 1998).

It is possible that some of the phosphorylation sites function as priming sites, which facilitate the recruitment of additional kinase molecules, which then could phosphorylate more sites in close proximity, e.g. polo-box recruits Plks to priming phospho-sites (Elia et al., 2003; Lowery et al., 2004). Since clusters of multiple phosphate groups are predicted to change the surface charge distribution significantly, these modifications could either induce structural changes within the kinetochore complex by altering subunit-interaction or they could change the affinity for molecules that are only temporarily associated with the kinetochore. We do not yet have a full insight into how the kinetochore proteins are regulated by each other and by post-translational modifications, therefore the detailed functional consequences of phosphorylation at the kinetochores remain unknown. Phosphorylation has a reversible nature and therefore could both loosen and tighten dynamic interactions between the complexes at the kinetochore, and thereby affect the attachment of the chromosomes to the mitotic spindle and the sensing of tension between sister chromatids.

Future challenges and the ultimate aim of this research would be to integrate the data of the protein-interaction and phosphorylation to generate a dynamic model for how the kinetochore is formed in mitosis, how it binds and detects microtubules, senses tension and coordinates the segregation of sister chromatids into daughter cells.

4. Materials and Methods

4.1. DNA and Cloning

4.1.1. Agarose gel electrophoresis

For 1% agarose gels, 0.5 g agarose was dissolved by heating in 50 ml 1x TAE buffer (40 mM Tris-acetate, 1 mM Na₂EDTA [pH 8.3]). After cooling down to ca. 60°C, the liquid was poured into the agarose gel caster. For visualization under UV light, 5 µl of 10 mg/ml ethidium bromide stock solution were added to 50 ml gel volume and distributed with the inserted comb. The gel was left to solidify for 30 min, running buffer TAE was added until it just covered the gel. As Molecular Weight Marker λ DNA digested with *Bst*EI was used. Samples were mixed with 6x loading buffer (0.25% bromophenol blue, 30% glycerol in water), the voltage was set to a constant 100 V and gel running time was typically 30 min.

4.1.2. Polymerase chain reaction (PCR)

PCR was performed in 50 µl reactions using the Long PCR enzyme mix (Fermentas), with 5 µl 10x PCR buffer (containing 15 mM MgCl₂), 1 µl of 10 mM dNTP, 0.5 µl of 100 µM primers, 0.5 µl DNA polymerase (Long-PCR enzyme mix [5 U/µl]), 1 µl template DNA (2.5 ng/µl) and topped up to 50 µl with nuclease-free water. The PCR reaction was performed in a MJ Research PTC-200 Peltier Thermal Cycler as follows: heating 2 min to 94°C to denature DNA strands, 30 amplification cycles with denaturation at 94°C for 20 seconds, annealing at determined annealing temperature for 30 seconds, extension at 68°C for 2-10 min depending on the length of the fragment (ca. 1 kB/min) and a final extension for 10 min. PCR products were separated on a 1% agarose gel and extracted with an PCR Purification Kit (Qiagen).

4.1.3. Primer design for cloning

PCR primer pairs were designed for amplifying kinetochore protein ORFs from cDNA (Table 2.1 and Table 4.2) clones. The strategy used for primer design was: a) the ORFs were inserted into the construct in-frame with the myc tag, b) the 3' end of PCR primers starting with a G or C nucleotide and c) reverse primers lacking STOP codons, except the reverse primer for Hec1 and Nuf2. Melting temperature (T_m) values were calculated (from ORF-derived section only) using the formula: $T_m = 4x (GC) + 2x (AT)$ and the website: www.pitt.edu/~rsup/OligoCalc.html. Designed primers are listed in Table 4.1.

Table 4.1. Primers used for cloning kinetochore ORFs.

Name	Sequence	Length	Tm	Description
SZ001	GGCTAGCTAGCATGGCGGGGTCTCCTGAG	29	60	DC8 Forward primer; <i>NheI</i> site
				DC8 Reverse primer; <i>XhoI</i> site
SZ023	GCCGCTCGAGCGTGTATCAAGATTAATTTTCTTTG	35	63	With 2 extra bases to put ORF in-frame with C-terminal tag.
SZ003	GGCTAGCTAGCATGACTTCAGTGACTAGATCAG	33	62	Q9H410 Forward primer; <i>NheI</i> site
				Q9H410 Reverse primer; <i>XhoI</i> site
SZ004	GCCGCTCGAGCGCTGACAAGATCCAGATCCAG	32	60	With 2 extra bases to put ORF in-frame with C-terminal tag.
SZ005	GGCTAGCTAGCATGTCTGTGGATCCAATGAC	31	58	Mis12 Forward primer; <i>NheI</i> site
				Mis12 Reverse primer; <i>XhoI</i> site
SZ006	GCCGCTCGAGCGAGATATTTTCAGTCGTTTCG	32	54	With 2 extra bases to put ORF in-frame with C-terminal tag.
SZ007	GGCTAGCTAGCATGTGGGAGCGGCTGAAC	29	58	Zwisch Forward primer; <i>NheI</i> site
				Zwisch Reverse primer; <i>NotI</i> site,
SZ022	ATAAGAATGCGGCCGCTCTTGAAATGCACCTGGCTG	36	68	With 1 extra base to put ORF in-frame with C-terminal tag.
SZ009	GGCTAGCTAGCATGGCCGCCCTTCCGC	26	52	Spc24 Forward primer; <i>NheI</i> site
				Spc24 Reverse primer; <i>XhoI</i> site
SZ021	GCCGCTCGAGCGCCACTCGGTGTCCACC	28	72	With 2 extra bases to put ORF in-frame with C-terminal tag.
SZ011	GGCTAGCTAGCATGGTAGAGGACGAACTGG	30	58	Spc25 Forward primer; <i>NheI</i> site
				Spc25 Reverse primer; <i>XhoI</i> site
SZ012	GCCGCTCGAGCGATTATAAACCGTGGCAGTAAAAG	35	62	With 2 extra bases to put ORF in-frame with C-terminal tag.
SZ017	GGGGTACCATGAAGCGCAGTTCAGTTTC	29	62	Hec1 Forward primer; <i>KpnI</i> site, with extra base to put ORF in-frame.
SZ018	CCCAGCTTTCATTCTTCAGAAGAGCTTAATTAG	34	66	Hec1 Reverse primer; <i>HindIII</i> site, with STOP codon.
SZ024	CTGCAGAAAGGTACCGATGGAACTTTGTCTTTCCCC	36	60	Nuf2 Forward primer; <i>KpnI</i> site, with extra base to put ORF in-frame.
SZ020	GGGGTACCTCAGGTTGACATTTGAACATC	30	60	Nuf2 Reverse primer; <i>KpnI</i> site, with STOP codon.

Legend: Following colour code is used: red, extra base-pairs (to increase the restriction enzyme cleavage efficiency for PCR products); blue, restriction site; black, sequence derived from the ORF (15-25 bp); underlined codon, STOP codon for reverse primers Hec1 and Nuf2.

4.1.4. Restriction enzyme digest

Digestions typically were done in a volume of 40 µl, containing 5 µg DNA (purified PCR-product or Vector-DNA), 4 µl 10x reaction buffer, 0.4 µl BSA (10 µg/µl), 1 µl restriction enzyme [10 U/µl] and topped up to 40 µl with water. Reactions were incubated at 37°C for 1-3 h. Dephosphorylation of the vector was achieved by adding 2 µl Alkaline Phosphatase (Roche) to the sample for 1 h at 37°C. The samples were separated on a preparative 1% agarose gel and fragments were cut out with a razor blade under UV illumination. DNA was extracted from the gel using a Gel Extraction Kit (Qiagen) and the DNA concentration of the elution was estimated comparing sample staining intensity to size marker intensity.

4.1.5. Ligation of PCR fragments into a vector

The ligation of insert and vector DNA was performed by using the Rapid DNA Ligation Kit (Fermentas). Ligation typically was done in a total volume of 20 µl, containing 4 µl 5x Rapid ligation buffer, 1 µl T4 DNA ligase (5 U/µl) and water. A molar ratio of insert to vector of 5:1 (cohesive ends) or 3:1 (blunt ends) was used. The ligation reaction was done at 20°C for 1 h.

4.1.6. Transformation

For transformation, DNA preparation, cloning and glycerol stocks competent *E.coli* DH5α cells were used. They have a more permeable cell membrane for a better uptake of foreign DNA. *E.coli* BL21 (DE3) cells were used for protein expression. Cells were slowly thawed on ice and 100 µl cells were added to the ligation reaction. The mix was incubated 15 min on ice and afterwards shifted to 42°C for 60 seconds for heat shock. After further 2 min of incubation on ice, 1 ml pre-warmed Luria Bertani (LB) medium (10 g bacto-tryptone, 5 g bacto-yeast extract, 10 g NaCl in 1 liter H₂O (pH 7.0)), without antibiotics, was added. The bacteria were incubated at 37°C for 30 min or 2 h with agitation to prepare for growth on ampicillin or kanamycin respectively. Cells were pelleted at 5000 rpm for 5 min, resuspended in 100 µl of the remaining supernatant, plated on an appropriate selection agar plate (LB + antibiotics) and grown at 37°C overnight.

4.1.7. Preparation of DNA

For mini-preps, a single colony was used to inoculate 4 ml LB + antibiotics. For maxi-preps, 4 ml of pre-culture were used to inoculate 250 ml LB + antibiotics. All cultures were grown at 37°C overnight. On the next day a fraction (0.5 ml) of the 4 ml overnight culture was mixed 1:1 with 87% glycerol, snap frozen and stored at -80°C for backup as a glycerol stock. DNA was prepared according to the mini- or maxi-prep manufacturer's protocols (both Qiagen).

The DNA was eluted in water, and the concentration was determined by measuring its absorption at 260 nm (assuming that, for double-stranded DNA, one A_{260} unit = 50 µg/ml). The size of the plasmid construct was confirmed by analysing a fraction of the sample on a 1% agarose gel. DNA was stored at -20°C.

4.1.8. cDNA

The pcDNA3.1_9myc vector contains 9 myc epitopes (the 1 his epitope is out of frame) and uses an ampicillin and a neomycin resistance cassette as selection marker for bacteria (*E.coli*) and human (HeLa) cells, respectively. The correct orientation and sequence of the inserts and junctions were confirmed by automated DNA sequencing.

Table 4.2. Kinetochore cDNA constructs used in this thesis.

Insert (size)	Vector (size)	5'	3'	Source
DC8 (846 bp)	pBluescriptR (2998 bp)	<i>Xho</i> I	<i>Bam</i> HI	RZPD, IRAKp961F1848Q2
Q9H410 (1071 bp)	pcMV-Sport6 (4400 bp)	<i>Sal</i> I	<i>Not</i> I	RZPD, IRAKp961K08119Q2
Mis12 (618 bp)	pOTB7 (1815 bp)	<i>Eco</i> R I	<i>Xho</i> I	Iain Cheeseman (IMC, La Jolla, USA)
Spc24 (594 bp)	pET28(+) (5370 bp)	<i>Nde</i> I	<i>Not</i> I	Todd Stukenberg (University of Virginia Medical School, Charlottesville, USA)
Spc25 (675 bp)	pET28(+) (5370 bp)	<i>Nde</i> I	<i>Not</i> I	Todd Stukenberg (University of Virginia Medical School, Charlottesville, USA)
Hec1 (1929 bp)	pcMV-Sport6 (4396 bp)	<i>Eco</i> R V	<i>Not</i> I	RZPD, IRATp970G0153D6
Nuf2 (1395 bp)	pDNR-LIB (4160 bp)	<i>Sfi</i> I	<i>Sfi</i> I	RZPD, IRAUp969D0245D6
Zwilch (1434 bp)	pWhitescript4stopEGFP	<i>Bam</i> HI	<i>Sal</i> I	Tim J Yen (Fox Chase Cancer Center, Philadelphia, USA)
Zw10 (2337 bp)	pBluescript II KS (3000 bp)	<i>Eco</i> R I	<i>Xho</i> I	Byron Williams (Cornell University, Ithaca, New York, USA)
DC8 (846 bp)	pcDNA3.1 9mycC (5830 bp)	<i>Xho</i> I	<i>Nhe</i> I	this thesis
Q9H410 (1071 bp)	pcDNA3.1 9mycC (5830 bp)	<i>Xho</i> I	<i>Nhe</i> I	this thesis
Mis12 (618 bp)	pcDNA3.1 9mycC (5830 bp)	<i>Xho</i> I	<i>Nhe</i> I	this thesis
Spc24 (594 bp)	pcDNA3.1 9mycN (5830 bp)	<i>Xho</i> I	<i>Nhe</i> I	this thesis
Spc25 (675 bp)	pcDNA3.1 9mycN (5830 bp)	<i>Xho</i> I	<i>Nhe</i> I	this thesis
Hec1 (1929 bp)	pcDNA3.1 9mycC(5830 bp)	<i>Kpn</i> I	<i>Hind</i> III	this thesis
Nuf2 (1395 bp)	pcDNA3.1 9mycC (5830 bp)	<i>Kpn</i> I	<i>Kpn</i> I	this thesis
Zwilch (1434 bp)	pcDNA3.1 9mycC (5830 bp)	<i>Nhe</i> I	<i>Not</i> I	this thesis

4.2. Expression and purification of recombinant protein

4.2.1. Expression in *E.coli* BL21 (DE3)

E.coli BL21 (DE3) codon plus competent cells were heat-shock transformed (section 4.1.6) with a pET28a expression plasmid containing the cDNA sequence for the desired protein (Spc24 or Spc25). This allows expression of the protein with a C-terminal His₆-tag, under a T7 promoter. Following transformation, cells were directly added to 20 ml LB-medium containing antibiotics (30 µg/ml kanamycin) and incubated overnight at 37°C with shaking at 220 rpm. For protein expression, the overnight cultures were diluted 1:100 in LB + Kan (small-scale: 25 ml, large-scale: 1 L), and incubated with shaking at 37°C. The OD₆₀₀ was measured at regular intervals until it had reached approximately 0.6, at which time expression was induced by adding isopropyl-β-D-thiogalactopyranoside (IPTG, final concentration 1 mM) to the cultures and continuing incubation at 37°C. 1 ml samples of the culture were taken before the IPTG induction and every hour during 5 hours for expression timepoint analysis. The OD₆₀₀ measurements were recorded, the cells were pelleted and resuspended in 2x sample buffer (SB), sonicated 5x 15 sec, heated to 95°C for 15 min, snap frozen and kept at 20°C for western blot (WB) analysis. To test the solubility of the expressed proteins, a 1 ml sample of the culture from the 5 h timepoint was spun down, resuspended in 20 µl 1xTBS-Tx + PIM, sonicated 5x 15 sec on ice and spun for 10 min at 3000 g, 4°C. The supernatant and the pellet (resuspended in 20 µl 1xTBS-Tx + PIM) were mixed with 2xSB and analysed by SDS-PAGE and Coomassie staining. The large-scale expression culture was pelleted at the 5 h post-IPTG timepoint by spinning for 20 min at 3000 g (4°C). The bacterial pellet was washed once with 40 ml ice-cold PBS, re-spun as before, snap frozen and kept at -80°C. Spc24-His₆ and Spc25-His₆ protein purification was performed as described in paragraph 4.3.2.

4.2.2. In vitro translation / transcription (IVT) and phosphoimaging

A coupled transcription-translation system ('TnT', Promega) was used for generation of radioactively labelled proteins. 25 µl 'TnT' rabbit reticulocyte lysate, 2 µl reaction buffer, 1 µl amino acids without methionine (1 mM), 2 µl ³⁵S-methionine (10.5 mCi/ml), 1 µl T7 or SP6 DNA polymerase and 1 µg plasmid DNA (maxi-prep) were incubated in a total volume of 50 µl. The reaction was performed for 90 min at 30°C. 2 µl of lysate were separated by SDS-PAGE and fixed in fixing solution (45% methanol, 10% acetic acid) for 15 min. Gels were dried on a vacuum gel drier at 80°C for 1.5 – 2 h. The dried gel was exposed to a phosphoimager screen (Molecular Dynamics) overnight. The signal was read using a Storm

860 Phosphoimager (Molecular Dynamics) and images were processed using ImageJ software (<http://rsb.info.nih.gov/ij/>).

4.3. Antibodies and peptides

4.3.1. Antibodies for western blotting

For Western blotting, all antibodies (Table 4.2) were diluted in TBS-Tw containing 5% non-fat dried milk (section 4.4.5). Primary antibody dilutions were stored with 0.04% NaN₃ and re-used several times. Secondary antibodies were HRP-coupled anti-rabbit or anti-mouse antibodies generated in goat and sheep, respectively (Sigma) and both were used at a 1:5000 dilution. When non-crosslinked antibodies were used for immunoprecipitations (IPs), antibodies may co-elute from the beads along with the desired immunoprecipitates. In these cases, 'Trueblot' secondary HRP-coupled anti-rabbit antibody (eBioscience) was used (at 1:7500). This reagent recognises native primary antibodies used for western blotting, but not antibody heavy (~55 kDa) and light chains (~23 kDa) co-eluting in the IP, which would be denatured during the SDS-PAGE/western-blotting procedure.

Table 4.2. Primary antibodies used for Western Blotting.

Epitope	Dilution	Species	Source, Ab code
Cdc27	1:1000	rabbit	Christian Gieffers (Gieffers et
DC8	1:1000	rabbit	this study, Ab1621
Hec1	1:1000	rabbit	Jim Hutchins, Ab510
His	1:500	mouse	Penta-His, Clontech
Mis12	1:500	rabbit	Jim Hutchins, Ab506
Myc	1:5000	mouse	Sigma, 9E10
Nuf2	1:1000	rabbit	Jim Hutchins, Ab507
Pds5B	1:2000	rabbit	Björn Hegemann, Ab1531
Q9H410	1:1000	rabbit	this study, Ab1622
Smc3	1:1000	rabbit	Iza Sumara, Ab727 (Sumara
Spc24	1:1000	rabbit	Todd Stukenberg, Ab460
Spc25	1:1000	rabbit	Todd Stukenberg, Ab463
Spc24	1:500	rabbit	this study, Ab889
Spc25	1:100	rabbit	this study, Ab887

4.3.2. Antibody generation

4.3.2.1. Peptide antibodies

In order to generate polyclonal antibodies against a peptide derived from a protein, it is important to choose a region of high antigenicity, of around 20 amino acid residues (Table 4.3). To predict the antigenicity of protein regions, Lasergene Protean software from

DNASTar was used. The selected peptides were synthesised (Madalinski M., IMP-IMBA Protein Chemistry Facility), covalently conjugated to keyhole limpet hemocyanin (KLH) and sent to Gramsch Laboratories (Schwabhausen, Germany) for rabbit immunisation. Antibodies specifically recognising the antigenic peptides were affinity purified on a column of immobilised peptide, coupled to a POROS epoxide matrix (Applied Biosystems), using a fast protein liquid chromatography (FPLC) system. After washing, antibodies were eluted first with counterions (1.5 M MgCl_2 in 100 mM potassium acetate, pH 5.2), then with low pH (100 mM glycine, 100 mM NaCl, pH 2.45). The eluates were both buffered to neutral pH with 2 M HEPES and referred to here as MgCl_2 and glycine eluates. Eluates were dialysed in Spectrum/Por dialysis tubing Molecular Weight Cut-Off (MWCO) 3.5 kDa against Hepes-buffered saline (HBS: 20 mM Hepes-KOH, pH 7.5, 150 mM NaCl) containing 10% glycerol, then concentrated to roughly 1 mg/ml using Amicon Centripreps (Millipore, MWCO 30 kDa). Antibody concentration was determined by photometric analysis at 280 nm ($\text{OD}_{280} = 1$ corresponds to 1.4 mg/ml antibody). Antibody aliquots were frozen in liquid N_2 and stored at -80°C . Working stocks containing 0.02% NaN_3 were stored at 4°C .

4.3.2.2. Recombinant protein antibodies

In order to raise polyclonal antibodies against recombinant proteins Spc24 and Spc25, these proteins were over-expressed in *E.coli* BL21 (DE3) cells (section 4.2.1), then purified via their His_6 tags, and sent to Gramsch Laboratories for rabbit immunisation. Specific antibodies were then purified from the immune sera.

Spc24- His_6 and Spc25- His_6 purification: Due to their insolubility, the recombinant proteins Spc24- His_6 and Spc25- His_6 were affinity purified with Ni-NTA beads (Qiagen) under denaturing conditions using the following (slightly modified) protocol from Todd Stukenberg (personal communication): Bacterial pellets were resuspended in 25 ml binding buffer (20 mM Tris-HCl pH 7.5, 0.5 M NaCl, 5 mM imidazole, PIM, PMSF) + 6 M guanidine hydrochloride (GuHCl). Before rotating (end-over-end) 20 min at 20°C , lysozyme was added to 0.2 mg/ml and NP40 to 0.5%. Afterwards, cells were sonicated 5x 15 sec, on ice. The lysate was spun at 11000 rpm (14000 g) in an SS34 rotor at 4°C for 20 min. To extract protein from the pellet, the pellet was resuspended in 25 ml binding buffer + 6 M GuHCl by vortexing, and re-spun as before. Ni-NTA beads were washed twice with binding buffer, then the extract supernatant was added and rotated at 4°C for 1 h to bind His_6 -tagged proteins. Beads were pelleted, washed 3x briefly with wash buffer (20 mM Tris-HCl pH 7.5, 0.5 M NaCl, 30 mM imidazole) + 6 M GuHCl and additionally washed 3x briefly with wash buffer + 6 M urea. Resuspended beads in 10 ml wash buffer + 6 M urea were poured into a 10 ml Poly-Prep column (Bio-Rad) and washed once with 10 ml wash buffer + 6 M urea. To elute

the proteins off the column, beads were resuspended in 1 ml elution buffer (20 mM Tris-HCl pH 7.5, 0.5 M NaCl, 300 mM imidazole, 8 M urea), mixed by end-over-end rotation for 10 min and the eluate was collected in a 1.5 ml eppendorf tube. A fraction of the eluates was analysed by SDS-PAGE and Coomassie staining, and their concentrations, assessed by the Bradford assay, were approximately 5 mg/ml. The Spc24-His₆ and Spc25-His₆ eluates were dialysed in Spectrum/Por dialysis tubing (MWCO 3.5 kDa) against PBS + 3 M urea at 4°C overnight and were TCA precipitated (by adding 2 volumes 20% trichloroacetic acid (TCA), incubating on ice for 10 minutes and spun at 13000 rpm for 1 min at 4°C). The supernatant was aspirated, and the protein pellet was washed with 1:1 ethanol:acetone, air dried, and sent to Gramsch for immunisation.

Preparation of Spc24-His₆ and Spc25-His₆ coupled columns: Antibodies specifically recognising the antigenic proteins, Spc24-His₆ and Spc25-His₆, were affinity purified by covalently coupling the proteins to Amersham CNBr-activated Sepharose beads (GE Healthcare), under denaturing conditions (in urea). Before coupling, 500 µg of Spc24-His₆ and Spc25-His₆ protein were dialysed overnight against coupling buffer (100 mM NaHCO₃ pH 8.2, 500 mM NaCl, 6 M Urea) and CNBr-activated Sepharose beads were prepared according to the manufacturer's instructions. For coupling, 500 µg of Spc24-His₆ and Spc25-His₆ protein, in coupling buffer, were each mixed with 100 µl beads and incubated in Poly-Prep columns with end-over-end rotation for 1 h at 20°C. The excess ligand was drained from the column, and the beads were washed with 5 bead-volumes (bv) of coupling buffer on the column and remaining active groups on the beads were blocked by adding 0.1 M Tris-HCl, pH 8.0 and incubating for 2 h at 20°C. After coupling, the beads were washed 2x with 10 ml PBS then 1x with 10 ml 10 mM Tris pH 7.5. The beads were pre-eluted by washing 1x with 10 ml 2 M MgCl₂, 1x with 10 ml 10 mM Tris pH 7.5 and 1x with 10 ml 0.1 M glycine pH 2.5 and 1x with 10 ml 10 mM Tris pH 7.5.

Antibody extraction: Immune sera were prepared as follows: 5 ml of each immune serum was mixed with an equal volume of Freon (trichlorotrifluoroethane). After centrifugation at 2000 rpm for 2 min, each serum had separated into three liquid phases: bottom = Freon; middle = lipid; top = aqueous. The upper phases of each, containing soluble proteins including extracted antibodies, were transferred into fresh Falcon tubes.

Negative selection: Extracted antibodies from each serum were subjected to negative selection on two His₆-peptide columns. To prepare these columns, the peptide SGSGHHHHHH (Kpep 1693) was coupled to POROS-maleimide beads at a density of 3.3 mg peptide per mg beads. 100 µl of these beads were washed twice with 10ml PBS in a Poly-Prep column, then the extracted antisera were added and incubated with end-over-end

rotation for 1 h at 4°C. Afterwards, the unbound sera (containing antibodies which do not recognise the His₆ tag) were allowed to pass through the columns and were collected.

Positive selection (affinity purification): The collected flow-throughs from the His₆-peptide columns were applied to their respective (Spc24-His₆ or Spc25-His₆)-coupled beads in Poly-Prep columns, and incubated with end-over-end rotation overnight at 4°C. The columns were washed twice with 10 ml 10 mM Tris pH 7.5 and twice with 10 ml 10 mM Tris pH 7.5, 0.5 M NaCl. Antibodies were eluted from the column first with 4 ml 2 M MgCl₂. The column was equilibrated with 10 ml 10 mM Tris pH 7.5, then antibodies were eluted with 4 ml 0.1 M glycine, pH 2.5 and neutralised with 0.4 ml 1 M Tris pH 8.0. Elutions were dialysed as described above (section 4.3.2.1).

Table 4.3. Antibodies and their respective antigens.

Protein	Rabbit no. (peptide)	Immunogenic region
ZW10 [601-621]	854 (kpep 1619)	CLERLSSARNFSNMDDEENYS
Zwilch [515-537]	844 (kpep 1620)	CRPTAVKNLYQSEKPKWVRVEIY
DC8 [265-282]	842 (kpep 1621)	CPQRKWYPLRPKKINLDT
Q9H410 [317-337]	838 (kpep 1622)	CVQLGKRSMQQLDPSPARKLL
Spc24	889	Full length protein plus His6 tag
Spc25	887	Full length protein plus His6 tag

Legend: Peptides of about 20 amino acid residues additionally including an C-terminal cysteine for coupling the to keyhole limpet hemocyanin (KHL). Spc24 and Spc25 antibodies were generated against the full-length protein including a His-tag.

4.4. Protein purification and analysis

4.4.1. Preparation of cell extract

Extracts were prepared freshly by thawing cell pellets at 37°C and adding freshly thawed extraction buffer (0.1% Triton X-100, 20 mM Tris-HCl (pH 7.5), 100 mM NaCl, 2 mM EGTA, 0.2% NP-40, 10% glycerol, 5 mM Na-pyrophosphate, 20 mM β-glycerophosphate, 10 mM NaF, 1 mM Na₂VO₄, 1 μM okadaic acid (OA), 1 mM DTT, 0.1 mM PMSF (phenylmethylsulphonylfluoride), 1x PIM (protease inhibitor mix, 10 μg/ml each chymostatin, leupeptine, pepstatin, in DMSO). 1 ml of buffer was used per approximately 65 x 10⁶ cells (1 Nunc dish) to obtain a protein concentration of 10 mg/ml. For lysis, cells were homogenized in a Potter-Elvehjem glass-Teflon homogenizer on ice for 20 min by repeated douncing (about 20 times in total). Afterwards, crude extracts were spun in centrifuge tubes suitable for Sorvall SS-34 rotor at 16000 g for 10 min at 4°C to pellet insoluble material. The supernatant ('S20') was transferred into a fresh tube, the pellet was discarded and the

protein concentration was determined by Bradford assay. Extracts were used directly for analysis and protein purification to avoid potential freezing artefacts.

4.4.2. SDS-polyacrylamide gel electrophoresis (SDS-PAGE)

Protein samples were separated under denaturing conditions on 10% or 8% - 12% gradient SDS-Polyacrylamide gels according to Laemmli (1970) in 1x running buffer (25 mM Tris-base, 192 mM glycine and 0.1% sodium dodecyl sulfate [SDS]). Gels consisting of a stacking gel and a separating gel (gel composition is shown in Table 4.4) were always prepared just before use. The standard 'Mini-gel' has a length, width and thickness of 8x 8x 0.075 cm, the 'Maxi-gel' 13 x 13 x 0.15 cm. The separating gel polymerised under iso-propanol before the stacking gel was pipetted into the gel system and a comb was inserted carefully into the stacking gel. The samples were mixed with 4 x SDS sample buffer (125 mM Tris-base (pH 6.8), 4% SDS, 20% glycerol, 200 mM dithiothreitol (DTT), 0.02% bromophenol blue), boiled for 5 min at 95°C and briefly spun before loading. For Coomassie staining and western blotting 10 µl SDS PAGE molecular weight marker (Bio-Rad) or PageRuler prestained protein ladder (Fermentas) and for silver staining 1 µl of the size marker was loaded. The gels were run with a constant current of 25 mA per 0.75 mm gel (thickness) until the dye just ran out of the gel.

Table 4.4. SDS polyacrylamide gel composition.

Separating gel	8%	10%	12%	Stacking gel	6%
(3 mini gels)				(3 mini gels)	
30% AA	4 ml	5 ml	6 ml	30% AA	1 ml
H ₂ O	6.75 ml	5.75 ml	4.75 ml	H ₂ O	3.62 ml
1.5 M Tris-base pH 9.2	4 ml	4 ml	4 ml	1.5 M Tris-base pH 9.2	0.3 ml
20% SDS	80 µl	80 µl	80 µl	20% SDS	25 µl
100% TEMED	15 µl	15 µl	15 µl	100% TEMED	5 µl
10% APS	150 µl	150 µl	150 µl	10% APS	50 µl

Legend: AA refers to 'Protogel' (30% acrylamide solution, 37.5:1 acrylamide to bisacrylamide, National Diagnostics).

4.4.3. Coomassie staining

Gels were soaked in staining solution (20% isopropanol, 7.5% acetic acid, 0.2% Coomassie Brilliant Blue R250) for 10 min and destaining solution (20% isopropanol, 7.5% acetic acid) until sufficiently destained. To accelerate the staining and destaining procedure, the solutions were heated.

4.4.4. Silver staining

After SDS-Page the gel was soaked in fixing solution (45% methanol, 10% acetic acid in water) for 15 min, transferred into freshly prepared Farmer's Reducer (0.99 g $K_3Fe(CN)_6$, 0.47 g Na_2SO_3 in 100 ml water) for exactly 2 min and destained with water washes until the yellow colour completely disappeared (30 min). Water was exchanged for freshly prepared 0.1% silver nitrate ($AgNO_3$) in water and the gel was shaken for at least 15 min. Then the gel was washed for 30 seconds in water and then in freshly prepared 2.5% Na_2CO_3 solution for 30 seconds. The silver stain was developed with 0.1% formaldehyde in 100 ml 2.5% Na_2CO_3 solution. The staining reaction was stopped by adding an excess of 10% acetic acid. Gels were stored in 0.1% acetic acid at 4°C. For each solution mentioned only mono-Q-purified water was used. Glassware was pre-washed with detergent, ethanol and acetone.

4.4.5. Western blotting

After SDS polyacrylamide gel electrophoresis, protein gels were equilibrated in transfer buffer (39 mM glycine, 48 mM Tris-base, 0.0375% SDS, 20% methanol) for 10 min before blotting. ImmobilonP polyvinyl difluoride (PVDF) membranes (Millipore) were activated with methanol for 2 min, washed with deionised water for 2 min and equilibrated in transfer buffer for 2 min. Membrane and gel were sandwiched by 6 layers of wet electrode paper (Novablot, Amersham) for blotting. The transfer was performed in a semi-dry blotting chamber at 1.7 mA/cm² for 1.5 h. After blotting, residual detergent was washed off the membrane with deionised water. Staining with Ponceau S (0.2% Ponceau S sodium salt, 5% acetic acid) for 5 min and destaining in H₂O revealed the marker bands and the efficiency of the transfer. The complete removal of the Ponceau S stain was achieved by shaking the membrane in Tris-buffered saline (TBS) (140 mM NaCl, 2.5 mM KCl, 25 mM Tris pH 8.0) containing 0.05% Tween-20 (TBS-Tw) for 10 min. To block unspecific binding sites the PVDF membrane was incubated with TBST-Tw containing 5% non-fat dried milk for 30 min. Antibodies were diluted in TBS-Tw containing 5% milk and used at the optimised concentration (ca. 2 µg/ml). Primary antibodies were incubated on the PVDF membrane for 1h at 20°C or overnight at 4°C. Five washes in 30 min with TBS-Tw were performed prior to adding the secondary antibody. As secondary antibodies anti-rabbit (1:5000) or anti-mouse (1:10000) antibodies coupled to horseradish peroxidase (HRP) (Sigma) were used. After 30 to 60 min secondary antibody incubation the immunoblots were washed 3 times for 5-10 min with TBST-Tw. The signal was generated using enhanced chemiluminescence (ECL) reagent (500 µl of 13 mg/ml coumaric acid in dimethylsulfoxide (DMSO), mixed with 1 ml of 44 mg/ml luminol in DMSO and dissolved in 200 ml 100 mM Tris-HCl [pH 8.5]) which was supplemented with 3% H₂O₂ (prepared from a 30% stock. The chemoluminescent signal was detected on high

performance chemiluminescence films (Hyperfilm ECL, Amersham) in 3 seconds to 20 min, depending on the intensity of the signal. Afterwards, blots were washed with water, dried on paper towels and stored at 20°C, the films were scanned and annotated using Adobe Photoshop software.

4.4.6. Stripping of PVDF membrane for reprobing

Membranes were reactivated with methanol, briefly washed in TBS-Tw and equilibrated in Stripping buffer (62.5 mM Tris-HCl pH 7.5, 2% SDS, 0.7% β -mercaptoethanol). Stripping was carried out in closed plastic boxes, shaking in a pre-warmed (55°C) water bath for 20 min. Afterwards the membrane was washed 3 times with TBS-Tw for 5 min and blocked with TBS-Tw containing 5% milk, followed by another round of antibody incubation. Alternatively, the membrane was stripped with 0.2 M NaOH for 10 min, followed by washing with TBS-Tw and blocking with 5% milk in TBS-Tw.

4.5. Immunoprecipitation and Mass Spectrometry

4.5.1. Antibody coupling and cross-linking

For immunoprecipitation antibodies were coupled and covalently cross-linked to Affi-Prep Protein-A beads (Bio-Rad) or protein-G beads ("Gamma Bind Plus Sepharose", GE Healthcare). Typically 1 μ g antibody was used per 1 μ l beads. Before coupling the beads were washed 3 times with 10 bead-volumes (bv) TBS-Tx (1x TBS + 0.04% Triton X-100) in a 1.5 ml Eppendorf tube. Antibodies were added to the beads after the third washing step, when the beads were still in solution. After gently mixing by flicking, the tube was incubated for 60 min with end-over-end rotation at 4°C. The beads were washed 3 times with 10 bv TBS-Tx after coupling. The coupled beads can be used for immunoprecipitation at this step, but following glycine elution, major bands for immunoglobulin heavy and light chains (50 and 25 kDa, respectively) would appear on SDS-PAGE, and would interfere with the identification of the proteins of interest by mass spectrometry. To avoid this, antibodies can be covalently cross-linked to the beads with dimethylpimelimidate (DMP, Sigma). After washing the beads 3 times in 0.2 M sodium borate (pH 9.2), DMP was added to a final concentration of 20 mM while mixing the beads with 10 bv sodium borate. Following 30 min end-over-end rotation at 20°C, the cross-linking reaction was stopped by washing the beads 3 times with 250 mM Tris-HCl (pH 8) and with 3 times TBS-Tx for 5 min at 4°C. Unbound immunoglobulins were eluted from the beads by washing 3 times briefly with ice-cold 100 mM glycine (pH 2) and 3 times with TBS-Tx to restore the pH value to 7. Beads were stored in TBST-Tx containing 0.02% NaN₃ at 4°C and re-used several times.

4.5.2. Immunoprecipitation (IP)

HeLa cell extracts were prepared as described. Depending on the experimental scale, the IPs were performed in 15 ml Falcon or in 0.5 ml Eppendorf tubes (low protein binding), containing antibody-coupled or cross-linked beads. Aiming to load the antibody-coupled beads with extract at sub-saturation levels, 4 mg protein per 20 μ l beads were used for a standard IP. After incubating the IP, rotating end-over-end for 1 h at 4°C, beads were pelleted and the supernatant (unbound proteins) was and kept for further analysis. Beads were washed 3 times briefly and 3 times for 10 min in 20-100 μ l ice-cold extraction buffer (section 4.4.1). Due to the interference with MS/MS analysis, detergent was removed by washes TBS when samples were prepared for mass-spectrometry. Before protein elution, the beads were washed once briefly with 150 mM NaCl to remove buffering agents. Proteins were eluted from the cross-linked beads with low pH by resuspending the beads for 1 minute in 1.5 μ l 0.1 M glycine (pH 2), pelleting the beads and carefully transferring the supernatant into a fresh Axygen low-retention 0.2 ml PCR tube containing 1.5 M Tris-HCl (pH 9.2) (5 μ l Tris per 100 μ l eluate). The eluates were taken up in 4x SDS sample buffer to be analysed by western blot, silver gel or further processed in in-solution digests for mass-spectrometry. Bands from silver gels were excised with sterile razorblades and submitted to the IMP-IMBA Protein Chemistry Facility, to perform the mass spectrometry analysis.

4.5.3. In-solution digest

An in-solution digest is the proteolytic digestion of a sample of dissolved proteins (as opposed to an excised gel-band) into peptides which can then be analysed by mass-spectrometry. By reducing the protein with dithiothreitol (DTT) and covalently modifying its cysteine residues with iodoacetamide (IAA), a proteolytic digest becomes possible because the protein becomes partially unfolded and is therefore better accessible for proteases. To identify proteins and binding partners, the digestion of the sample with a single protease, trypsin (Try) is sufficient. Trypsin specifically cleaves proteins on the carboxyl side (or 'C-terminal') of lysine and arginine residues (Olsen et al., 2004), except when either is followed by proline. But for detection of protein modifications such as phosphorylation sites, a higher sequence coverage was necessary (Yates et al., 2000). Therefore the samples were split into three and separately digested with two additional proteases, GluC (which selectively cleaves peptide bonds C-terminal to glutamic and aspartic acid residues) and chymotrypsin (Cht) (which cleaves peptides at the carboxyl side of tyrosine, tryptophan and phenylalanine, although over time it also hydrolyses carboxyl sides of leucine and isoleucine. The pH of the glycine eluates was checked (using a pH indicator strip, range pH 6.5-10.0) and adjusted to pH 8.0 using concentrated Tris (e.g. 5 μ l of 1.5 M Tris-HCl, pH 9.2 per 100 μ l 0.1 M glycine

eluate, pH 2.0). For reduction of cysteine residues, a fresh solution of DDT (0.5 mg/ml, Roche 708984, dissolved in 50 mM NH_4HCO_3 , Fluka 09830) was prepared. 2 μl of DTT solution were added per 100 μl of protein sample, and incubated in an Eppendorf Thermomixer at 56°C at 900 rpm for at least 30 min. To alkylate reduced cysteine residues with iodoacetamide (IAA), a fresh solution of 2.5 mg/ml IAA (Sigma I 6125, dissolved in 50 mM NH_4HCO_3) was prepared, 2 μl of this were added per 100 μl of protein sample, followed by incubation for 30 min at 20°C in the dark. Afterwards the protease solutions were prepared as follows: **Trypsin (Try)**: 100 μg Promega 'Trypsin Gold, MS Grade' #V5280 were dissolved in 1 ml 50 mM acetic acid and diluted 1:1 with NH_4HCO_3 to 50 ng/ μl . 4 μl of the Try dilution were added to the protein sample. After incubating at 37°C for 2 h, 4 μl more Trypsin were added and incubated at 37°C overnight. **Chymotrypsin (Cht)**: 25 μg Cht sequencing grade, Roche Diagnostics 1418467, were dissolved in 250 μl 1 mM HCl (stock = 100 ng/ μl), 4 μl of this Chy solution were added to the protein sample. After incubating at 25°C for 2 h, 4 μl more Cht were added and incubated at 25°C, 2 h. **Glu-C**: 50 μg Glu-C, Roche #11420399001, were dissolved in 500 μl water and diluted 1:1 with NH_4HCO_3 to 50 ng/ μl . 4 μl of the Glu-C dilution were added to the protein sample and incubated 25°C for 2 h. Afterwards additional 4 μl Glu-C were added and incubated at 25°C overnight. To stop the proteolytic digestion and to lower the pH for the subsequent HPLC step, 10% trifluoroacetic acid (TFA, Pierce 28904), was added to give a final concentration of 1%. If analysis was to be performed on the same day, samples were stored at 4°C, otherwise they were snap-frozen and stored at -80°C.

4.5.4. Mass spectrometry

Proteolytically-digested protein complexes were analysed by nano-HPLC-ESI-MS/MS as follows (Yates et al., 2000): samples were injected into an HPLC machine, where they were first applied to a precolumn (PepMAP C18, 0.3 x 5 mm, Dionex) to remove buffer salt and other perturbing substances, then eluted onto an analytical column (PepMAP C18, 75 μm x 150 mm, Dionex) at a flowrate of 200 nl/min. Bound peptides were eluted from the analytical column over a 4-hour gradient, and introduced via electrospray ionisation (nanospray ion source interface, Proxeon) into an ion trap mass spectrometer coupled to a Fourier transform ion cyclotron resonance mass detector (LTQ-FT, Thermo Finnigan). The mass spectrometer cycled through seven scans: one full mass scan (duty scan) followed by six tandem mass scans of the six most intense ions; if 'neutral-loss' was observed a neutral-loss dependent MS^3 was performed. Sequenced peptides were put onto a dynamic exclusion list for one minute. All spectra from one analysis were saved as a Finnigan RAW file, and converted into

a Mascot Generic Format (MGF) file for data analysis. The mass spectrometry runs were performed by the IMP-IMBA Protein Chemistry Facility.

Data analysis: All tandem mass spectra (MGF file) were searched against the human KBMS database (Celera Genomics), using the algorithms included in the MASCOT 2.1 program (Matrix Science), to identify proteins in the sample. A subsequent search was performed with a 'variable modification' option to identify putative phosphopeptides in proteins. Any phosphopeptide matched by computer searching algorithms was verified manually. For valid identification of phosphorylation sites, mass spectra have to comply with the following criteria: (1) Mass spectrum of a peptide has to contain a fragment ion representing the mass of the peptide fragment plus the mass of a phosphate residue. (2) The MS/MS spectrum has to be of good quality, i.e. fragment ions have to be above the baseline noise. (3) There has to be certain continuity to the b or y ion series. (4) The y ions, which correspond to a proline residue, should be intense ions. (5) Unidentified, intense fragment ions either correspond to +2 or +3 fragment ions or the loss of one or two amino acids from one of the ends of a peptide. After going through this process we have a high confidence in the phosphorylation sites identified. This analysis was mainly performed by the IMP-IMBA Protein Chemistry Facility.

Phospho-site identification: Sets of validated phosphopeptide data from interphase and mitotic samples produced by Mascot searches were compared using MS-Excel to determine which phospho-sites are mitosis-specific.

4.6. Cell culture and immunofluorescence microscopy

4.6.1. Growth and harvesting of HeLa cells

Adherent HeLa cells were grown as monolayers on 13.5 cm diameter round (Cellstar, Greiner), or on 24.5 cm square cell culture dishes (Nunc) in 20 ml or 100 ml, respectively, high-glucose Dulbecco's Modified Eagle Medium (DMEM), supplemented with 10% fetal calf serum (FCS) and PSG (100 units/ml penicillin, 0.3 µg/ml L-glutamine, 100 µg/ml streptomycin) in a humidified 5% CO₂ incubator at 37°C. Cells were grown to 80% confluence either logarithmically (log), for predominantly interphase cells or were arrested in mitosis (prometaphase state) by the microtubule drug nocodazole (100 ng/ml for 16 h at 37°C). Nocodazole (Noc) disrupts tubulin self assembly and also promotes depolymerization of preformed microtubule structures (Samson and Himes, 1979), such as the mitotic spindle, thus activating the spindle assembly checkpoint and inducing a mitotic (prometaphase) arrest. Harvesting of the cells was done by scraping them off the culture dishes with a cell scraper and spinning the cell suspension in a 1-litre centrifuge vessel at 5000 rpm for 10 min

at 4°C in a Sorvall ultracentrifuge (Sorvall HLR6 rotor). The cells were washed by re-suspending the pellet in 40 ml cold PBS, transferring it into a 50 ml Falcon tube and spinning at 2000 rpm for 2 min at 4°C in a Heraeus biofuge. The washing step was repeated once more with 40 ml PBS and once with 10 ml PBS. After the supernatant was removed, the cell pellet was frozen in liquid N₂ and stored at -80°C. This method of freezing cell pellets, rather than cell extracts, has in some cases been found to yield more stable protein complexes.

4.6.2. siRNA transfection

HeLa cells were seeded the day before transfection into 13.5 cm diameter round culture dishes. The cells should be 40-60% confluent, depending on the oligo, incubation time, further analysis etc. On the day of the siRNA transfection, two tubes were prepared: tube A should be a 1.5 ml Eppendorf tube and tube B a 2.0 ml Eppendorf tube. The 20 µM annealed siRNA (Ambion) stock was thawed and aliquoted. In tube A 40 µl OptiMem (Gibco/Invitrogen) was mixed with 10 µl Oligofectamine (Invitrogen), in tube B 425 µl OptiMem was mixed with 25 µl of 20 µM annealed siRNA (final concentration on the cells was 100 nM) in tube B. Both tubes were mixed by inverting and incubated for 5 min at 20°C. Afterwards, contents of tube A and B were mixed by pipetting A drop-wise into B, mixed by tapping or inverting and incubated for 30 min at 20°C. Meanwhile, the growth medium was replaced with 4.5 ml OptiMem supplemented with 0.3% FCS. The transfection mixture was dropped onto the cells, which were subsequently incubated for 4 h with 0.3% FCS only to increase the transfection efficiency. Afterwards, 550 µl FCS were added to obtain a final concentration of 10%. The cells were incubated at 37°C for 24, 48 or 72 h, to compare knock-down efficiencies.

Table 4.5. Sequences of used small interfering RNAs (siRNAs).

Internal ID	Ambion ID	Target Gene (protein)	Sequence (5'→ 3') Sense
44	203452	ZWILCH (Zwilch)	CCCAUUUGAAGAUUAAUCUtt
45	203453	ZWILCH (Zwilch)	GCUUAUCACAACAAACAACtt
46	203455	SPBC24 (Spc24)	GCUCUCCAGGAAAUUCAUCtt
47	203456	SPBC24 (Spc24)	AGAGCUCAAGGAGAUUGAGtt
48	203459	SPBC25 (Spc25)	GCUGUCUGUGAAAUUAAGtt
49	203460	SPBC25 (Spc25)	GGCAAAAAGCAGGAUUUGGtt
50	203465	C20ORF172 (Q9H410)	AGUUGGAUUCCGAUUGUAAtt
51	203466	C20ORF172 (Q9H410)	UCAAGUCUCAGUCCUGUGGtt
52	203462	C1ORF48 (DC8)	GCUGUGCAAGAGAAUAUCAtt
53	203463	C1ORF48 (DC8)	GCUCUUUCUGUUUUUUUGtt
58	203514	ZW10 (Zw10)	GCAUGGAGCUCACAAUACAAtt
59	203515	ZW10 (Zw10)	CCAUCUGAAGUUUUUACAAtt

4.6.3. Establishment of stable cell pools

Cell transfection was performed with Lipofectamine PLUS reagent (Invitrogen) according to the manufacturer's protocol using HeLa cells at 80% confluence. The amount of DNA used was dependent on the size of the transfected plate and the construct. The selection was started at 72 h after transfection by using 1 µg/µl Geneticin (G418). After three weeks, when colonies became visible, the concentration of G418 was reduced to 500 µg/µl and cell pools were cultivated as described above. The selection was continued until single colonies of about 200-300 cells were obtained. For picking the clones, metallic rings were placed on top of the colonies (using grease to seal the connection between the ring and the plate surface) in order to apply trypsin locally. Afterwards, candidates were split on 24-well plates and screened for positive clones by immunofluorescence or western blotting.

4.6.4. Immunofluorescence microscopy

4.6.4.1. Growth and fixation on cover slips

5×10^4 cells were seeded on ethanol-cleaned 18 mm coverslips in 12-well cell culture dishes and grown overnight at 37°C. The next day, medium was taken off and cells were washed once in PBS. In some cases pre-extraction, to extract cytoplasmatic proteins, was performed by adding PBS containing 0.1% Triton X-100 for 2 min and washing 3 min with PBS. To fix the cells, 4% paraformaldehyde (PFA; prepared in phosphate buffer (pH 7.4) by dissolving 0.8 g PFA in 17 ml 0.1 M Na_2HPO_4 (base) under heating, stirring and then adding 3 ml 0.1 M NaH_2PO_4 (acid)) was added for 20 min. After fixation, cells were washed once with PBS and afterward extracted with PBS containing 0.01% Tx (PBS-Tx) for 10 min at 20°C. The samples were washed with PBS-Tx and blocked with PBS-Tx containing 10% goat serum for 1 h at 20°C with gentle agitation. Antibodies were diluted in PBS-Tx containing 10% goat serum. The primary antibodies mouse-anti-myc (9E10) and human-CREST (calcinosis, Raynaud's phenomenon, esophageal dysmotility, sclerodactyly, telangiectasias) antiserum (staining centromeric domains) were used in a 1:1000 dilution and typically incubated for 1 h. As secondary antibodies, goat-anti-human Alexa 488 (green), goat-anti-rabbit-Alexa 568 (red) or goat-anti-mouse Alexa 568 (all from Molecular Probes/Invitrogen) were used in a 1:500 dilution. Incubation was done for 1 h at 20°C. Three washes with PBS-Tx for 5 min each were done between and after antibody incubation. Double or triple staining was usually done at the same time. DNA was stained by incubation with 1 µg/ml Hoechst 33342 (diluted in PBS) for 5 min. Cover slips were mounted onto glass slides with 'Prolong Gold' (Invitrogen) mounting medium. After drying for 30 min at 20°C, slides were sealed with nail

varnish. Samples were analysed with a fluorescence microscope (Axioplan2 imaging/coolsnap HQ, Zeiss) and stored at 4°C.

4.6.4.2. Cytospins

For cytopins, cells were seeded in a suitable density on 10 cm dishes and grown overnight. On the next day, slides were washed with 100% ethanol. Using a lipomarker, a circle was drawn at those spots where the cells would later be spun to the glass slide. The medium was taken off from the 10 cm dishes except for 2 ml and transferred into a 15 ml Falcon tube. Mitotic cells were shaken off in the remaining medium by tapping against the dish. The 2 ml containing the mitotic cells were put into the same 15 ml Falcon tube and spun at 1100 rpm for 5 min at 20°C. The supernatant, containing the FCS, was discarded. For hypotonic treatment, the cells were resuspended in 2 ml serum free medium and 3 ml pre-warmed water was added for 5 min. Mixing was done by gently inverting the tubes. For isotonic cytopins, the cells were resuspend in an appropriate volume of PBS. In the meantime, the cytopins funnels were assembled and the filter papers pre-wetted with PBS. In general, about 100 µl of cell suspension was added to the cytospin funnels (5.6×10^6 cells = 50% density of a 10 cm plate, resuspended in 5 ml). Cells were spun onto the glass slides at 1500 rpm for 5 min at 20°C. Afterwards, cells were pre-extracted with 0.1% Tx for 2 min. Further washes and immunofluorescence staining was performed as described in section 4.6.4.1.

5. Appendix

A) DC8/NSL1 (Q96IY1)

```

hDC8      MAGSPE-----LVVLDPPWDKELAAQTESQALVSATPREDFVRCTSKRAVTEMLQ  51
cDC8      MAGAPV-----SGVPSRPRGVEREARPDDGASVAASSREDCRVRCTSKRAVTEME  51
mDC8      MAAVSE-----TVLVSAPQDHDAQASDPQATAADSPLDFVRCTLKRAVMEVME  51
gDC8      MPPPHARPRPREGRGGGAVGCASGPAFSVRRRREMAAGPPARQDWRVQCCSRRGLDEVVG  60
          * . . . . . . . . . . : * * * * : * : * :

hDC8      LCGRFVQKLGDALPEEIREPALRDAQWTFESAVQENISINGQAWQEASDNCFMDS-DIKV  110
cDC8      LCGRFVDKLGDALPEEIRGPALRDVQWTFESAVQENVISINGQAWQEASDSLIVDS-DIKV  110
mDC8      MCGRFVQELGAVLPEDVRELALRDAQWTFESAVQENVSFNGQAWEEAKEHGLMDS-DIKV  110
gDC8      LCAPFLRGLAQGPQGA-AAAVDDAIWNFEAAVRENTINGQPWAETSADSEPNSANIKI  119
          : * : * : * : * : * : * : * : * : * : * : * : * : * : * : * :

hDC8      LEDQFDEIIVDIATKRKQYPRKILECVIKTIKAKQEILKQYHPVVHPLDLKYDPDPAPHM  170
cDC8      LEDQFDEIIVDIATKRKQYPRKILECVIKTIKAKQEILKQYCPVVHPLDLKYDPDPGESM  170
mDC8      LEDEFDELIVDVATKRKQYPRRILESVIKTLKAQHASKQYHPVVHPLDLKCDPDPASRV  170
gDC8      LEDQLDELIVETATKRKQWPKKILVHAIQTMKAEQEMLKLYQPVVTPPEEIKSQPSQDAYV  179
          * * * : * * * : * * * : * * * : * * * : * * * : * * * : * * * :

hDC8      ENLKRGETVAKEISEAMKSLPALIEQGEFGFSQVLRMQPVIHLQRIHQEVFSSCHRPDA  230
cDC8      F-ICGKSETLVCIYCCFLFKSLPALIEQGDGFSQVLKMQPIIQLQRVHQEVFSGCYKKPDT  229
mDC8      EDLKRGEAIAKEMSEAMKALPVLIEQGEFGFSQVLKMRPVIQLQRINQEVFSSLYRKADS  230
gDC8      ADLKQVTEMASEQIGEAMKSLPALIERAEGFSQALTWQPTLELCKLRQEVFAGCNAKEEN  239
          : * : * * * * : * * * * : * : * : * : * : * : * :

hDC8      KPENFITQIETTPETETASRKTSMDVLKRKQTKDCPQRKWYPLRPKKINLDT  281
cDC8      KPESFITQIETTPETETSTRKATDVVLKRRQTEDCPQRKRYPLRPKRINLD-  279
mDC8      KPDRTRVTHVETTPAETGARKASDIVLKRKKAPDCAQRKRYPLRLQRIINLDM  281
gDC8      SVQNFVSPAEVTPTDADSTNNPYTLFKRKAADTPQRRYPLRRRKITLST  290
          . : . : * : * : : : . : * * : * : * : * : * : * : * :

```

B) C20orf172/Mis13/DSN1 (Q9H410)

```

hQ9H410    MTSVTRSEIIDE----KGPVMSKTHDHQLESLSLSPVEVFAKTSASLEMN-QGVSEERIHL  55
cQ9H410    MSSVIRSEAIIEEQVLEEVPVTSKYTDHPLKSDPIPVEVCSKSPASLEMI-QRVSEERIHP  59
mQ9H410    MTSVTRSE-----DQEPMTSETQDRPLQPSLKPLEALPQSSAYQEMMTQGVSEKNHL  53
gQ9H410    MEGRPEGSFRLRS--EERRQRAAGLETSLTGSFLRADGGAPEPDGEGKKDVGKPPKPTDL  58
          * . . . . : : : * . : . . * . : .

hQ9H410    GSSPKKGGNCDLSHQERLQSKSLHLSPQEQSASYQDRRQSWRRASMKETNRRKSLHPIHQ  115
cQ9H410    GSSPKMGGNCDLIHQEGLQSRSLHLAPQEQSPDRQDKSQSWRRASMKEISRKSLPAFHQ  119
mQ9H410    GSNPGEGESGADHQEGSQLSRSLHLSPQEQSIRPQDRRQSWRRASMKEVNRRKSLAPFHP  113
gQ9H410    AAVSQENATPEAAAGKTSHG-SLSSVKSPNTTSCQTKRRSWRRSSLKGSKRKSLPPFHE  117
          . : . . . : : * : . : : * : * * * : * : * * * : * :

hQ9H410    GITELSRSISVDLAESKRLGCLLLSSFQFSIQKLEPFLRDTKGFSLESFRAKASSLSEEL  175
cQ9H410    GITELSRSISANLAESKRLGALLSSFFQFSVQKLEPFLKDMEGFSLESFRAKASSLSEEL  179
mQ9H410    GITELCRSISVKLAQSQRLLGALLSSFFQFSVEKLEPFLKNTKDFSLFCFRAKASSLSEEL  173
gQ9H410    DVTALSQAISLDLPEADRLSMLLLSSFQFSAQKLEHVLEQTEGFSPEAFKASVNSASEDL  177
          . : * : * : * : * : * : * : * : * : * : * : * : * : * : * : * :

hQ9H410    KHFDAGLETDTGLQKCFE-DSNGKASDFSLEASVAEMKEYITKFSLERQTDQDLLLHYQQ  234
cQ9H410    KHFAESLESNGTLQKCFE-DSKGKASDLSLETSAEMKEYITKFSLERQSWDQLLQHYQM  238
mQ9H410    KHFTDRLGNDGTGLQKCFVEDSKEAADFSLEASVAEVKEYITKFSLERQAWDRLLQYQK  233
gQ9H410    KRYIEKLLDGTLRSCIE-KAEGDSSDSVDESVCakeCIARFSAECQAWDELLQRYQK  236
          * : : * : * * : * : : * : : * : * : * : * : * : * : * : * :

hQ9H410    EAK-EILSRGSTeAKITEVKVEPMTYLGSSQNEVLNTPDYQKILQNQSKVFDCMELVMD  293
cQ9H410    EAE-EITSRTSAETKVTEVEVEPKTYLGSSQSEVLSTKPDYQKILQNQNKFVDFYMELVMD  297
mQ9H410    EVPEEMPRGSTETRITEVVDPAAYLRSSQKEVLSTKPDYQRIVDQDNQVFAYVELVMD  293
gQ9H410    DAE--ETSRQLEECRSKEGRAEPPNYLQTSQAEVLSTKPNYQRIILDEQGEVLSCMELVLD  294
          : . . * : * : * : * : * : * : * : * : * : * : * : * : * :

hQ9H410    ELQGSVKQLQAFMDESTQCFQKVSQVLGKRSMQQLDPSARKLLKLQLQNPPAIHSGSGS  353
cQ9H410    ELQGSVKQLLHAFMDESTQCFQKVSQVLGKRSTQQLDPSARKLLKLQLQNPPTHCSR--  355
mQ9H410    ELQGSVKQLQALMDESTQYLQKVSQVLGKRSMQQLDSSARKLLKLPLQSSPSTQ-----  348
gQ9H410    ELQQAAKLLRAFSEDSRQHLRGLFELL-----  321
          * * * : * * * : * * * : : : *

```

5. Appendix

hQ9H410 SCQ 356
cQ9H410 SCQ 358
mQ9H410 ---
gQ9H410 ---

C) SPAG5/Astrin/MAP126 (Q96R06)

hSPAG5 MWRVKKLSLSLSPQGTGKPSMRTPRLRELTLQPGALTN⁵SGKRSPACSSSLTPSLCKLGLQE 60
cSPAG5 MWRVKALSVSGSPSPQPGKPMRTPLRELVLQPGAFTTS⁵SGKPPVCHSPTSSLYKLGLQE 60
mSPAG5 MWRVKTLNLGLSPSPQKGKPMAMSTPLRELKLQPEALADSGKGPMSMISALTPYLCLRELKE 60
***** .: .: ***** *: : ***** * : : * : . : . : * : * : *

hSPAG5 GSNNSSPVDFVNNKRTDLSSEHFSHSSKWLETCQHESD---EQPLDPIPQISSTPKTSEE 117
cSPAG5 DSNTASPLDFVNAKRTDSSSEQFSPHPSKCLEACHRES---EQSLDLNPQTNSTPRISEE 117
mSPAG5 RCNNSSPVDFIN-TENNFLSEQFSPHPSHIEACQRESDPPTESNSLFHTLEEAETVDDF 119
. : . : * : * : * : . : . : * : * : * : . : . : * : . : . : . : . :

hSPAG5 AVDPLGNYMVKTIIVLVPSPLGQQQDMIFEARLDTMAETN⁵ISLNGPLRTDDLVRREEVAPC 177
cSPAG5 AVDPLDNSVFKTMFLVPSVPVQQQDVLTLEAHLDTMAETNNTSPDEPLNPGDLLREGVAAC 177
mSPAG5 VVDPRDDSIIVSMVLLPFLSGQQQDMLQAHLDTTAERTKSSLNESLGLLEDLVGKEVAPC 179
. * : . : . : . : * : . : * : * : . : . : * : * : . : . : * : . : * : *

hSPAG5 MGDRFSEVAASV-EKPIFQESPSHLLSESPNPCSEQLHCS⁵KESSLS-SRTEAVREDLVPS 235
cSPAG5 LEDSLKEVPTMPEKPTFQHPSPSHILEYLPNTCSEQQPHCSKECFRGSRTAEAVVEDLVPS 237
mSPAG5 VEDSLTEIVAIRPEQPTFQDEP-----LGPSTEDAPVDLVPS 217
: * : . : . : . : * : * : * : . : . : * : * : . : * : * : *

hSPAG5 ESNAFLPSSSVLWLS⁵PSSTALAADFRVNHVDPEEEIVEHGAMEREMRFPHPKESETEDQA 295
cSPAG5 ESNTSLPSSMFWLSPSTDLATDFLVSHVDPGEEIVEHRSVEEKELSFILPEEVELGDQA 297
mSPAG5 EN--VLNFSLARLS⁵PSAVLAQDFSDVHDVPGREETVENRVLQEMETSFPPTFEEAELGDQA 275
* . * * : * : * : * : * : * : * : * : * : * : * : * : * : * : * : *

hSPAG5 LVSSVEDILSTCLTPNLVEMESQEAPGPAVEDVGRILGSDTESW⁵SP⁵PLAWLEKGVNTSV⁵ 355
cSPAG5 LVSNMEATPFTCLTPNPREMESQTAAGPTVEDTGRVLISDTGPWMS⁵PLAWLEKDINTSV⁵ 357
mSPAG5 PAANAEAVSPLYLTSSLVEMGPRAEPGPTVEDASRIPGLESETWMS⁵PLAWLEKGVNTSV⁵ 335
. : . : * * : . : * : . : * : * : * : . : . : * : * : * : * : * : *

hSPAG5 LENLRQSLSLPSMLRDAAICTTPFSTCSVGTWFTPSAPQEKSTNTSQTGLVGTKHSTSET 415
cSPAG5 LENLRQSLSLPSMLRDTAISTTPFPTCSVGTWFTPPVAQEKSTNTSQTGPAGVKDGTSET 417
mSPAG5 LQNLQRQSLSFSSVLQDAAVGNTPLATCSVGTSFTPPAPLE-----VGTKDSTSET 385
* : * : * : * : . : * : * : * : . : * : . : * : * : * : * : * : * : * : *

hSPAG5 EQLLCG-RPPDLTALSRRHLEDNLLSSVLVILEVLSRQLRDWKSQ⁵LAVPHPETQDSSTQTD 474
cSPAG5 EHLLWGNRPLDLTALSRRHLEDNLLNSVLVILEVLSRQLRDWKSQ⁵LTVPHEVQDSSTQTD 477
mSPAG5 ERLLGCRPPDLATLSRRHLEDNLLNSVLVILEVLSHQLQAWKSQ⁵LTVPHEARDSTQTD 445
* : * : * * * : * : * : * : * : * : * : * : * : * : * : * : * : * : * : *

hSPAG5 TSHSGITNKLQHLKESHEMGQALQQARNVMQSWVLIS-KELISLLHLSLLHLEEDKTTVS 533
cSPAG5 TSPGGINKKPQHLQESQEIQVQLQARNVMYLWVSCEDKEWRILRHVPIGSLGLTTFTF 537
mSPAG5 SSPCGVTKTPKHLQDSKEIRQALLQARNVMQSWGLVS-GDLLSLLHLSLTHVQEGRVTVS 504
: * * : . : . : * : * : * : * : * : * : * : . : . : * : * : . : . : *

hSPAG5 -QESRRAETLVCCCFDLLKKLRKALQSLKAEREERHREEMALRGKDAAEIVLEAFCAHA 592
cSPAG5 STASRLIETMVSCCDVLRKLKARLQSLKAEKEEAMHKEEMALRGKDAAEAVLEAFCAHA 597
mSPAG5 -QESQRSKTLVSSCSRVLKKLAKLQSLKTECEEARHSKEMALKGKAAAEAVLEAFRAHA 563
* : . : * : . : * : * : * : * : * : * : * : * : * : * : * : * : * : * : *

hSPAG5 SQRISQLEQDLASMRFRGLLKDAQTQLVGLHAKQEELVQQT⁵TVSLTSTLQQDWRSMQLDY 652
cSPAG5 SQRISQLEQDLASMGDFRGLLKETQTQLVGLHTEQEEVAQQT⁵TVSLTSTLQQDWRSMQLDY 657
mSPAG5 SQRISQLEQGLTSMQEFGRGLLQEAQTQLIGLHTEQKELAQQT⁵TVSLSSALQQDWT⁵SVQLNY 623
* : * : * : * : * : * : * : * : * : * : * : * : * : * : * : * : * : * : *

hSPAG5 TTWTALLSRSRQLTEKLT⁵VKSQQALQERDVAIEEKQEVSRVLEQVSAQLEECKGQTEQLE 712
cSPAG5 ITWTALLSRSRQLTEKLTAKSRQALQERDAAIEEKQQVSRELEQATTHLEDCKGRIEQLE 717
mSPAG5 GIWAALLWSRELTKLTA⁵KSRQALQERDAAIEEKQVVEVEQVSAHLEDCKGQIEQLK 683
* : * : * : * : * : * : * : * : * : * : * : * : * : * : * : * : * : * : *

hSPAG5 LENSRLATDLRAQLQILANMDSQLKELQSQHTHCAQDLAMKDELLCQLTQSNEEQAAQWQ 772
cSPAG5 LENSCLATDLQAQLQILASMESQLNELQSQAHAQDLAMKDELLCQLTQSNEEQAAQWQ 777
mSPAG5 LENSRLTADLSAQLQILTSTESQLKEVRSQHSRCVQDLAVKDELLCQLTQSNKEQATQWQ 743
* : * : * : * : * : * : * : * : * : * : * : * : * : * : * : * : * : * : *

Figure 5.1. Analysis of the conservation of the phospho-site residues amongst vertebrate species. For A) kinetochore protein DC8 (UniProt AC: Q96IY1), in B) for kinetochore protein Q9H410 (UniProt AC: Q9H410) in human, dog, mouse and chicken and C) for SPAG5 (UniProt AC: Q96R06) in human, dog and mouse. The sequences were retrieved from Ensembl (Hubbard et al., 2007) and the multiple sequence alignment was performed using ClustalW (1.83). Red labeled AS are certain phospho-sites, blue labeled AS are uncertain positions of phosphorylation. Ortholog sequence positions are highlighted in yellow.

86

5. Appendix

Rank	Identified proteins	Number of similar matches	Accession number	MW [kDa]	Inter-phase	Mitosis
1	SPAG5, Astrin, Mitotic spindle associated protein p126, Deepest	1	sp Q96R06	134.4	70	71
2	RAB GTPase activating protein 1, RABGAP1	1	trm Q9Y3P9	114.0	65	67
3	Chromodomain helicase DNA binding protein 4	5	spt Q14839	219.4	63	44
4	Rho guanine nucleotide exchange factor (GEF) 17	3	trm Q96PE2	221.6	35	41
5	NRAA Best Hit: similar to KIAA0870 protein	1	cra hCP38365.4	144.2	27	26
6	ELP4, elongation protein 4 (DKFZp564P2272)	1	trm Q9NX11	46.6	29	25
7	C15orf23, HSD11, TRAF4 associated factor 1	4	trm Q6P2S5	354	20	23
8	6-phosphofructo-2-kinase, PFKFB2	3	spt Q60825	58.5	24	25
9	Thyroid hormone receptor-associated protein	1	trm Q5VTK6	108.6	18	22
10	DEAD (Asp-Glu-Ala-Asp) box polypeptide 3	7	spt Q00571	73.3	23	19
11	Hypothetical protein BC007653	2	trm Q8WY93	76.3	22	14
12	Claspin	1	rf NP_071394.2	151.1	17	16
13	Q9H410, C20orf172 protein	2	cra hCP1858063	40.5	19	10
14	TMEM103, transmembrane protein 103	2	trm Q9BW57	297.8	13	15
15	p66 alpha	5	spt Q86YP4	68.0	15	12
16	CD2-associated protein	2	spt Q9Y5K6	71.4	12	14
17	DC8/DC31 protein	3	sp Q96Y1	32.1	12	10
18	Metastasis-associated gene family, member 2	3	spt Q94776	75.0	11	14
19	PRP19/PSO4	2	spt Q9UMS4	55.2	14	12
20	Hypothetical protein FLJ10154	3	trm Q9NW66	33.2	9	12
21	Hec1, hNdc80 'cmere/kchore' (KNTC2)	3	sp O14777	73.9	18	4
22	HSPC002, DERP6	1	trm Q9Y2Q4	18.5	11	8
23	Vimentin	8	spt P08670	53.6	10	11
24	Potassium channel tetramerisation domain containing 3	4	trm Q9Y597	89.0	19	0
25	Bcl-2-associated transcription factor	4	spt Q9NYF8	106.1	0	18
26	Mis12 kinetochore protein	1	tr Q9H081	24.1	9	7
27	RelA-associated inhibitor	1	cra hCP1891982	89.1	11	7
28	LIM domain binding 1	1	cra hCP1897154	46.3	8	6
29	Bcl-2-associated transcription factor	2	cra hCP1876075	100.2	11	0
30	Retinoblastoma binding protein 7	3	spt Q16576	47.8	4	10
31	Histone deacetylase 2	4	trm Q8NEH4	55.3	4	8
32	MYCBP, c-myc binding protein	5	trm Q6IB68	11.9	5	5
33	PMF1, Polyamine-modulated factor 1 (RP11-54H19.4-001)	2	cra hCP1859428	23.3	11	4
34	Cylindromatosis (turban tumor syndrome)	5	spt Q9NQC7	107.1	4	6
35	Complement component 1	5	spt Q07021	31.3	4	5
36	Dynein light chain 1, cytoplasmic, DLC8	2	sp P63167	10.3	3	3
37	Kinetochore protein Nuf2, CDCA1	2	cra hCP1767287.1	54.3	8	0
38	Kinetochore protein Spc24	1	tr Q8NBT2	22.4	9	2
39	MCTP2	1	trm Q6DN12	99.6	3	7
40	Enhancer of rudimentary homolog	3	spt P84090	12.2	3	4
41	Transcription elongation factor B (SIII)	8	spt Q15370	17.8	3	3
42	Insulinoma protein	3	trm Q9UDC2	17.0	2	3
43	Interleukin enhancer binding factor 3	7	spt Q12906	94.9	5	3
44	Dedicator of cytokinesis protein 1, DOCK180, DOCK1	2	spt Q14185	215.3	9	0
45	Kinetochore protein Spc25	1	tr Q9HEM1	26.1	5	0
46	DEAD (Asp-Glu-Ala-Asp) box polypeptide 23	3	trm Q9BUQ8	95.5	3	4
47	SEC13-like 1	7	spt P55735	37.5	4	3
48	histone 1, H1c	3	spt P16403	21.3	3	2
49	LIM domain binding 1	4	trm Q9UGM4	46.5	0	6
50	poly(A) binding protein, cytoplasmic 1	10	spt P11940	70.6	0	7
51	adenosine monophosphate deaminase 2 (isoform L)	12	trm Q5T694	92.0	4	3
52	hypothetical protein FLJ20403	5	trm Q72638	65.6	2	2
53	LIM domain only 4	3	spt P61968	18.0	2	2
54	similar to hypothetical protein FLJ10883	6	trm Q658R8	21.0	2	2
55	HP1-gamma (CBX3)	7	sp Q13185	20.8	3	2
56	KIAA0179	3	spt Q14684	84.0	0	4
57	Single stranded DNA binding protein 3	4	spt Q9BWW4	37.7	3	0
58	Engulfment and cell motility 2	11	spt Q96JU3	82.6	4	0
59	Hypothetical protein FLJ16420	1	trm Q6ZN53	155.0	0	2
60	Spermatogenesis associated 2	5	spt Q9UM82	58.4	0	3
61	Retinoblastoma binding protein 4	4	spt Q09028	47.6	0	3
62	KIAA0664 protein	1	cra hCP46321.3	147.5	2	0
63	Histone deacetylase 1	4	spt Q13547	55.1	0	3
64	S-phase 2 protein	5	trm Q9BUB2	34.8	2	2
65	CDK2-associated protein 1	6	spt Q75956	31.6	2	2
66	DEAD (Asp-Glu-Ala-Asp) box polypeptide 48	5	spt P38919	46.8	0	4
67	Chromosome 20 open reading frame 36	4	spt Q9NV79	41.1	2	0
68	Transcription elongation factor B (SIII)	6	spt Q15369	12.5	2	0
69	Inhibitor of kappa light polypeptide gene enhancer in B-cells	10	trm Q8N516	158.1	2	0
70	Protein-L-isoaspartate (D-aspartate) O-methyltransferase	10	trm Q5VYC1	17.7	0	2
71	Arg/Abi-interacting protein ArgBP2b (Fragment)	1	trm Q60593	70.6	2	0
72	sorting nexin 8	3	spt Q9Y5X2	52.5	2	0
73	Spectrin, alpha, non-erythrocytic 1 (alpha-fodrin)	11	trm Q5VXV6	284.5	2	0
74	Related to the N terminus of tre	4	spt Q92738	94.1	2	0

Protein legend:

gold: bait protein

yellow: kinetochore complex partners

grey: other proteins, chosen for further analysis

bold: further proteins which were top hits in Mascot search

Probability legend:

over 95%

80% to 94%

50% to 79%

20% to 94%

6. References

- Abend, M., Blakely, W.F. and van Beuningen, D. (1995) Simplified and optimized kinetochore detection: cytogenetic marker for late-G2 cells. *Mutat Res*, **334**, 39-47.
- Acquaviva, C., Herzog, F., Kraft, C. and Pines, J. (2004) The anaphase promoting complex/cyclosome is recruited to centromeres by the spindle assembly checkpoint. *Nat Cell Biol*, **6**, 892-898.
- Ahonen, L.J., Kallio, M.J., Daum, J.R., Bolton, M., Manke, I.A., Yaffe, M.B., Stukenberg, P.T. and Gorbsky, G.J. (2005) Polo-like kinase 1 creates the tension-sensing 3F3/2 phosphoepitope and modulates the association of spindle-checkpoint proteins at kinetochores. *Curr Biol*, **15**, 1078-1089.
- Andrews, P.D., Knatko, E., Moore, W.J. and Swedlow, J.R. (2003) Mitotic mechanics: the auroras come into view. *Curr Opin Cell Biol*, **15**, 672-683.
- Backer, J.M., Myers, M.G., Jr., Shoelson, S.E., Chin, D.J., Sun, X.J., Miralpeix, M., Hu, P., Margolis, B., Skolnik, E.Y., Schlessinger, J. and et al. (1992) Phosphatidylinositol 3'-kinase is activated by association with IRS-1 during insulin stimulation. *Embo J*, **11**, 3469-3479.
- Bain, J., McLauchlan, H., Elliott, M. and Cohen, P. (2003) The specificities of protein kinase inhibitors: an update. *Biochem J*, **371**, 199-204.
- Bharadwaj, R., Qi, W. and Yu, H. (2004) Identification of two novel components of the human NDC80 kinetochore complex. *J Biol Chem*, **279**, 13076-13085.
- Biggins, S. and Walczak, C.E. (2003) Captivating capture: how microtubules attach to kinetochores. *Curr Biol*, **13**, R449-460.
- Brinkley, B.R. and Stubblefield, E. (1966) The fine structure of the kinetochore of a mammalian cell in vitro. *Chromosoma*, **19**, 28-43.
- Buffin, E., Lefebvre, C., Huang, J., Gagou, M.E. and Karess, R.E. (2005) Recruitment of Mad2 to the kinetochore requires the Rod/Zw10 complex. *Curr Biol*, **15**, 856-861.
- Cahill, D.P., Kinzler, K.W., Vogelstein, B. and Lengauer, C. (1999) Genetic instability and darwinian selection in tumours. *Trends Cell Biol*, **9**, M57-60.
- Chan, G.K., Jablonski, S.A., Starr, D.A., Goldberg, M.L. and Yen, T.J. (2000) Human Zw10 and ROD are mitotic checkpoint proteins that bind to kinetochores. *Nat Cell Biol*, **2**, 944-947.
- Chan, G.K., Liu, S.T. and Yen, T.J. (2005) Kinetochore structure and function. *Trends Cell Biol*, **15**, 589-598.
- Cheeseman, I.M., Anderson, S., Jwa, M., Green, E.M., Kang, J., Yates, J.R., 3rd, Chan, C.S., Drubin, D.G. and Barnes, G. (2002) Phospho-regulation of kinetochore-microtubule attachments by the Aurora kinase Ipl1p. *Cell*, **111**, 163-172.
- Cheeseman, I.M., Chappie, J.S., Wilson-Kubalek, E.M. and Desai, A. (2006) The Conserved KMN Network Constitutes the Core Microtubule-Binding Site of the Kinetochore. *Cell*, **127**, 983-997.
- Cheeseman, I.M., Niessen, S., Anderson, S., Hyndman, F., Yates, J.R., 3rd, Oegema, K. and Desai, A. (2004) A conserved protein network controls assembly of the outer kinetochore and its ability to sustain tension. *Genes Dev*, **18**, 2255-2268.
- Chen, Y., Riley, D.J., Chen, P.L. and Lee, W.H. (1997) HEC, a novel nuclear protein rich in leucine heptad repeats specifically involved in mitosis. *Mol Cell Biol*, **17**, 6049-6056.

- Ciferri, C., De Luca, J., Monzani, S., Ferrari, K., Ristic, D., Wyman, C., Stark, H., Kilmartin, J., Salmon, E.D. and Musacchio, A. (2005) Architecture of the human HEC1/NDC80 complex, a critical constituent of the outer kinetochore. *J Biol Chem*.
- Cimini, D. and Degross, F. (2005) Aneuploidy: a matter of bad connections. *Trends Cell Biol*, **15**, 442-451.
- Cimini, D., Wan, X., Hirel, C.B. and Salmon, E.D. (2006) Aurora kinase promotes turnover of kinetochore microtubules to reduce chromosome segregation errors. *Curr Biol*, **16**, 1711-1718.
- Cleveland, D.W., Mao, Y. and Sullivan, K.F. (2003) Centromeres and kinetochores: from epigenetics to mitotic checkpoint signaling. *Cell*, **112**, 407-421.
- Comings, D.E. and Okada, T.A. (1971) Fine structure of kinetochore in Indian muntjac. *Exp Cell Res*, **67**, 97-110.
- Corthals, G.L., Aebersold, R. and Goodlett, D.R. (2005) Identification of phosphorylation sites using microimmobilized metal affinity chromatography. *Methods Enzymol*, **405**, 66-81.
- Cuif, M.H., Possmayer, F., Zander, H., Bordes, N., Jollivet, F., Couedel-Courteille, A., Janoueix-Lerosey, I., Langsley, G., Bornens, M. and Goud, B. (1999) Characterization of GAPCenA, a GTPase activating protein for Rab6, part of which associates with the centrosome. *Embo J*, **18**, 1772-1782.
- Davies, S.P., Reddy, H., Caivano, M. and Cohen, P. (2000) Specificity and mechanism of action of some commonly used protein kinase inhibitors. *Biochem J*, **351**, 95-105.
- De Antoni, A., Pearson, C.G., Cimini, D., Canman, J.C., Sala, V., Nezi, L., Mapelli, M., Sironi, L., Faretta, M., Salmon, E.D. and Musacchio, A. (2005) The Mad1/Mad2 complex as a template for Mad2 activation in the spindle assembly checkpoint. *Curr Biol*, **15**, 214-225.
- De Wulf, P., McAinsh, A.D. and Sorger, P.K. (2003) Hierarchical assembly of the budding yeast kinetochore from multiple subcomplexes. *Genes Dev*, **17**, 2902-2921.
- DeLuca, J.G., Gall, W.E., Ciferri, C., Cimini, D., Musacchio, A. and Salmon, E.D. (2006) Kinetochore microtubule dynamics and attachment stability are regulated by Hec1. *Cell*, **127**, 969-982.
- Desai, A., Rybina, S., Muller-Reichert, T., Shevchenko, A., Hyman, A. and Oegema, K. (2003) KNL-1 directs assembly of the microtubule-binding interface of the kinetochore in *C. elegans*. *Genes Dev*, **17**, 2421-2435.
- Diella, F., Cameron, S., Gemund, C., Linding, R., Via, A., Kuster, B., Sicheritz-Ponten, T., Blom, N. and Gibson, T.J. (2004) Phospho.ELM: a database of experimentally verified phosphorylation sites in eukaryotic proteins. *BMC Bioinformatics*, **5**, 79.
- Dong, Y., Vanden Beldt, K.J., Meng, X., Khodjakov, A. and McEwen, B.F. (2007) The outer plate in vertebrate kinetochores is a flexible network with multiple microtubule interactions. *Nat Cell Biol*, **9**, 516-522.
- Elia, A.E., Cantley, L.C. and Yaffe, M.B. (2003) Proteomic screen finds pSer/pThr-binding domain localizing Plk1 to mitotic substrates. *Science*, **299**, 1228-1231.
- Elledge, S.J. (1996) Cell cycle checkpoints: preventing an identity crisis. *Science*, **274**, 1664-1672.
- Elowe, S., Hummer, S., Uldschmid, A., Li, X. and Nigg, E.A. (2007) Tension-sensitive Plk1 phosphorylation on BubR1 regulates the stability of kinetochore microtubule interactions. *Genes Dev*, **21**, 2205-2219.

- Evans, T., Rosenthal, E.T., Youngblom, J., Distel, D. and Hunt, T. (1983) Cyclin: a protein specified by maternal mRNA in sea urchin eggs that is destroyed at each cleavage division. *Cell*, **33**, 389-396.
- Flemming, W. (1891) Neue Beiträge zur Kenntnis der Zelle: II. *Theil. Arch. Mikr. Anat.*, **37**, 685-751.
- Foltz, D.R., Jansen, L.E., Black, B.E., Bailey, A.O., Yates, J.R., 3rd and Cleveland, D.W. (2006) The human CENP-A centromeric nucleosome-associated complex. *Nat Cell Biol*, **8**, 458-469.
- Friedlander, M.L., Hedley, D.W. and Taylor, I.W. (1984) Clinical and biological significance of aneuploidy in human tumours. *J Clin Pathol*, **37**, 961-974.
- Fukagawa, T. (2004) Assembly of kinetochores in vertebrate cells. *Exp Cell Res*, **296**, 21-27.
- Gandhi, T.K., Zhong, J., Mathivanan, S., Karthick, L., Chandrika, K.N., Mohan, S.S., Sharma, S., Pinkert, S., Nagaraju, S., Periaswamy, B., Mishra, G., Nandakumar, K., Shen, B., Deshpande, N., Nayak, R., Sarker, M., Boeke, J.D., Parmigiani, G., Schultz, J., Bader, J.S. and Pandey, A. (2006) Analysis of the human protein interactome and comparison with yeast, worm and fly interaction datasets. *Nat Genet*, **38**, 285-293.
- Gieffers, C., Dube, P., Harris, J.R., Stark, H. and Peters, J.M. (2001) Three-dimensional structure of the anaphase-promoting complex. *Mol Cell*, **7**, 907-913.
- Gieffers, C., Peters, B.H., Kramer, E.R., Dotti, C.G. and Peters, J.M. (1999) Expression of the CDH1-associated form of the anaphase-promoting complex in postmitotic neurons. *Proc Natl Acad Sci U S A*, **96**, 11317-11322.
- Goshima, G., Kiyomitsu, T., Yoda, K. and Yanagida, M. (2003) Human centromere chromatin protein hMis12, essential for equal segregation, is independent of CENP-A loading pathway. *J Cell Biol*, **160**, 25-39.
- Gould, K.L. and Nurse, P. (1989) Tyrosine phosphorylation of the fission yeast cdc2+ protein kinase regulates entry into mitosis. *Nature*, **342**, 39-45.
- Griffin, D.K. (1996) The incidence, origin, and etiology of aneuploidy. *Int Rev Cytol*, **167**, 263-296.
- Gruber, J., Harborth, J., Schnabel, J., Weber, K. and Hatzfeld, M. (2002) The mitotic-spindle-associated protein astrin is essential for progression through mitosis. *J Cell Sci*, **115**, 4053-4059.
- Hartwell, L.H. and Weinert, T.A. (1989) Checkpoints: controls that ensure the order of cell cycle events. *Science*, **246**, 629-634.
- Hassold, T. and Hunt, P. (2001) To err (meiotically) is human: the genesis of human aneuploidy. *Nat Rev Genet*, **2**, 280-291.
- Hauf, S. (2003) Fine tuning of kinetochore function by phosphorylation. *Cell Cycle*, **2**, 228-229.
- Hauf, S., Cole, R.W., LaTerra, S., Zimmer, C., Schnapp, G., Walter, R., Heckel, A., van Meel, J., Rieder, C.L. and Peters, J.M. (2003) The small molecule Hesperadin reveals a role for Aurora B in correcting kinetochore-microtubule attachment and in maintaining the spindle assembly checkpoint. *J Cell Biol*, **161**, 281-294.
- Hauf, S., Waizenegger, I.C. and Peters, J.M. (2001) Cohesin cleavage by separase required for anaphase and cytokinesis in human cells. *Science*, **293**, 1320-1323.
- Hawkes, N.A., Otero, G., Winkler, G.S., Marshall, N., Dahmus, M.E., Krappmann, D., Scheidereit, C., Thomas, C.L., Schiavo, G., Erdjument-Bromage, H., Tempst, P. and

- Svejstrup, J.Q. (2002) Purification and characterization of the human elongator complex. *J Biol Chem*, **277**, 3047-3052.
- Hilliker, C.E., Darville, M.I., Aly, M.S., Chikri, M., Szpirer, C., Marynen, P., Rousseau, G.G. and Cassiman, J.J. (1991) Human and rat chromosomal localization of two genes for 6-phosphofructo-2-kinase/fructose-2,6-bisphosphatase by analysis of somatic cell hybrids and in situ hybridization. *Genomics*, **10**, 867-873.
- Hori, T., Haraguchi, T., Hiraoka, Y., Kimura, H. and Fukagawa, T. (2003) Dynamic behavior of Nuf2-Hec1 complex that localizes to the centrosome and centromere and is essential for mitotic progression in vertebrate cells. *J Cell Sci*, **116**, 3347-3362.
- Hornbeck, P.V., Chabra, I., Kornhauser, J.M., Skrzypek, E. and Zhang, B. (2004) PhosphoSite: A bioinformatics resource dedicated to physiological protein phosphorylation. *Proteomics*, **4**, 1551-1561.
- Howell, B.J., Moree, B., Farrar, E.M., Stewart, S., Fang, G. and Salmon, E.D. (2004) Spindle checkpoint protein dynamics at kinetochores in living cells. *Curr Biol*, **14**, 953-964.
- Hoyt, M.A., Totis, L. and Roberts, B.T. (1991) *S. cerevisiae* genes required for cell cycle arrest in response to loss of microtubule function. *Cell*, **66**, 507-517.
- Hubbard, T.J., Aken, B.L., Beal, K., Ballester, B., Caccamo, M., Chen, Y., Clarke, L., Coates, G., Cunningham, F., Cutts, T., Down, T., Dyer, S.C., Fitzgerald, S., Fernandez-Banet, J., Graf, S., Haider, S., Hammond, M., Herrero, J., Holland, R., Howe, K., Johnson, N., Kahari, A., Keefe, D., Kokocinski, F., Kulesha, E., Lawson, D., Longden, I., Melsopp, C., Megy, K., Meidl, P., Ouverdin, B., Parker, A., Prlic, A., Rice, S., Rios, D., Schuster, M., Sealy, I., Severin, J., Slater, G., Smedley, D., Spudich, G., Trevanion, S., Vilella, A., Vogel, J., White, S., Wood, M., Cox, T., Curwen, V., Durbin, R., Fernandez-Suarez, X.M., Flicek, P., Kasprzyk, A., Proctor, G., Searle, S., Smith, J., Ureta-Vidal, A. and Birney, E. (2007) Ensembl 2007. *Nucleic Acids Res*, **35**, D610-617.
- Janke, C., Ortiz, J., Lechner, J., Shevchenko, A., Magiera, M.M., Schramm, C. and Schiebel, E. (2001) The budding yeast proteins Spc24p and Spc25p interact with Ndc80p and Nuf2p at the kinetochore and are important for kinetochore clustering and checkpoint control. *Embo J*, **20**, 777-791.
- Jimenez, J.L., Hegemann, B., Hutchins, J.R., Peters, J.M. and Durbin, R. (2007) A systematic comparative and structural analysis of protein phosphorylation sites based on the mtcPTM database. *Genome Biol*, **8**, R90.
- Johnson, L.N., Noble, M.E. and Owen, D.J. (1996) Active and inactive protein kinases: structural basis for regulation. *Cell*, **85**, 149-158.
- Jokelainen, P.T. (1967) The ultrastructure and spatial organization of the metaphase kinetochore in mitotic rat cells. *J Ultrastruct Res*, **19**, 19-44.
- Karess, R. (2005) Rod-Zw10-Zwilch: a key player in the spindle checkpoint. *Trends Cell Biol*.
- Karess, R.E. and Glover, D.M. (1989) rough deal: a gene required for proper mitotic segregation in *Drosophila*. *J Cell Biol*, **109**, 2951-2961.
- Karsenti, E., Bravo, R. and Kirschner, M. (1987) Phosphorylation changes associated with the early cell cycle in *Xenopus* eggs. *Dev Biol*, **119**, 442-453.
- Keller, A., Nesvizhskii, A.I., Kolker, E. and Aebersold, R. (2002) Empirical statistical model to estimate the accuracy of peptide identifications made by MS/MS and database search. *Anal Chem*, **74**, 5383-5392.

- Khokhlatchev, A.V., Canagarajah, B., Wilsbacher, J., Robinson, M., Atkinson, M., Goldsmith, E. and Cobb, M.H. (1998) Phosphorylation of the MAP kinase ERK2 promotes its homodimerization and nuclear translocation. *Cell*, **93**, 605-615.
- Kim, J.H., Lane, W.S. and Reinberg, D. (2002) Human Elongator facilitates RNA polymerase II transcription through chromatin. *Proc Natl Acad Sci U S A*, **99**, 1241-1246.
- King, E.M., Rachidi, N., Morrice, N., Hardwick, K.G. and Stark, M.J. (2007) Ipl1p-dependent phosphorylation of Mad3p is required for the spindle checkpoint response to lack of tension at kinetochores. *Genes Dev*, **21**, 1163-1168.
- Kittler, R., Pelletier, L., Ma, C., Poser, I., Fischer, S., Hyman, A.A. and Buchholz, F. (2005) RNA interference rescue by bacterial artificial chromosome transgenesis in mammalian tissue culture cells. *Proc Natl Acad Sci U S A*, **102**, 2396-2401.
- Kiyomitsu, T., Obuse, C. and Yanagida, M. (2007) Human Blinkin/AF15q14 is required for chromosome alignment and the mitotic checkpoint through direct interaction with Bub1 and BubR1. *Dev Cell*, **13**, 663-676.
- Kline, S.L., Cheeseman, I.M., Hori, T., Fukagawa, T. and Desai, A. (2006) The human Mis12 complex is required for kinetochore assembly and proper chromosome segregation. *J Cell Biol*, **173**, 9-17.
- Knowlton, A.L., Lan, W. and Stukenberg, P.T. (2006) Aurora B is enriched at merotelic attachment sites, where it regulates MCAK. *Curr Biol*, **16**, 1705-1710.
- Kops, G.J., Kim, Y., Weaver, B.A., Mao, Y., McLeod, I., Yates, J.R., 3rd, Tagaya, M. and Cleveland, D.W. (2005) ZW10 links mitotic checkpoint signaling to the structural kinetochore. *J Cell Biol*, **169**, 49-60.
- Kotwaliwale, C. and Biggins, S. (2006) Microtubule capture: a concerted effort. *Cell*, **127**, 1105-1108.
- Kraft, C., Herzog, F., Gieffers, C., Mechtler, K., Hagting, A., Pines, J. and Peters, J.M. (2003) Mitotic regulation of the human anaphase-promoting complex by phosphorylation. *Embo J*, **22**, 6598-6609.
- Kunitoku, N., Sasayama, T., Marumoto, T., Zhang, D., Honda, S., Kobayashi, O., Hatakeyama, K., Ushio, Y., Saya, H. and Hirota, T. (2003) CENP-A phosphorylation by Aurora-A in prophase is required for enrichment of Aurora-B at inner centromeres and for kinetochore function. *Dev Cell*, **5**, 853-864.
- Lee, M.G. and Nurse, P. (1987) Complementation used to clone a human homologue of the fission yeast cell cycle control gene *cdc2*. *Nature*, **327**, 31-35.
- Lenart, P., Petronczki, M., Steegmaier, M., Di Fiore, B., Lipp, J.J., Hoffmann, M., Rettig, W.J., Kraut, N. and Peters, J.M. (2007) The small-molecule inhibitor BI 2536 reveals novel insights into mitotic roles of polo-like kinase 1. *Curr Biol*, **17**, 304-315.
- Lengauer, C., Kinzler, K.W. and Vogelstein, B. (1997) Genetic instability in colorectal cancers. *Nature*, **386**, 623-627.
- Lengauer, C., Kinzler, K.W. and Vogelstein, B. (1998) Genetic instabilities in human cancers. *Nature*, **396**, 643-649.
- Lew, D.J. and Burke, D.J. (2003) The spindle assembly and spindle position checkpoints. *Annu Rev Genet*, **37**, 251-282.
- Li, R. and Murray, A.W. (1991) Feedback control of mitosis in budding yeast. *Cell*, **66**, 519-531.
- Liebel, U., Kindler, B. and Pepperkok, R. (2004) 'Harvester': a fast meta search engine of human protein resources. *Bioinformatics*, **20**, 1962-1963.

- Lin, Y.T., Chen, Y., Wu, G. and Lee, W.H. (2006) Hec1 sequentially recruits Zwint-1 and ZW10 to kinetochores for faithful chromosome segregation and spindle checkpoint control. *Oncogene*, **25**, 6901-6914.
- Liu, X., McLeod, I., Anderson, S., Yates, J.R., 3rd and He, X. (2005) Molecular analysis of kinetochore architecture in fission yeast. *Embo J*, **24**, 2919-2930.
- Lowery, D.M., Mohammad, D.H., Elia, A.E. and Yaffe, M.B. (2004) The Polo-box domain: a molecular integrator of mitotic kinase cascades and Polo-like kinase function. *Cell Cycle*, **3**, 128-131.
- Mack, G.J. and Compton, D.A. (2001) Analysis of mitotic microtubule-associated proteins using mass spectrometry identifies astrin, a spindle-associated protein. *Proc Natl Acad Sci U S A*, **98**, 14434-14439.
- Mann, M. (2006) Functional and quantitative proteomics using SILAC. *Nat Rev Mol Cell Biol*, **7**, 952-958.
- Mann, M., Ong, S.E., Gronborg, M., Steen, H., Jensen, O.N. and Pandey, A. (2002) Analysis of protein phosphorylation using mass spectrometry: deciphering the phosphoproteome. *Trends Biotechnol*, **20**, 261-268.
- Mazanek, M., Mituloviae, G., Herzog, F., Stingl, C., Hutchins, J.R., Peters, J.M. and Mechtler, K. (2007) Titanium dioxide as a chemo-affinity solid phase in offline phosphopeptide chromatography prior to HPLC-MS/MS analysis. *Nat Protoc*, **2**, 1059-1069.
- McAinsh, A.D., Tytell, J.D. and Sorger, P.K. (2003) Structure, function, and regulation of budding yeast kinetochores. *Annu Rev Cell Dev Biol*, **19**, 519-539.
- McClelland, M.L., Kallio, M.J., Barrett-Wilt, G.A., Kestner, C.A., Shabanowitz, J., Hunt, D.F., Gorbsky, G.J. and Stukenberg, P.T. (2004) The vertebrate Ndc80 complex contains Spc24 and Spc25 homologs, which are required to establish and maintain kinetochore-microtubule attachment. *Curr Biol*, **14**, 131-137.
- McEwen, B.F., Hsieh, C.E., Mattheyses, A.L. and Rieder, C.L. (1998) A new look at kinetochore structure in vertebrate somatic cells using high-pressure freezing and freeze substitution. *Chromosoma*, **107**, 366-375.
- Meijer, L., Borgne, A., Mulner, O., Chong, J.P., Blow, J.J., Inagaki, N., Inagaki, M., Delcros, J.G. and Moulinoux, J.P. (1997) Biochemical and cellular effects of roscovitine, a potent and selective inhibitor of the cyclin-dependent kinases cdc2, cdk2 and cdk5. *Eur J Biochem*, **243**, 527-536.
- Morgan, D.O. (1997) Cyclin-dependent kinases: engines, clocks, and microprocessors. *Annu Rev Cell Dev Biol*, **13**, 261-291.
- Murray, A.W. (2004) Recycling the cell cycle: cyclins revisited. *Cell*, **116**, 221-234.
- Musacchio, A. and Salmon, E.D. (2007) The spindle-assembly checkpoint in space and time. *Nat Rev Mol Cell Biol*, **8**, 379-393.
- Nakajima, H., Toyoshima-Morimoto, F., Taniguchi, E. and Nishida, E. (2003) Identification of a consensus motif for Plk (Polo-like kinase) phosphorylation reveals Myt1 as a Plk1 substrate. *J Biol Chem*, **278**, 25277-25280.
- Nasmyth, K. (2002) Segregating sister genomes: the molecular biology of chromosome separation. *Science*, **297**, 559-565.
- Nasmyth, K., Peters, J.M. and Uhlmann, F. (2000) Splitting the chromosome: cutting the ties that bind sister chromatids. *Science*, **288**, 1379-1385.

- Nesvizhskii, A.I., Keller, A., Kolker, E. and Aebersold, R. (2003) A statistical model for identifying proteins by tandem mass spectrometry. *Anal Chem*, **75**, 4646-4658.
- Neumann, B., Held, M., Liebel, U., Erfle, H., Rogers, P., Pepperkok, R. and Ellenberg, J. (2006) High-throughput RNAi screening by time-lapse imaging of live human cells. *Nat Methods*, **3**, 385-390.
- Nigg, E.A. (1993) Cellular substrates of p34(cdc2) and its companion cyclin-dependent kinases. *Trends Cell Biol*, **3**, 296-301.
- Nigg, E.A. (2001) Mitotic kinases as regulators of cell division and its checkpoints. *Nat Rev Mol Cell Biol*, **2**, 21-32.
- Nousiainen, M., Sillje, H.H., Sauer, G., Nigg, E.A. and Korner, R. (2006) Phosphoproteome analysis of the human mitotic spindle. *Proc Natl Acad Sci U S A*, **103**, 5391-5396.
- Obuse, C., Iwasaki, O., Kiyomitsu, T., Goshima, G., Toyoda, Y. and Yanagida, M. (2004) A conserved Mis12 centromere complex is linked to heterochromatic HP1 and outer kinetochore protein Zwint-1. *Nat Cell Biol*, **6**, 1135-1141.
- Okamura, A., Pendon, C., Valdivia, M.M., Ikemura, T. and Fukagawa, T. (2001) Gene structure, chromosomal localization and immunolocalization of chicken centromere proteins CENP-C and ZW10. *Gene*, **262**, 283-290.
- Olsen, J.V., Ong, S.E. and Mann, M. (2004) Trypsin cleaves exclusively C-terminal to arginine and lysine residues. *Mol Cell Proteomics*, **3**, 608-614.
- Ong, S.E., Blagoev, B., Kratchmarova, I., Kristensen, D.B., Steen, H., Pandey, A. and Mann, M. (2002) Stable isotope labeling by amino acids in cell culture, SILAC, as a simple and accurate approach to expression proteomics. *Mol Cell Proteomics*, **1**, 376-386.
- Orr-Weaver, T.L. and Weinberg, R.A. (1998) A checkpoint on the road to cancer. *Nature*, **392**, 223-224.
- Perkins, D.N., Pappin, D.J., Creasy, D.M. and Cottrell, J.S. (1999) Probability-based protein identification by searching sequence databases using mass spectrometry data. *Electrophoresis*, **20**, 3551-3567.
- Peters, J.M. (2006) The anaphase promoting complex/cyclosome: a machine designed to destroy. *Nat Rev Mol Cell Biol*, **7**, 644-656.
- Rajagopalan, H., Jallepalli, P.V., Rago, C., Velculescu, V.E., Kinzler, K.W., Vogelstein, B. and Lengauer, C. (2004) Inactivation of hCDC4 can cause chromosomal instability. *Nature*, **428**, 77-81.
- Ris, H. and Witt, P.L. (1981) Structure of the mammalian kinetochore. *Chromosoma*, **82**, 153-170.
- Ruchaud, S., Carmena, M. and Earnshaw, W.C. (2007) Chromosomal passengers: conducting cell division. *Nat Rev Mol Cell Biol*, **8**, 798-812.
- Sironi, L., Mapelli, M., Knapp, S., De Antoni, A., Jeang, K.T. and Musacchio, A. (2002) Crystal structure of the tetrameric Mad1-Mad2 core complex: implications of a 'safety belt' binding mechanism for the spindle checkpoint. *Embo J*, **21**, 2496-2506.
- Sluder, G. and McCollum, D. (2000) Molecular biology. The mad ways of meiosis. *Science*, **289**, 254-255.
- Smith, D.A., Baker, B.S. and Gatti, M. (1985) Mutations in genes encoding essential mitotic functions in *Drosophila melanogaster*. *Genetics*, **110**, 647-670.
- Smith, T.F., Gaitatzes, C., Saxena, K. and Neer, E.J. (1999) The WD repeat: a common architecture for diverse functions. *Trends Biochem Sci*, **24**, 181-185.

- Starr, D.A., Saffery, R., Li, Z., Simpson, A.E., Choo, K.H., Yen, T.J. and Goldberg, M.L. (2000) HZWint-1, a novel human kinetochore component that interacts with HZW10. *J Cell Sci*, **113** (Pt 11), 1939-1950.
- Starr, D.A., Williams, B.C., Hays, T.S. and Goldberg, M.L. (1998) ZW10 helps recruit dynactin and dynein to the kinetochore. *J Cell Biol*, **142**, 763-774.
- Starr, D.A., Williams, B.C., Li, Z., Etemad-Moghadam, B., Dawe, R.K. and Goldberg, M.L. (1997) Conservation of the centromere/kinetochore protein ZW10. *J Cell Biol*, **138**, 1289-1301.
- Steegmaier, M., Hoffmann, M., Baum, A., Lenart, P., Petronczki, M., Krssak, M., Gurtler, U., Garin-Chesa, P., Lieb, S., Quant, J., Grauert, M., Adolf, G.R., Kraut, N., Peters, J.M. and Rettig, W.J. (2007) BI 2536, a potent and selective inhibitor of polo-like kinase 1, inhibits tumor growth in vivo. *Curr Biol*, **17**, 316-322.
- Sumara, I., Gimenez-Abian, J.F., Gerlich, D., Hirota, T., Kraft, C., de la Torre, C., Ellenberg, J. and Peters, J.M. (2004) Roles of polo-like kinase 1 in the assembly of functional mitotic spindles. *Curr Biol*, **14**, 1712-1722.
- Sumara, I., Vorlaufer, E., Gieffers, C., Peters, B.H. and Peters, J.M. (2000) Characterization of vertebrate cohesin complexes and their regulation in prophase. *J Cell Biol*, **151**, 749-762.
- Sumara, I., Vorlaufer, E., Stukenberg, P.T., Kelm, O., Redemann, N., Nigg, E.A. and Peters, J.M. (2002) The dissociation of cohesin from chromosomes in prophase is regulated by Polo-like kinase. *Mol Cell*, **9**, 515-525.
- Taira, T., Maeda, J., Onishi, T., Kitaura, H., Yoshida, S., Kato, H., Ikeda, M., Tamai, K., Iguchi-Ariga, S.M. and Ariga, H. (1998) AMY-1, a novel C-MYC binding protein that stimulates transcription activity of C-MYC. *Genes Cells*, **3**, 549-565.
- Takahashi, K., Yamada, H. and Yanagida, M. (1994) Fission yeast minichromosome loss mutants mis cause lethal aneuploidy and replication abnormality. *Mol Biol Cell*, **5**, 1145-1158.
- Tanaka, T.U. (2002) Bi-orienting chromosomes on the mitotic spindle. *Curr Opin Cell Biol*, **14**, 365-371.
- Tanaka, T.U., Rachidi, N., Janke, C., Pereira, G., Galova, M., Schiebel, E., Stark, M.J. and Nasmyth, K. (2002) Evidence that the Ipl1-Sli15 (Aurora kinase-INCENP) complex promotes chromosome bi-orientation by altering kinetochore-spindle pole connections. *Cell*, **108**, 317-329.
- Tanaka, T.U., Stark, M.J. and Tanaka, K. (2005) Kinetochore capture and bi-orientation on the mitotic spindle. *Nat Rev Mol Cell Biol*, **6**, 929-942.
- Vigneron, S., Prieto, S., Bernis, C., Labbe, J.C., Castro, A. and Lorca, T. (2004) Kinetochore localization of spindle checkpoint proteins: who controls whom? *Mol Biol Cell*, **15**, 4584-4596.
- Waizenegger, I.C., Hauf, S., Meinke, A. and Peters, J.M. (2000) Two distinct pathways remove mammalian cohesin from chromosome arms in prophase and from centromeres in anaphase. *Cell*, **103**, 399-410.
- Warburton, P.E., Cooke, C.A., Bourassa, S., Vafa, O., Sullivan, B.A., Stetten, G., Gimelli, G., Warburton, D., Tyler-Smith, C., Sullivan, K.F., Poirier, G.G. and Earnshaw, W.C. (1997) Immunolocalization of CENP-A suggests a distinct nucleosome structure at the inner kinetochore plate of active centromeres. *Curr Biol*, **7**, 901-904.
- Wei, R.R., Al-Bassam, J. and Harrison, S.C. (2007) The Ndc80/HEC1 complex is a contact point for kinetochore-microtubule attachment. *Nat Struct Mol Biol*, **14**, 54-59.

- Westermann, S., Cheeseman, I.M., Anderson, S., Yates, J.R., 3rd, Drubin, D.G. and Barnes, G. (2003) Architecture of the budding yeast kinetochore reveals a conserved molecular core. *J Cell Biol*, **163**, 215-222.
- Wigge, P.A. and Kilmartin, J.V. (2001) The Ndc80p complex from *Saccharomyces cerevisiae* contains conserved centromere components and has a function in chromosome segregation. *J Cell Biol*, **152**, 349-360.
- Winey, M., Goetsch, L., Baum, P. and Byers, B. (1991) MPS1 and MPS2: novel yeast genes defining distinct steps of spindle pole body duplication. *J Cell Biol*, **114**, 745-754.
- Wong, O.K. and Fang, G. (2007) Cdk1 phosphorylation of BubR1 controls spindle checkpoint arrest and Plk1-mediated formation of the 3F3/2 epitope. *J Cell Biol*, **179**, 611-617.
- Yaffe, M.B. (2002) Phosphotyrosine-binding domains in signal transduction. *Nat Rev Mol Cell Biol*, **3**, 177-186.
- Yaffe, M.B. and Smerdon, S.J. (2001) PhosphoSerine/threonine binding domains: you can't pSERious? *Structure*, **9**, R33-38.
- Yates, J.R., 3rd, Link, A.J. and Schieltz, D. (2000) Direct analysis of proteins in mixtures. Application to protein complexes. *Methods Mol Biol*, **146**, 17-26.
- Yuan, J., Tang, W., Luo, K., Chen, X., Gu, X., Wan, B. and Yu, L. (2006) Cloning and characterization of the human gene DERP6, which activates transcriptional activities of p53. *Mol Biol Rep*, **33**, 151-158.
- Zhang, X., Ye, J., Jensen, O.N. and Roepstorff, P. (2007) Highly efficient phosphopeptide enrichment by calcium phosphate precipitation combined with subsequent serial immobilized metal ion affinity chromatography (IMAC) enrichment. *Mol Cell Proteomics*.

7. Abbreviations

APS	- ammonium peroxodisulfate
BSA	- bovine serum albumin
bv	- bead volume
CREST	- calcinosis, Raynaud's phenomenon, esophageal dysmotility, sclerodactyly, telangiectasias
DMEM	- Dulbecco's modified Eagle's medium
DMP	- dimethylpimelimidate
DMSO	- dimethylsulfoxide
DTT	- dithiothreitol
E	- eluate
ECL	- enhanced chemiluminescence
EGTA	- ethylene glycol tetraacetic acid
ESI	- electrospray ionisation
FCS	- fetal calf serum
Fig.	- Figure
FPLC	- Fast Protein Liquid Chromatography
FRAP	- Fluorescence Recovery After Photobleaching
GuHCl	- guanidine hydrochloride
GST	- glutathione S-transferase
HBS	- HEPES buffered saline
HPLC	- High-performance liquid chromatography
HRP	- horseradish peroxidase
IF	- immunofluorescence
IMAC	- immobilized metal ion affinity chromatography
IP	- immunoprecipitation
IPTG	- isopropyl- β -D-thiogalactopyranoside
IVT	- in vitro transcription / translation
KLH	- keyhole limpet hemocyanin
LBamp	- Luria broth medium with ampicillin resistancy
log	- exponentially grown cells
min	- minutes
MOC	- Metal Oxide Chromatography
MS	- mass spectrometry
MS/MS or MS ²	- tandem mass spectrometry
MS ³	- three-step mass spectrometry

Ni/NTA	- nickel nitrilo-triacetic-acid agarose resin
NP40	- nonidet P-40
OA	- okadaic acid
PBS	- phosphate buffered saline
PAGE	- polyacrylamide gel electrophoresis
PCR	- polymerase chain reaction
PFA	- paraformaldehyde
PI	- phosphoimager
PIM	- phosphatase inhibitor mix
rpm	- revolutions per minute
PSG	- penicillin streptomycin glutamate
PVDF	- polyvinyl difluoride
S14	- supernatant after spinning cell lysate at 14000 g
SILAC	- stable isotope labelling of amino acids in cell culture
SDS	- sodium dodecylsulfate
SMS	- Specific Mascot Score
TEMED	- tetramethylethylenediamine
TBS-Tw	- Tris buffered saline containing detergent Tween-20
TRIS	- 2-amino-2-hydroxymethyl-1,3-propanediol
Tw	- Tween-20
Tx	- Triton X-100
Tm	- melting temperature
U	- fraction of proteins remaining unbound to the beads after IP bead binding
WB	- western blot
MWCO	- Molecular Weight Cut-Off

Acknowledgements

In the first place I wish to thank to Jan-Michael for giving me the opportunity to work in his lab, for his remarkable expertise and enthusiasm, as well as his constant encouragement during my work.

I want to express my deep gratitude to my two supervisors Jim and Björn for the time they invested in explaining and interpreting my experiments, for joyful discussions and of course for helping me to improve my scientific skills and knowledge. Many thanks also to Martina who was helping me in generating the cell-lines.

Thanks to all the Peters lab members, past and present, for providing a very pleasant working atmosphere and for all the helpful discussions.

And finally many thanks to all my friends and family, especially my parents who supported me in various ways during the time of my studies and of course to my daughter Lena-Marie who is brightening every day of my life.



Peters lab members, December 2005

Curriculum Vitae

Personal data:

Full name: Stephan Zettl
Gender: male
Date of birth: June 8th, 1977
Place of birth: Berlin, Germany
Citizenship: German
Children: 1 daughter *2005

Education:

2003 – 2009 Diploma programme in Molecular Biology, University of Vienna, Austria
06/2005 - 06/2006 Diploma thesis under supervision of Dr. Jan-Michael Peters, Institute of Molecular Pathology (IMP), Vienna, Austria

1998 - 2003 Study of Biology and Geography, University of Wuerzburg, Germany

1997 - 1998 Military Service, Hildesheim and Prenzlau, Germany

1990 - 1997 Secondary School C.-F.-Gauss Gymnasium, Schwedt, Germany

1984 - 1990 Primary School, Polytechnische Oberschule 8, Schwedt, Germany